Theses and Dissertations

1993

An experimental investigation of real-time product quality sensing during molding processes

Akihisa Kikuchi
Lehigh University

Follow this and additional works at: http://preserve.lehigh.edu/etd

AUTHOR:

Kikuchi, Akihisa

TITLE:

An Experimental
Investigation of Real-Time
Product Quality Sensing
During Molding Processes

DATE: January 16, 1994

An Experimental Investigation of Real-Time Product Quality Sensing During Molding Processes

by

Akihisa Kikuchi

A Thesis

Presented to the Graduate and Research Committee

of Lehigh University

in Candidacy for the Degree of

Master of Science

in

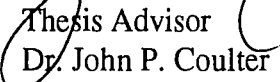The Department of Mechanical Engineering and Mechanics

Lehigh University

1993

CERTIFICATE OF APPROVAL

This thesis is accepted and approved in partial fulfillment of the requirements for the Master of Science.

Dec. 7, 1993
_____
Date

Thesis Advisor
Dr. John P. Coulter

_____
Chairperson
Dr. Robert P. Wei

Acknowledgments

Table of Contents

List of Tables

List of Figures

Nomenclature

∂P = pressure difference between two points

∂x = distance between two points in x-direction

∂y = distance between two points in y-direction

μ = viscosity of fluid

$\bar{u}$ = mean velocity of fluid in x-direction

$\bar{v}$ = mean velocity of fluid in y-direction

K_x = permeability in x-direction

K_y = permeability in y-direction

C = capacitance

q = electric charge

V = potential voltage

ε^* = complex permittivity

ε' = permittivity in real part

ε'' = permittivity in imaginary part

C_0 = air filled replaceable capacitance of the measuring cell

C_{mat} = capacitance of material (resin)

G_{mat} = conductance of material (resin)

f = frequency

ε'_d, ε''_d = dipolar component of both real and imaginary part of complex permittivity

ε'_i, ε''_i = ionic component of both real and imaginary part of complex permittivity

ε_0 = limiting low frequency value of ε

ε_∞ = limiting high frequency value of ε

τ = characteristic relaxation time

β = parameter measures the distribution in relaxation time

Z^* = electrode impedance induced by the ions

σ = electrical conductivity

P_b = Rayleigh backscattered power

α_s = power attenuation coefficient due to Rayleigh scattering

P_0 = optical pulse of peak power

S = recapture ratio of Rayleigh scattered power back into the fiber

W = optical pulse of width

t = time for returning the pulse to laser source from laser source

υ = velocity of the pulse

l = location of the failure in the fiber

ΔV_1 = voltage drop across the fixed resistor

V_{ps} = voltage applied by power supply

R_1 = fixed resistor

R_2 = total resistance obtained from the sensor

R_{res} = resistance of resin at one sensing gap

ϕ_e = volume fraction of epoxy

ϕ_c = volume fraction of curing agent

ρ_{res} = density of resin

ρ_e = density of epoxy

ρ_c = density of curing agent

ε = critical voltage drop gradient level

A = cross sectional area of sensing gap

L = distance of two fibers at a sensing gap

N = number of sensing gap filled with resin

Abstract

The present investigation focused on the need for real-time sensing subsystems for the monitoring of resin flow dynamics during injection molding (IM) and resin transfer molding (RTM) processes. Such subsystems, when combined with process parameter control, will produce intelligent manufacturing systems that will significantly improve molding process manufacturing capabilities. Product quality will improve while both manufacturing process development time and cost will be reduced. A precise review of potential process monitoring methodologies is included. The concept chosen is based on embedded electronic sensors, and during the present study a real-time resin front monitoring system based on a modified version of the concept originally investigated at the U.S. Army Materials Technology Laboratory was developed. Electrically conductive wires were embedded orthogonally in a non-intersecting manner within mold cavities. Subsequent resin flow was sensed by monitoring the electrical characteristics of circuits which resulted during processing. A novel modification of circuitry was included to allow for the monitoring of multiple locations with a single electronic circuit. The net result of this modification was a faster response time of the overall sensing subsystem. The concept was verified experimentally through the performance of both one dimensional (1-D) and two dimensional (2-D) experiments. The resin system utilized consisted of a mixture of epoxy resin (Shell, EPON 826) and a curing agent (Anhydrides & Chemicals Incorporated, MHHPA). The study included an analysis of the effects of variations in relative resin to curing agent ratio. The sensed flow front progression information was validated through controlled injection rate experimentation and flow visualization results obtained with transparent molds.

Chapter 1. INTRODUCTION TO POLYMER PRODUCT MANUFACTURING

The present study focused on the development of a product quality monitoring subsystem specifically applicable to molding processes such as injection molding (IM) and resin transfer molding (RTM). With such processes, there is a need to monitor both flow conditions and material rheological properties within closed molds during manufacturing. This chapter presents an introduction to polymer materials and polymer product manufacturing. Following this, chapter 2 presents characteristics and needs specifically related to molding processes.

1.1 Polymeric Materials and Polymeric Matrix Composites

The discovery and improvement of new materials has influenced human societies since mankind was created. In a way, new or advanced materials can be viewed as symbols of human evolution [1]. At the beginning of the industrial revolution, metals were the primary engineering materials of choice for many applications. Since the early 1900's, however, many traditionally metal products have been replaced by those based on polymeric materials.

The first polymeric material, discovered in its natural form in 1908, was "celluloid". Following this, the first synthetic polymeric material, which was "phenol," was discovered in 1909 [2]. Since then, many types of synthetic polymers have been discovered and they can be characterized in two classes, namely thermosets and thermoplastics. Thermosets are materials that react or cure irreversibly when heat, pressure, and/or some other reaction energy providing mechanism is supplied. Once

2

cured, thermosetting materials do not soften and flow with the subsequent application of heat and pressure. Thermoplastic polymers, on the other hand, change phases reversibly, and do soften and flow every time that critical pressure and temperature conditions are imposed. Thus, most thermoplastic materials can be remolded many times.

Since World War II, many types of thermoplastics have been developed and improved. Table 1.1.1 [3] includes examples of commonly utilized polymers. Some of the important characteristics of various polymers are presented in Table 1.1.2 [3].

In the early years of polymer development, thermosets were brittle and had low impact strength. Likewise, thermoplastics were brittle at room temperature and had very low mechanical strength below 100°C [2]. Due to these reasons, early polymeric materials were inferior to metals in mechanical strength and usable temperature range.

Polymers which were useful for unique applications began to be developed in the 1950's. These polymers became known as engineering plastics, an example of which is polyacetal. Polyacetal was first presented in commercial form as "Delrin," and was found to possess good fatigue resistance and lubricant characteristics. For these reasons, Delrin rapidly secured a position as a replacement for metal in products such as gears and camshafts. Another important polymer which was discovered in the 1950's was polycarbonate, which had high impact strength and high temperature resistance. A additional polymer, "Nylon," was also developed and found to have good friction characteristics, high temperature resistance, and high mechanical strength. Nylon quickly became well recognized as a useful industrial material. As is evident from the discussion above, engineering plastics have characteristics such as:

- o High mechanical strength and/or impact strength.
- o Resistance to softening at high temperature.
- o Unique or special performance related to industrial applications.

Table 1.1.1 Commonly used polymers

Acetal (POM)
Acrylics
   Polyacrylonitrile (PAN)
   Polymethylmethacrylate (PMMA)
Acrylonitrile butadiene styrene (ABS)
Alkyd
Allyl diglycol carbonate (CR-39)
Allyls
   Diallyl isophthalate (DAIP)
   Diallyl phthalate (DAP)
Aminos
   Melamine formaldehyde (MF)
   Urea formaldehyde (UF)
Cellulosics
   Cellulose acetate (CA)
   Cellulose acetate butyrate (CAB)
   Cellulose acetate propionate (CAP)
   Cellulose nitrate
   Ethyl cellulose (EC)
Chlorinated polyether
Epoxy (EP)
Ethylene vinyl acetate (EVA)
Ethylene vinyl alcohol (EVOH)
Fluorocarbons
   Fluorinated ethylene propylene (FEP)
   Polytetrafluoroethylene (PTFE)
   Polyvinyl fluoride (PVF)
   Polyvinylidene fluoride (PVDF)
Furan
Ionomer
Ketone
Liquid crystal polymer (LCP)
   Aromatic copolyester (TP polyester)
Melamine formaldehyde (MF)
Nylon (polyamide) (PA)
Parylene
Phenolic
   Phenol formaldehyde (PF)
Phenoxy
Poyallomer
Polyamide (nylon) (PA)
Polyamide-imide (PAI)
Polyarylether
   Polyaryletherketone (PAEK)
   Polyaryl sulfone (PAS)
Polyarylate (PAR)
Polybenzimidazole (PBI)
Polycarbonate (PC)

Polyetherketone (PEK)
Polyetheretherketone (PEEK)
Polyetherimide (PEI)
Polyimide (PI)
   Thermoplastic PI
   Thermoset PI
Polymethylmethacrylate (acrylic) (PMMA)
Polymethylpentene
Polyolefins (PO)
   Chlorinated PE (CPE)
   Cross-linked PE (XLPE)
   High density PE (HDPE)
   Ionomer
   Linear LDPE (LLDPE)
   Low density PE (LDPE)
   Polyallomer
   Polybutylene (PB)
   Polyethylene (PE)
   Polypropylene (PP)
Ultra-high-molecular weight PE (UHMWPE)
Poly oxymethylene (POM)
Polyphenylene ether (PPE)
Ployphenylene oxide (PPO)
Polyphenylene sulfide (PPS)
Polyurethane (PUR)
Silicone (SI)
Styrene
   Acrylic styrene acrylonitrile (ASA)
   Acrylonitrile butadiene styrene (ABS)
   General-purpose PS (GPPS)
   High-impact PS (HIPS)
   Polystyrene (PS)
   Styrene acrylonitrile (SAN)
   Styrene butadiene (SB)
Sulfones
   Polyether sulfone (PES)
   Polyphenyl sulfone (PPS)
   Polysulfone (PSU)
Urea formaldehyde (UF)
Vinyls
   Chrolinate PVC (CPVC)
   Polyvinyl acetate (PVAC)
   Polyvinyl alcohol (PVA)
   Polyvinyl butyrate (PVB)
   Polyvinyl chloride (PVC)
   Polyvinylidene chloride (PVDC)
   Polyvinylidene fluoride (PVF)
Polyesters
   Aromatic polyester (TS poyester)
   Thermoplastic polyesters
     Crystalized PET (CPET)
     Polybutylene terephthalate (PBT)
     Polyethylene terephthalate (PET)
   Unsaturated polyester (TS polyester)

Properties	Thermoplastics	Thermosets
Low temperature	TFE	DAP
Low cost	PP, PE, PVC, PS	Phenolic
Low gravity	Polypropylene methylpentene	Phenolic/nylon
Thermal expansion	Phenoxy glass	Epoxy-glass fiber
Volume resistivity	TFE	DAP
Dielectric strength	PVC	DAP, Polyester
Elasticity	EVA, PVC, TPR	Silicone
Moisture absorption	Chlorotrifluorethylene	Alkyd-glass fiber
Steam resistance	Polysulfone	DAP
Flame resistance	TFE, PI	Melamine
Water immersion	Chlorinated polyether	DAP
Stress craze resistance	Polypropylene	All
High temperature	TFE, PPS, PI	Silicones
Gasoline resistance	Acetal	Phenolic
Impact	UHMW PE	Epoxy-glass fiber
Cold flow	Polysulfone	Melamine-glass fiber
Chemical resistance	TFE, FEP, PE, PP	Epoxy
Scratch resistance	Acrylic	Allyl diglycol carbonate
abrasive wear	Polyurethane	Phenolic-canvas
Colors	Acetate, PS	Urea, melamine

Table 1.1.2   Properties of common polymers

In addition to engineering plastics, there are other polymers more applicable to structural applications, such as polyethylene, polystyrene, polypropylene, phenol, and unsaturated polyester. Also, new polymers have been discovered recently which can be classified as high performance engineering plastics. Examples of these materials include polyimide, polyethersulfone, and polyamideimide. To date these materials remain low in production rate and high in cost.

Apart from being used for products made completely from polymers, polymers have been found to be very applicable as matrix components of composite materials. A polymer matrix composite material (or fiber reinforced plastic "FRP") is defined as a material consisting of a polymeric matrix reinforced by strengthening fibers. Today,

composite materials are highly attractive to a wide variety of industries. The most common reinforcements used in polymer composites are graphite fibers, glass fibers, or aramid fibers. Typical properties of these reinforcements are presented and compared to metals in Table 1.1.3.

Types	Density (g/cc)	Tensile strength (GPa)	Tensile elastic Modulus (GPa)
Glass			
E monofilament	2.54	3.45	72.4
12 end roving	2.54	2.56	72.4
S monofilament	2.54	4.58	85.5
12 end roving	2.54	3.79	85.5
Boron			
(Tungsten substrate)			
4 mil or 5.6 mil	2.63	3.10	400
Graphite			
High strength	1.80	2.76	262
High modulus	1.94	2.07	380
Intermediate	1.74	2.48	190
Organic			
Aramid	1.44	2.76	124
Metal			
H. T. Steel	7.80	1.40	210
Duralmin	2.70	0.51	73
Ti-6 Al-4 V	4.40	1.00	112

Table 1.1.3   Commonly used fiber reinforcements

As seen in the table, polymeric matrix composites can be preferable to metal products, specifically when a high strength to weight ratio is desired. In addition, their performance level can be controlled by selecting the type, location, direction and amount of fibers for the required strength.

1.2 Polymeric Product and Polymeric Matrix Composite Manufacturing Processes

Polymers can be molded, formed, cast, machined, and joined into desired product shapes. For this reason, polymeric products and polymeric matrix composites are manufactured in many ways. One benefit associated with polymer manufacturing is that the operating temperatures during polymer manufacturing are usually lower than those present during the processing of metals. In this section, processes used for the manufacture of polymeric material based products and polymeric matrix composites are briefly explained.

1.2.1 Polymeric Product Manufacturing Processes

1.2.1.1 Extrusion

Extrusion processes are characterized by the forcing of a material through a die to form a constant cross section product of desired shape. In most cases involving the extrusion of polymers, thermoplastics are used in the form of granules, pellets or powder. The raw material is placed into a hopper and then fed into an extruder barrel. A screw inside the barrel pushes the pellets down the barrel. The pellets are melted while traveling through the barrel due to both internal friction from the mechanical action of the screw and heat applied from heaters. The molten polymer is then forced through a die, and the extruded product is subsequently cooled.

1.2.1.2   Injection Molding (IM)

Injection molding processes are used during the manufacturing of both thermoplastic and thermosetting polymer products. Detailed descriptions of several classes of injection molding processes follow.

i)   Basic IM :

A schematic diagram of a typical injection molding machine is shown in Figure 1.2.1. Thermoplastic polymer pellets are fed into a reciprocating screw from a hopper. The rotating screw forces the polymer into a heated extruder barrel where it softens enough to flow. The polymer accumulates in the barrel until a suitable shot size required to fill the desired mold is reached. Once this condition exists, the screw stops turning and moves axially to force the polymer through the nozzle and into the mold. During injection, very high pressure levels, as high as 300 psi., can be reached. Following injection and packing, the mold is cooled down, and the polymer fully solidifies. The mold is then opened, and the part is ejected.

With thermosets, the resin is injected into an empty closed mold from a resin supply system. The mold is then heated up to induce curing of the polymer. After curing, the part is released from the mold.

Mold
Molded parts
Gate
Sprue
Hopper
Hydraulic cylinder
Nozzle
Runner
Screw
Molded parts
Pump
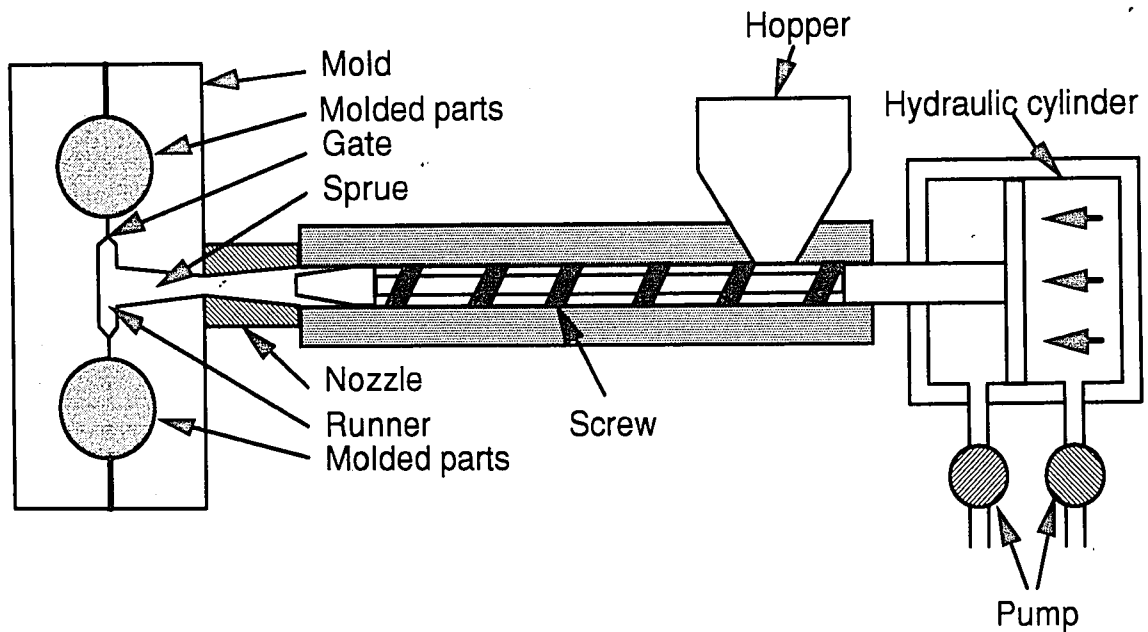
Figure 1.2.1:   Schematic of Injection Molding Apparatus

ii)   Hollow Gas Injection Molding :

Hollow gas injection molding is mostly used with thermoplastic materials. The initial stage of this process is the same as that for basic injection molding. The difference with hollow gas injection molding is that the molten polymer within the mold is combined with a high pressure inert gas, such as nitrogen. The gas does not mix with polymer, but instead forms a continuous channel through the thicker sections of the mold to maintain the pressure throughout the molding cycle. As a result the thicker sections of the resulting products are commonly hollow. A main advantage of this process is that the mold clamping force required to produce quality parts is lessened. In addition, thick and thin sections can be combined without leading to sinking or warping, and molded parts with higher stiffness/weight ratios can be produced. This process also produces parts with low residual stresses and therefore little post-molding warpage.

9

iii)   Co-Injection (Sandwich) Molding :

Co-injection molding involves the injection of two separate polymers through individual feed screw and hopper systems. This process produces parts consisting of skin and core sections. During the initial stage of the process the skin material is injected. Following this, the core material is injected into the inside of the skin to let the skin expand. At the end of the injection stage, the core material typically fills 70 to 90% of the mold, and the skin material surrounds the core in a continuous fashion. Advantages of the co-injection molding process include the ability to control the color of the surface material and the ability to reduce cost by using less expensive core materials. A disadvantage of this process is decreased surface finish quality compared to that obtained with conventional injection molding.

iv)   Fusible Core Injection Molding :

This process involves the usage of a fusible core during the injection molding of parts that can not be easily formed or released. The usage of a core makes the injection molding of complex parts possible. The core is commonly a die-cast tin-bismuth alloy that has a low melting temperature (lower than the polymer injected). During the initial stage of the process, the alloy core is inserted into the mold. The polymer is then injected into the mold and forms around the core to produce the skin. The mold is then cooled down to let the skin solidify. After this, the part is released from the mold and heated up to melt out the low melting temperature core without melting the skin. An advantage of the fusible core process is the part weight reduction that can be achieved. In many cases, fusible core produced polymer products have replaced previously aluminum parts and yielded a weight reduction of 50%. Also, fusible core molded parts are ready to be used while the die-cast parts usually require post-casting-machining .

v)   Push-Pull Injection Molding :

This relatively new injection molding technique utilizes a conventional twin-component injection system with two mold inlet injection gates. The primary injection unit pushes polymer through one inlet gate, and it is injected until the mold is overfilled. The overfill of polymer flows into the other gate and the secondary unit. The secondary unit then pushes the polymer back into the mold again. This process is continuously repeated, while the outer layer solidifies on the mold surface little by little. At the end of the process, the mold is filled with solid polymer.

vi)   Reaction Injection Molding (RIM) :

RIM is the most commonly used injection molding process for thermosetting polymer. The initial set-up is the same as for basic injection molding. The difference exists when the resin is injected into the mold. The resin used in this process, however, consists of two parts, which are mixed together just before the polymer is injected. During injection, very high pressure are used, and the cure reaction occurs during filling. The result is a very fast product manufacturing cycle time.

1.2.1.3   Blow Molding

Blow molding is a modification of an extrusion or injection molding process specifically employed to produce hollow parts such as bottles and tubes. Extrusion blow molding is usually used to produce tubes or pipes. In extrusion blow molding, a tube is extruded and clamped into a mold with a cavity larger than the tube diameter. The tube is then blown outward to fill the mold cavity usually with an air blast at a pressure of 350 - 700 kPa.

Injection blow molding is usually used to produce bottles and hollow containers. In injection blow molding, a short tubular piece is injection molded, then the dies open and the tubular piece is transferred to a blow molding die. Hot air is then injected into the tubular piece to expand and fill the mold cavity.

1.2.1.4   Rotational Molding

Rotational molding is used to produce large hollow parts, usually out of thermoplastic materials. The process involves the usage of a two piece female mold which is designed to be rotated about two perpendicular axes. A premeasured quantity of powdered polymer which is obtained from a polymerization process that precipitates a powder from a liquid is placed in a warm mold. The mold is then rotated about the two axes while being heated the heat and tumbling motion causes the polymer to simultaneously melt and cast the inside of the mold. The suggested cooling of the mold produces a hollow polymer product.

1.2.1.5   Thermoforming

Thermoforming is a process of forming thermoplastic sheet or film against a mold by simultaneously applying heat and pressure. In thermoforming, a sheet is heated in an oven to the softening point that is below the melting point. The sheet is then removed from the oven and formed into a mold by the application of a vacuum to pull the sheet against the mold. The shape of the product is set upon contacting the mold since the mold is usually at room temperature.

1.2.1.6 Compression Molding

In compression molding, a premeasured charge of material is placed directly in a heated mold cavity. Forming is completed under pressure with a plug or the upper half of the die. Typical products made by this process are dishes, handles, container caps, fittings, electrical components, washing machine agitators, and housings.

1.2.1.7 Casting

Some thermoplastic and thermoset polymer products are produced by casting into rigid or flexible molds. In casting thermoplastics, a mixture of monomer, catalyst, and various additives is heated and poured into the mold. The part is formed after polymerization takes place.

1.2.2 Polymeric Matrix Composite Manufacturing Process

1.2.2.1 Hand Lay-up

Hand lay-up is the oldest, the simplest and the most versatile method for composite material production. The process consists of the manual placement of layers of mat, fabric, or both on a one piece mold. During the placement process, the layers are simultaneously saturated with a liquid thermosetting polymer resin. The resultant product is sequentially cured. The hand lay-up process is slow and labor intensive, and the variety of parts that can be produced is limited to relatively simple geometries.

1.2.2.2 Spray-up

During spray-up processes, an air spray gun equipped with a roller cutter chops fiber rovings to a controlled length. The resulting short fibers are then blown in a random

13

pattern onto a surface of the mold simultaneously with a spray of catalyzed resin. The chopped fibers are coated with the resin as they exit the gun's nozzle. The resulting mass is consolidated with serrated rollers to squeeze out air and excess resin.

1.2.2.3   Vacuum Bag Molding

This method was developed to reduce or eliminate resin-rich or resin-starved areas resulting from hand-lay-up or spray-up process in which curing occurred without the application of external pressure. In vacuum bag molding, the wet liquid resin composite and mold are enclosed in a flexible membrane or bag and the bag or the membrane is vacuumed. Atmospheric pressure on the outside then presses the bag or membrane uniformly against the composite. Pressure usually ranges from 69 to 96.6 kPa (10-14 psi).

1.2.2.4   Pressure Bag Molding

Pressure bag molding is used to produce seamless containers, tanks, pipes, and so on. In this process, an inflatable elastic pressure bag is placed within a preform and the assembly is put into a closed mold. Resin is then injected into the preform and the pressure bag is inflated to about 345 kPa. Heat is applied and the part is cured within the mold. After cure is complete, the bag is deflated and removed through an opening at the end of the mold. The part is then removed from the mold.

1.2.2.5   Resin Transfer Molding

The resin transfer molding (RTM) process was developed in the 1950's. Today, RTM processes are still used for the manufacture of many fiber reinforced composite plastic products. Detailed descriptions and the various RTM methods are as follows.

a)   Basic RTM:

A diagram of basic RTM is shown in Figure 1.2.2. The mold surface is first treated with a release agent. A dry reinforcement called a preform is cut into a desired shape and is placed into the mold. The mold is then closed and a resin feeding system is attached.   It should be noted that the mold must have air vents to avoid the air entrapment during filling. The valve is opened to let the resin usually of thermosetting type flow into the mold. When the mold is filled, the valve is closed, and the resin feeding system removed.   The mold is then heated up and cure reaction takes place. After curing is completed, the mold is opened, and the finished part is released.

b)   Thermal Expansion RTM (TERTM) [4,5]:

This process was developed and licensed by TERTM Inc. in Winona, Minnesota. This process is basically the same as basic RTM but it utilizes a foam core material which is placed in the center of the preform within the mold. The foam core and preform are cut into a desired shape and placed into the mold. The mold is closed, the resin feeding system is attached, and the resin is transferred to the mold. When the mold is filled, the resin feeding system is removed from the mold. Then, as the mold is heated, the foam core expands and squeezes excess resin out of the mold through the vents. The heating in this process is very fast to avoid the curing of resin before the expansion of the foam core. When the process is complete and the post cured, the result is more fully consolidated product due to the added pressure realized during core expansion.
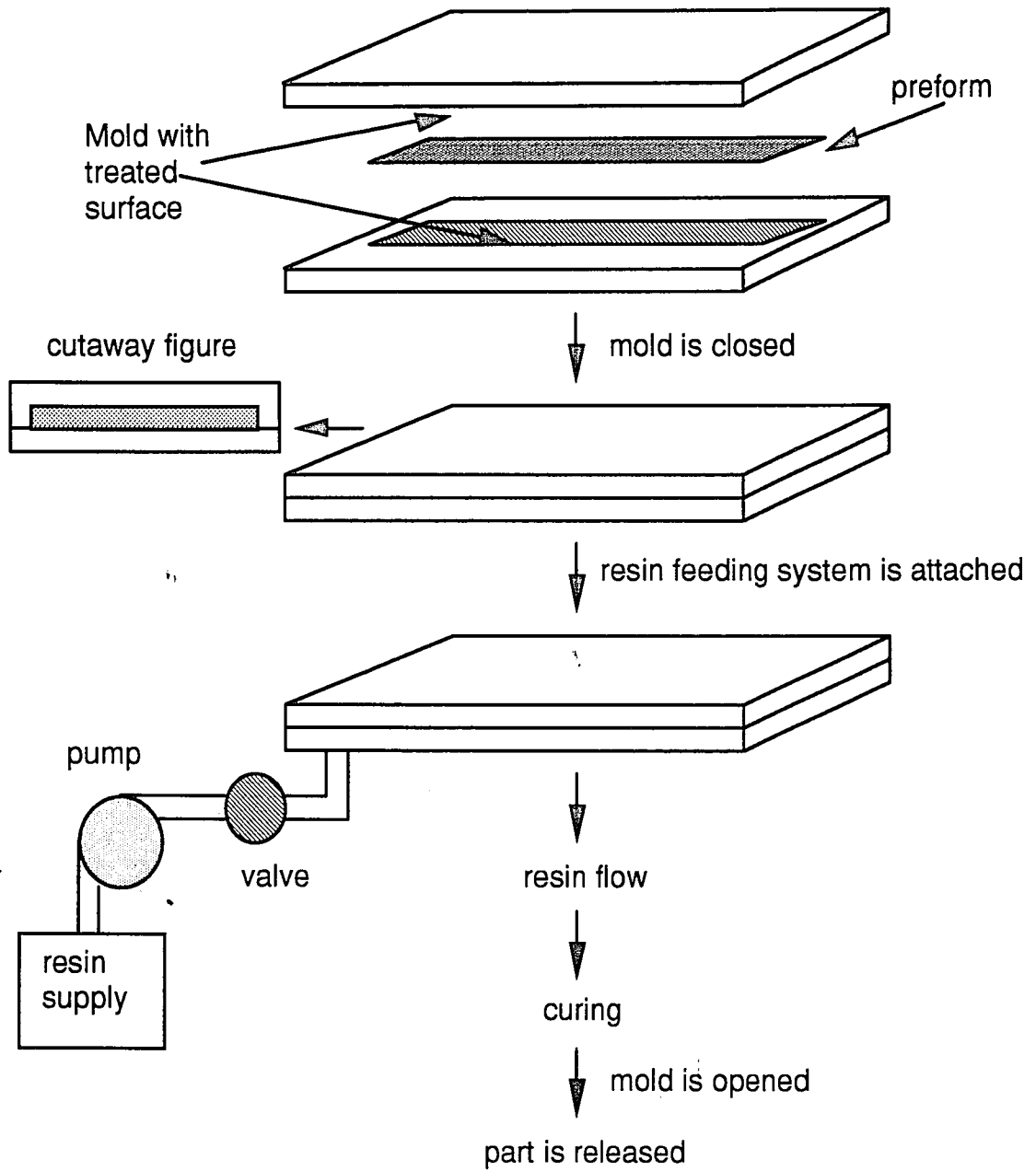
Figure 1.2.2: The Basic Resin Transfer Molding Process

c)   Vacuum Assisted Resin Injection (VARI) [4]:

The process is the same as basic RTM with the exception being that a vacuum pump is used for the evacuation of the air inside the mold during filling. The existence of this vacuum simply enhances the flow of resin into the mold.

d)   High Speed RTM (HSRTM) [6]:

This high speed RTM process was developed by Ford Motor Co. As is evident from the name, HSRTM process have faster process cycles than those for basic RTM. The HSRTM process is similar to basic RTM. The only difference is that HSRTM utilizes a higher quality aluminum or steel mold to contain moderately higher molding pressures (100 to 500 psi) and enhance heat transfer. The ability to work with higher pressures brings with it an increase in viable resin injection rates. Likewise, enhanced mold heat transfer permits faster cure of final products.

e)   Structural Reaction Injection Molding (SRIM)

and Reinforced Reaction Injection Molding(RRIM):

RRIM and SRIM are resin transfer molding processes characterized by curing of the resin during mold filling. RRIM processes usually produce short fiber composites, while SRIM processes involves continuous fiber preforms. The resin used in these processes consists of two parts, which are mixed together just before injection into the mold at very high pressure. Injection occurs at a very high rate. No subsequent curing stage is required since the cure is usually completed when the mold is filled.

1.2.2.6   Stamping

In stamping, a reinforced thermoplastic sheet material is precut to a required size and preheated in an oven. After heating, the sheet is quickly formed into the desired shape in cooler matched-metal dies using conventional stamping presses.

1.2.2.7   Pultrusion

In pultrusion, a combination of liquid thermosetting or thermoplastic resin and continuous fibers is pulled continuously through a heated die of the shape required. The resin is cured or solidified as it exits from the die.

1.2.2.8   Filament Winding

In filament winding, continuous filaments are wound onto a mandrel after passing through a resin bath. The shape of the mandrel is the internal shape of the finished part. The configuration of the winding depends on the relative speed of rotation of the mandrel and the rate of travel of the reinforcement-dispersing mechanism. There are three common windings, helical winding, circumferencial winding and polar winding. In some cases, pre-impregnated filament tows are used, and no in-situ wet resin bath is required.

Among the manufacturing processes described before, injection molding for polymeric products and resin transfer molding for polymeric matrix composites were focused on during the present study. Further discussion specifically related to these processes, leading to the need for the present investigation, appears in the next chapter.

Chapter 2. MOLDING PROCESSES: PRACTICE AND NEEDS

2.1   Advantages of Molding Processes

Injection molding and resin transfer molding both offer a number of advantages, the most outstanding of which is a manufacturing cost reduction compared to other manufacturing processes. A cost comparison of RTM versus sheet molding compound (SMC) compression and IM is presented in Table 2.1.1 [3]. Specific advantages of both injection molding and resin transfer molding are listed in the following sections.

	RTM	SMC Compression	IM
Process operation:			
Production requirement, annual units per press	5,000 -10,000	50,000	50,000
Capital investment	Moderate	High	High
Labor cost	High	Moderate	Moderate
Skill requirement	Considerable	Very low	Lowest
Finishing	Trim flash, etc.	Very little	Very little
Product:			
Complexity	Very complex	Moderate	Greatest
Size	Very large parts	Big flat parts	Moderate
Tolerance	Good	Very good	Very good
Surface appearance	Gel coated	Very good	Very good
Voids / Wrinkles	Occasional	Rarely	Least
Reproducibility	Skill-dependent	Very good	Excellent
Cores / Inserts	Possible	Very difficult	Possible
Material usage:			
Raw material cost	Lowest	Highest	High
Handling / Applying	Skill dependent	Easy	Automatic
Waste	Up to 3 %	Very low	Sprues, runners
Scarp	Skill dependent	Cuts reusable	Low
Reinforcement flexibility	Yes	No	No
Mold:			
Initial cost	Moderate	Very high	Very high
Cycle life	3,000-4.000 parts	Years	Years
Preparation	In factory	Special mold making shop	Special mold making shop
Maintenance	In factory	Special machine shop	Special machine shop

Table 2.1.1   Cost comparison of RTM vs. SMC Compression and IM

19

2.1.1 Advantages of the Injection Molding process

i) Labor Savings

Since injection molding is a high volume process, the labor cost per part is quite low. The machine operator skill requirement for injection molding is also low.

ii) Design / Material Selection Flexibility

Many polymers can be utilized with injection molding. IM allows design possibilities, such as the incorporation of a form core material for strength and weight reduction.

iii) Surface Finish

Both sides of IM products have a high quality finished surface. In addition, various finishing effects can be designed into the mold surface.

iv) Dimensional Tolerances

IM parts can be designed with very tight tolerances (i.e. $\pm$ 0.005 inches).

v) Low voids/wrinkles

The melt during injection molding is subjected to a compression load or vacuum , which is beneficial in that it causes a release of air from the mold.

vi) Part Reproducibility

The tight tolerances characteristics of injection molding provide for excellent reproducibility on a part to part basis.

vii)   Faster Production

The cycle time during injection molding processes depends on the resin system, part size, and many other factors. In general, however, injection molding processes are fast, and with multiple mold cavities more than one part per cycle can be produced.

viii)   Environmental Compliance

Since the process utilizes a closed mold, styrene monomer emission is kept to a minimum. Without ventilation, IM produces less than 10% of the emission of a corresponding hand lay-up process.

ix)   Long mold life cycle

The life cycle of the mold depends on the mold material. The mold is usually made of steel, so that, it has a long life cycle.

2.1.2 Advantages of the Resin Transfer Molding Process

i)   Low Start Up Cost

Equipment, tooling and other start up costs for resin transfer molding are associated with matched die operation. Since RTM is usually a low pressure process, the initial capital equipment expenditure for the process is relatively low.

ii)   Design Flexibility

Many possible resin / fiber combinations can be used with RTM. In addition, the orientation of fiber can be controlled. Also, like injection molding, RTM allows for the incorporation of foam core materials for strength and weight reduction.

iii)   Surface Finish

Both sides of RTM products have a high quality finished surface and various finishing effects can be designed into the mold surface.

iv)   Dimensional Tolerances

RTM parts can be designed with very tight tolerances (i.e. ± 0.005 inches).

v)   Faster Production

RTM production rates depend on resin reactivity, part size, and other factors. In general, however, RTM can produce parts at a rate of 5 to 20 times faster than other conventional composite manufacturing methods (i.e. prepreg / autoclave type).

vi)   Low raw material, cost

RTM material costs the resin system and preform used during product production. While resins and preforms can be expensive, they remain much cheaper than composite prepreg materials.

vii)   Low waste

Resin waste amount during RTM processes are generally less than 3%. The only waste is that the left in the injection system, and that comes out of the vents when the mold is filled.

viii)   Part Reproducibility

Like injection molding, the tight tolerances common to RTM provide for excellent reproducibility on a part to part basis.

ix)   Higher Volume Fraction

RTM allows for fiber volume fractions as high as 70 % while other molding processes allows for volume fractions in the range of 15 to 30%. The higher the volume fraction, the greater the strength of finished parts.

x)   Environmental Compliance

Since the process utilizes a closed mold, styrene monomer emission is kept minimum. Without ventilation, RTM processes produce less than 10% of the emissions of hand lay-up.

The many advantages of injection molding and resin transfer molding processes have led to their worldspread usage. There are various applications of the products made with those processes. These applications for which these processes are commonly used are presented in the following section.

2.2   Application of the Molding Processes

Selected typical products made with injection molding and resin transfer molding processes are listed in Table 2.2. These processes were traditionally used for simple parts where high mechanical strength or high temperature resistance was not required. Today, however, due to the continuous improvement of polymers, the processes are also used for aerospace products [6,7] and automotive structural parts [6]. While injection molding and resin transfer molding processes are widely used, they could be significantly improved. The disadvantages associated with these processes are described in the next section.

Field	IM products	RTM products
Automotive	Urethane bumper Front exterior parts Rear exterior parts Brake reservoir tank Distributor cap Washer tank Radiator grill Instrumental panel	Corvette rear under body, bumper, hood GM pick-up track boxes BMW Z-1 hood and deck Ford Aerostar's chassis cross member Drive shaft Truck cab, fender, hood, door Truck sleeper cab, air deflector
Aerospace	Control surface	Helicopter drive shaft, rotor blades Small missile wing, fin, body Submunition dispenser for Tomahawk missile Propellers Launch tube Fuel tank Access cover and door Control surface
Marine	Control surface	Boat hull Cabin cover Deck Propeller Radar bridge
Construction	Pipe Curtain rods, rail Gutter Wall panel	Column and post Kiosk and booth Sign Grocery display table
Electronics	Fan Refrigerator Air conditioner TV, VCR Cassette deck Micro wave Iron Calculator Cash register Copy machine Type writer Fax	Business machine housing Computer work station Satellite dish antenna
Sports & Leisure (Recreational)	Boomerang Frisbee	Tennis racket Baseball bat Canoe paddle Bicycle frame and handle bar Golf club shaft Kayak Sail board Surf board

Table 2.2   Sample products manufactured by IM and RTM processes

24

2.3 Disadvantages of Molding Processes

The major disadvantages of both IM and RTM processes are associated with the understanding and control of resin flow dynamics, solidification and cure kinetics. Poor curing or solidification causes the potential failure of products, and undesired flow progression can cause both air entrapment within finished parts and the formation of weld lines in inappropriate areas. For the time being, production practice with molding processes has been mostly developed by a traditional trial-and-error scheme. This process is usually done by varying the injection rates, the temperature of resin injected, the cure cycle, the mold temperature, the cooling cycle, the resin inlet location, the number of inlets, the number of vents, the location of vents, and the resin system. Although it often leads to success, the trial-and-error technique does not guarantee the manufacturing of products with desired quality. In addition, even when successful, it is very costly and time consuming. As can be seen in Table 2.1.1, the initial cost and the raw material cost are high for IM and the labor cost is high for RTM. These costs can be reduced by eliminating the trial-and-error method without loss of product quality. In pursuit of this goal, computer simulation models for these processes have been developed in order to facilitate the designing of new products. At present, these process models are good but they are not good enough to eliminate the trial-and-error process development methodology. What is needed an intelligent manufacturing methodology that involves the sensing of product quality during manufacturing and the real-time adjustment of processing conditions of optimize quality.

2.4. Present Investigation Objective

Figure 2.4.1 shows an intelligent manufacturing scenario for improved process cycle development through the incorporation of in-situ product quality monitoring and process condition adjustment during production. For any specific class of processes, the realization of intelligent processing requires that both knowledge-based process condition modification and product quality monitoring subsystems be developed. Process condition modification tools can be based on either experiential knowledge or knowledge obtained from process models. While such tools are being investigated as part of the current effort, they are not the subject of this particular study. The present study focused on the development of a product quality monitoring subsystem specifically applicable to molding processes such as injection molding (IM) and resin transfer molding (RTM). With such processes, there is a need to monitor both flow conditions and material rheological properties within closed molds during manufacturing.
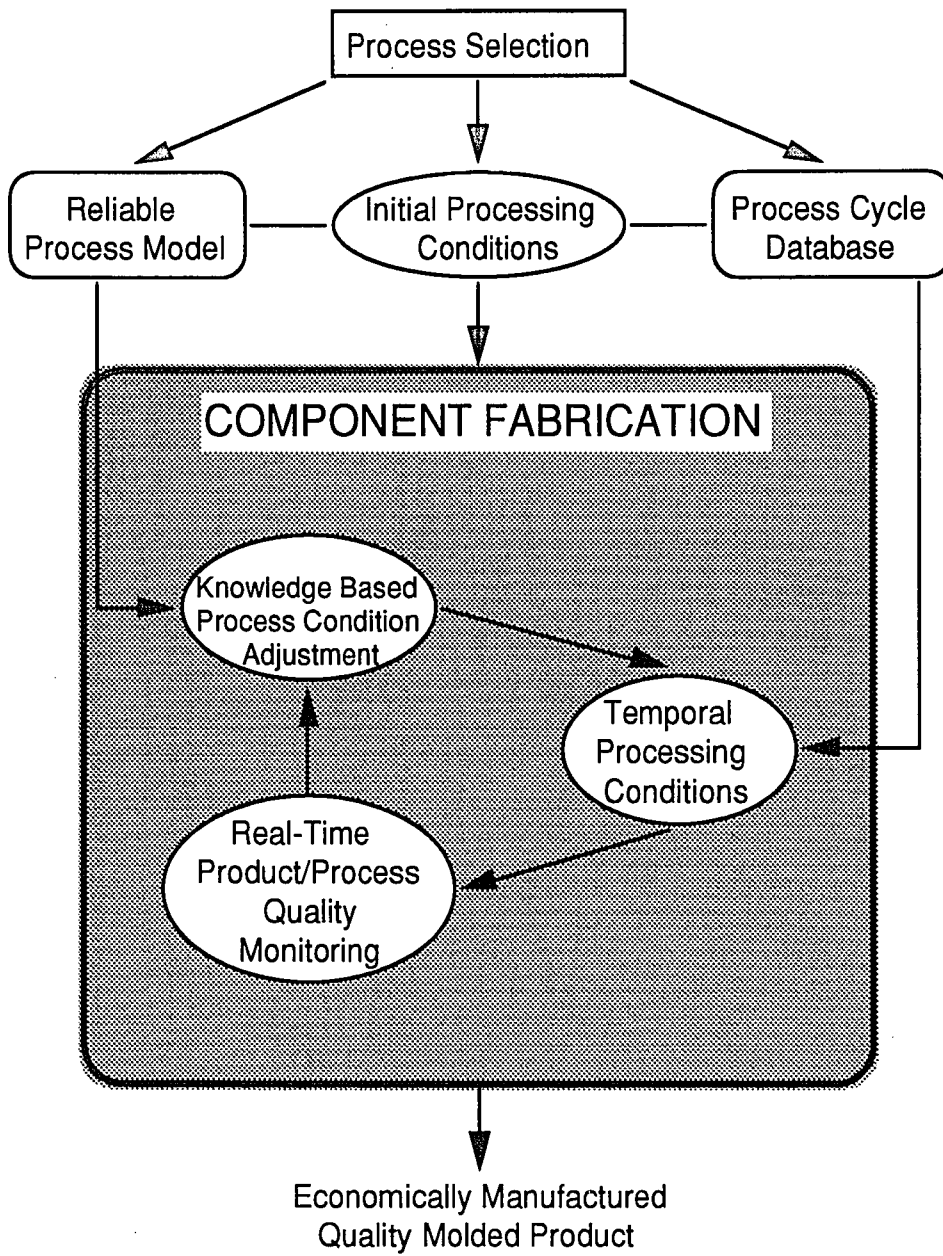
Figure 2.4.1: A diagram of a generic intelligent manufacturing concept

Chapter 3. REVIEW OF SENSING TECHNIQUES

Sensor subsystems for these molding processes must sense one, or all of the important molding process variables below:

- o   Pressure distribution
- o   Temperature distribution
- o   Degree of cure / Change of viscosity
- o   Flow front progression

During molding processes, the temporal progression of flow is extremely important. In addition, the degree of cure (for thermosets) or the change of viscosity (for thermoplastics) are also critical factors. These factors, which affect the quality of finished parts, are affected by molding process conditions.

The sensor types appropriate for molding process can be categorized into two classes, distributed sensors and point sensors. Distributed sensors can sense at multiple locations while point sensors can monitor conditions only where the sensor is placed. There are also two approaches for the utilization of sensors. The embedded approach utilizes sensors that remains in the part after fabrication, while the non-embedded approach involves sensors that are reusable. Overall, a useful sensor subsystem should be inexpensive, durable, as simple as possible, and capable of real-time process monitoring. In the following sections, existing and potential sensing methodologies applicable to molding processes are discussed.

3.1   Previous Molding Process Monitoring Investigation

In this section, the sensing methodologies actually used for monitoring one or more of the important process variables during molding are described. Sensing methodologies have been used for the measurement of pressure distribution, degree of cure and/or flow front location. Both non-embedded sensors and embedded sensors have been applied. The non-embedded sensors have for the most part been used for the verification of molding process models. Embedded sensors, on the other hand, have been utilized to develop monitoring systems for the intelligent manufacturing. Embedded sensors have also been used to determine preform permeabilities for RTM processes.

3.1.1 Non-Embedded Sensors

3.1.1.1   Video camera / Camera:

Cameras and the video cameras have been used to visualize and record resin flow during molding processes. A primary goal in these case was the verification of the process simulation models. Visualization was made possible through the usage of transparent mold. These sensing methods can not be used with real molding processes because of the high temperatures and processes typically involved.

3.1.1.2   Photovoltaic / Photoelectric sensors :

Photovoltaic sensors have been used during molding processes to measure the velocity of the flow front. The photoelectric sensor is a system composed of a light transmitter and light receiver. The light is directed to the object by the transmitter which is usually a light emitting diode (LED). The receiver is a cadmium sulfide cell that allows

current to flow and energize a relay when reflected light originating from the transmitter is detected. The resulting signal from photoelectric sensors is often modified with time logic, scaling, or offset adjustments prior to output. There are two ways of sensing using this methodology. One is thru-beam sensing and the other is reflex sensing as shown in Figure 3.1.1.

The features of thru-beam sensing include wide optical range, high possible signal strength, high light / dark contrast ratio, little effect of surface color and reflectivity and good trip-point repeatability. The limitations include the requirements of two components passing through the detection zone and, difficult alignment. The features of reflex sensing are that it has long optical range, high light / dark contrast ratio, little effect of surface color and reflectivity, and easy installation and alignment. The limitation of reflex sensing is that it can be falsely triggered by mirrorlike objects unless polarized optics are used.
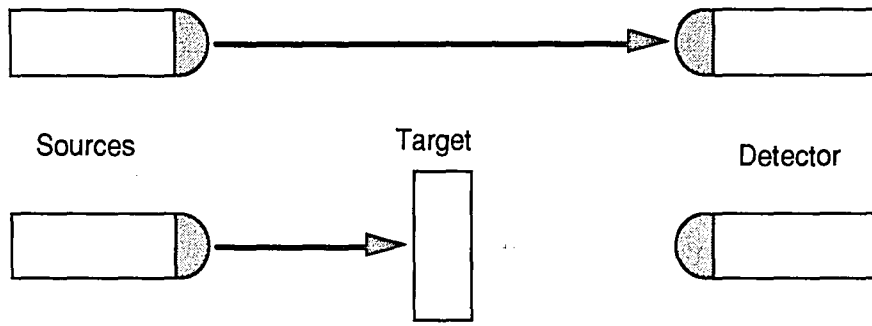
(a) Thru-Beam Sensor Configuration
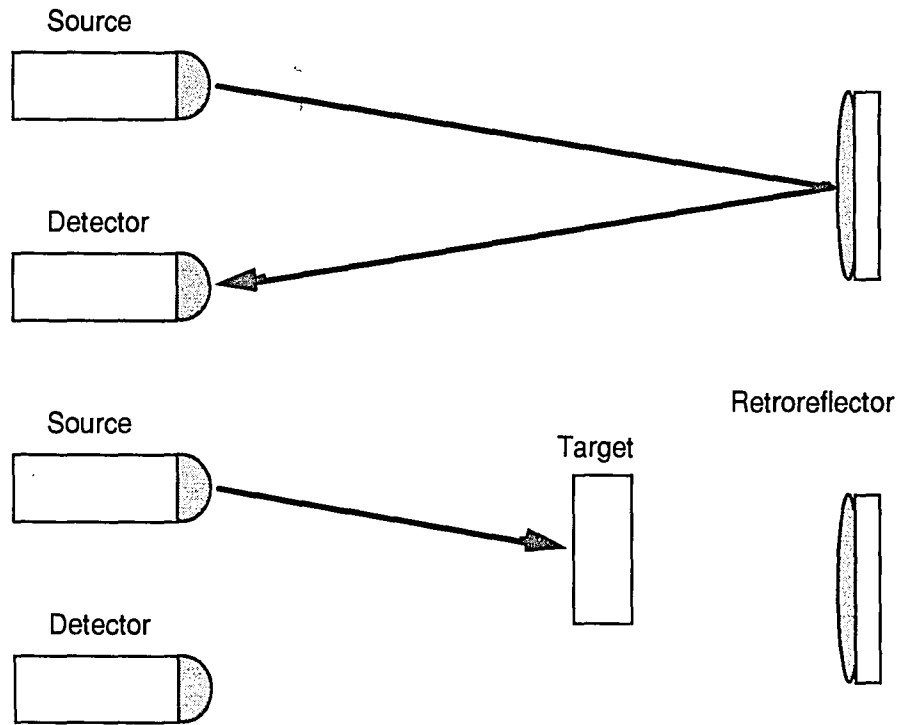
(b) Reflex Sensor Configuration

Figure 3.1.1:   Photoelectric sensor configurations.

3.1.1.3   Pressure Transducers:

Pressure transducers have been used with RTM processes to obtain the pressure difference between two points for the measurement of permeability and to obtain the pressure distribution within a closed mold.   Preform permeability is a critical factor in RTM processing, as it significantly affects flow front progression. The permeability for a two dimensional impregnation flow can be obtained by using "Darcy's law" which is as follows:

$$\frac{\partial P}{\partial x} + \frac{\mu}{K_x}\bar{u} = 0 \qquad\qquad (3.1.1)$$

$$\frac{\partial P}{\partial y} + \frac{\mu}{K_y}\bar{v} = 0 \qquad\qquad (3.1.2)$$

In these equations, K_x, K_y are the permeabilities in x - and y - directions, respectively, ∂P is the pressure difference between two different locations, $\partial x, \partial y$ are the distances between the two points where the pressure is measured, μ is the resin viscosity, and $\bar{u}, \bar{v}$ are the mean velocities of the resin flow in the x - and y - directions, respectively. The pressure sensing methodology is mostly used to obtain permeability values.   It can, however, also be used to sense both pressure distribution and flow front locations by monitoring the change of pressure at each sensor location when resin replaces air.

3.1.2 Embedded Sensors

3.1.2.1   Dielectric sensors:

Dielectric sensors were originally used for molding processes by Kranbuehl et al [9-11]. These sensors are based on resin dielectric properties which change as a function of viscosity and/or degree of cure. Dielectric sensors have been used to monitor changes in resin viscosity during cure processes. They can also be used to sense flow front location since the electrical properties of resin differs from those of air. Measurements have been made of capacitance, C, and of conductance, G. The capacitance, C, is the amount of charge for a given voltage defined as follows:

$$C = \frac{q}{V} \qquad (3.1.3)$$

where q is the total charge of either conductor and V is the potential difference between conductors. The capacitance is a function of physical dimensions of a system and permittivity of the dielectric (dielectric constant). Once obtained, the capacitance and conductance can be used to calculate the complex permittivity, ε^*, defined as follows:

$$\varepsilon^* = \varepsilon' - i\varepsilon'' \qquad (3.1.4)$$

where ε' and ε'' are as follows:

$$\varepsilon' = \frac{C_{mat}}{C_0} \qquad (3.1.5)$$

33

$$\varepsilon'' = \frac{G_{mat}}{C_0 2\pi f} \qquad (3.1.6)$$

In the above relations, C_0 is the air filled replaceable capacitance of the measuring cell, C_{mat} is the capacitance of the resin to be measured, G_{mat} is the conductance of the resin to be measured and f is the frequency. Also, both the real and imaginary part of the complex permittivity have a dipolar and an ionic component as follows:

$$\varepsilon' = \varepsilon'_d + \varepsilon'_i \qquad (3.1.7)$$

$$\varepsilon'' = \varepsilon''_d + \varepsilon''_i \qquad (3.1.8)$$

where $\varepsilon'_d, \varepsilon''_d$ are the dipolar components, $\varepsilon'_i, \varepsilon''_i$ are the ionic components. The dipolar component comes from molecular dipole moments. The polar component, depending on the frequency, is defined by the Cole-Davidson function as follows:

$$\varepsilon^* = \varepsilon_\infty + \frac{\varepsilon_0 - \varepsilon_\infty}{(1 + i\omega\tau)^\beta} \qquad (3.1.9)$$

where ε_0 and ε_∞ are the lowest and highest frequency values of ε, τ is a characteristic relaxation time and β is a parameter which relates to the relaxation times. The dipolar term is usually the main component of the dielectric signal at high frequency or for highly viscous media.

The ionic component, ε_i^*, often dominates ε^* at low frequencies, low viscosities or higher temperatures. The presence of mobile ions gives rise to localized layers of charge near the electrodes. Since these space charge layers are very small molecular

distances on the order of A^o, the corresponding space charge capacitance can become extremely large, with ε' on the order of 10^6. Johnson and Cole derived empirical equations for the ionic contribution to ε^*. In their equations, these space charge ionic effects have the form as follows:

$$\varepsilon'_I = C_0 Z_0 \sin\frac{n\pi}{2} \omega^{-(n+1)} \left(\frac{\alpha}{8.85 \times 10^{-14}}\right)^2 \qquad (3.1.10)$$

The electrode impedance induced by the ions, Z^*, with n between 0 and 1 is defined as follows:

$$Z^* = Z_0 (i\omega)^{-n} \qquad (3.1.11)$$

The ionic component of the imaginary part of the complex permittivity is defined as follows:

$$\varepsilon''_0 = \frac{\sigma}{8.85 \times 10^{-14} \omega} C_0 Z_0 \cos\frac{n\pi}{2} \omega^{-(n+1)} \left(\frac{\sigma}{8.85 \times 10^{-14}}\right)^2 \qquad (3.1.12)$$

where σ is the conductivity. The first term in equation 3.1.12 is due to the conductance of ions translating through the medium. The second term, electrode polarization, makes dielectric measurements increasingly difficult to interpret and use as the frequency of measurement becomes lower. The ionic parameter, σ, and the dipolar parameter, τ, are directly related on a molecular level to the rate of ionic translational diffusion and dipolar rotational mobility which directly relate to the viscosity of resin.

3.1.2.2   Frequency Dependent ElectroMagnetic Sensors (FDEMS):

This sensing methodology was recently developed by the Dek Dyne [12-17]. The technique is based on the dielectric sensing methodology, and focuses on the frequency applied to the sensing system. This is because the frequency directly affects the dipolar term which is the major part of the dielectric signal at high frequencies and in highly viscous media. The dipolar parameter or dipolar relaxation time, τ, is defined as follows:

$$\tau = \frac{1}{\omega} \tag{3.1.13}$$

where $\qquad\qquad \omega = 2\pi f \tag{3.1.14}$

The dipolar relaxation time is used to determine the state of the cure process. A particular relaxation time, τ, occurs at the time and temperature when the dipolar term, ε''_d, in equation 3.1.8 is a maximum at corresponding frequency peaks. This sensor is distinguished from the ordinary dielectric sensor as it is an inert, disposable, planar, and geometrically independent microsensor system. The sensor consists of two interdigitated comb electrodes. It is intended for the monitoring of cure including reaction onset, point of and magnitude of maximum flow, fluidity, solvent evolution, buildup in modulus, approach to T_g, reaction completion, and degradation.

3.1.2.3   Sensors Mounted As Roving Thread (S.M.A.R.T.) weave:

This sensing technique was originally investigated at the U.S. Army Materials Technology Laboratory [18]. Figure 3.1.2 shows the schematic concept of the methodology, which involves the creation of a sensing grid between the layers of fiber reinforcement. These sensing grids are made of electrically conductive fibers in an

orthogonally non-intersecting manner. The system senses the presence of the resin as it advances through the reinforcement as shown in Figure 3.1.3 for RTM. All sensing circuits are initially open, and indivdual circuits are closed as the resin fills each sensing gap. When this occurs, current flows through the circuit, and the signal at that particular location differs from the one before the resin filled the gap.

Electrically conductive fibers
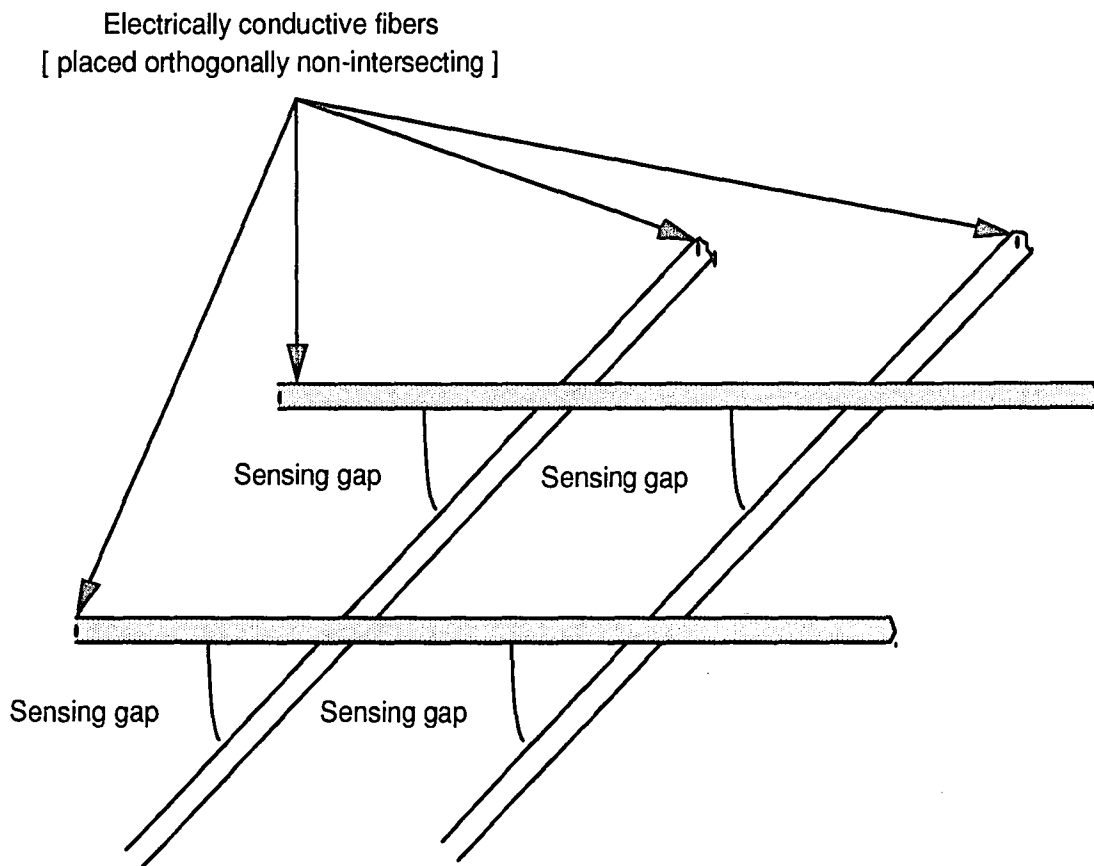[placed orthogonally non-intersecting]

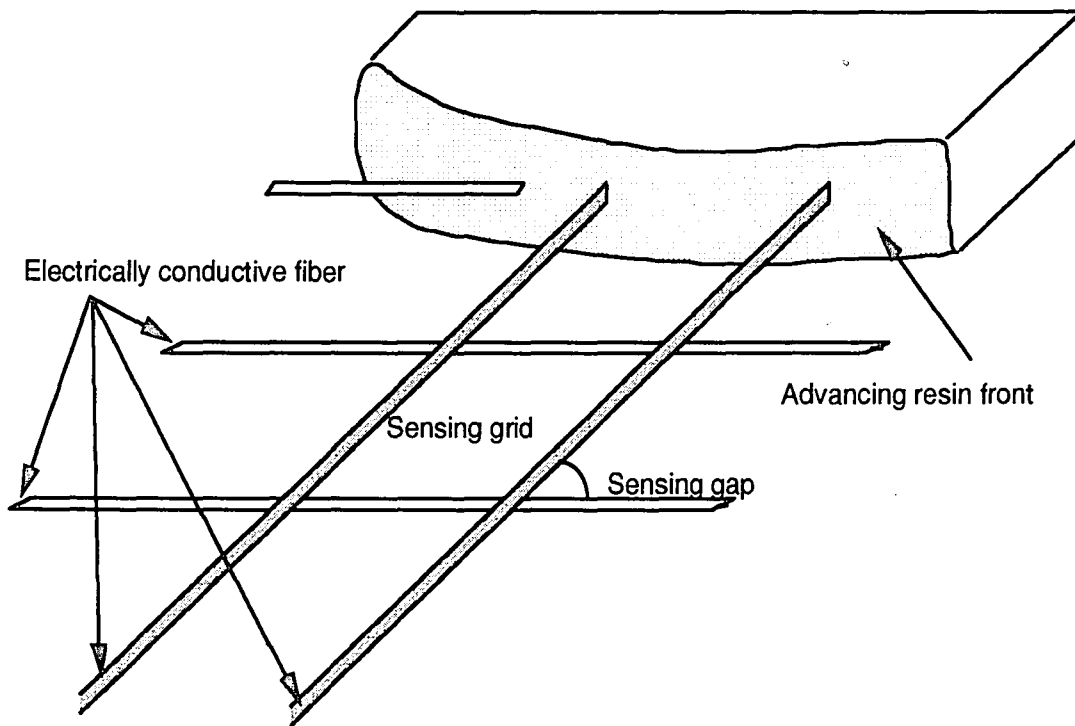Figure 3.1.2: Creation of sensing gap

Figure 3.1.3:   How S.M.A.R.T. weave senses

The overall system set-up is shown in Figure 3.1.4. One end of a fiber (i.e. longitudinal direction) is connected to a positive side of a multiplexer which is a rapid switching system including a power supply, and one end of the other fiber (i.e. horizontal direction) is grounded to the multiplexer. The multiplexer is then connected to a computer for conditioning and presentation of data.
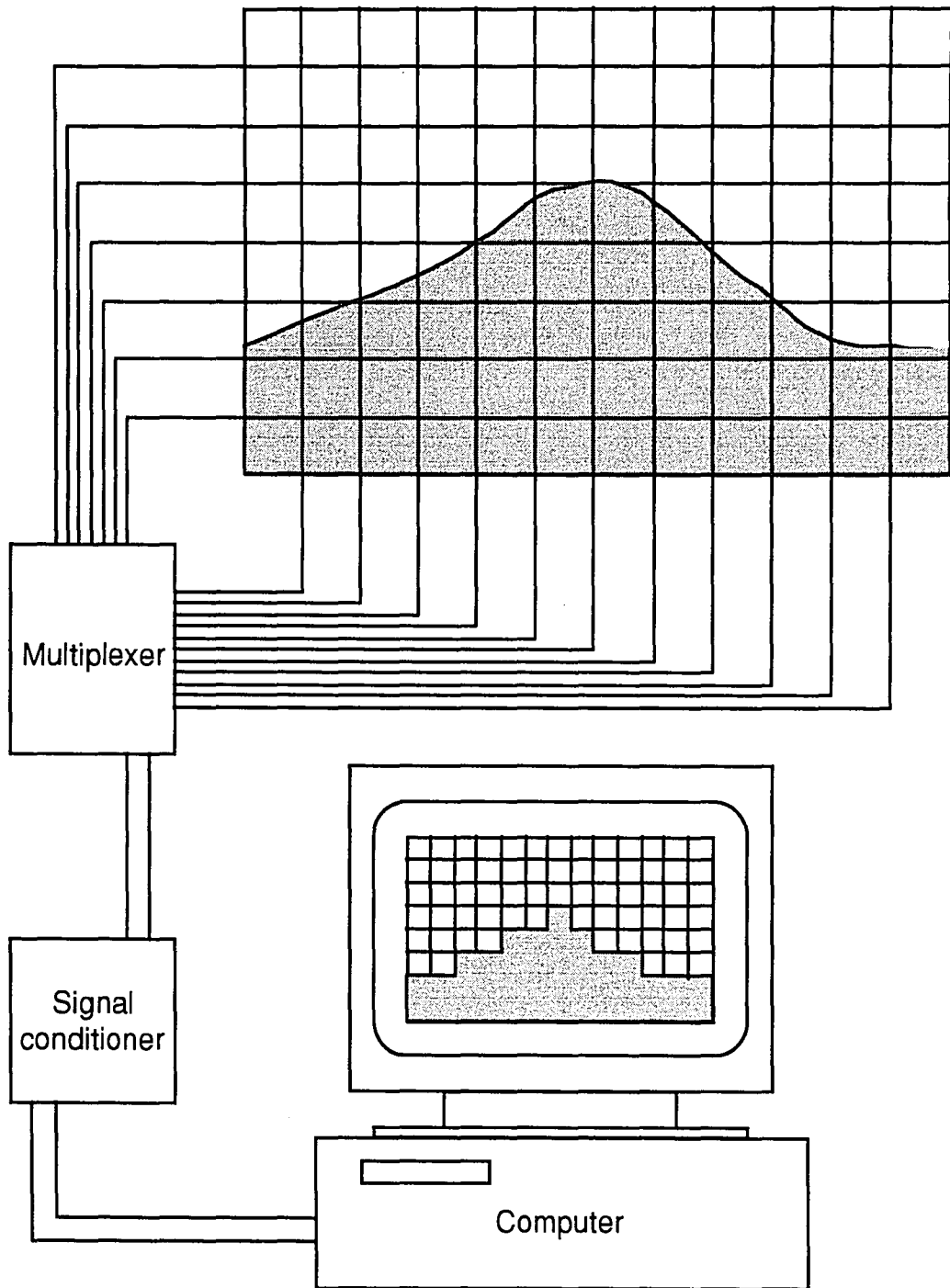
38

Figure 3.1.4: Schematic of S.M.A.R.T. weave set-up

3.2 Possible Sensor Candidates

The sensing methodologies discussed in the following sections have the potential usage as sensors for molding processes. In the case of optical fibers, they are already experimentally used as embedded stress/strain sensors for FRP products, such as air-plane wings. Optical fibers, therefore, can possibly be used as sensors to monitor both the manufacturing process and the lifelong condition and health of finished parts.

3.2.1 Non-Embedded Sensors

3.2.1.1   Infrared (IR) thermometer / Infrared (IR) sensors:

Infrared energy is that which lies in the segment of the spectrum which ranges from 1μm to 1mm in wavelength , as seen in Figure 3.2.1. An IR thermometer scans the energy in this region to evaluate the variation of intensity of infrared radiation. Any warm object emits energy in the infrared range due to thermal emissivity. Thermal emissivity is very critical to infrared thermometers since the thermal emissivity is defined as the ratio of the energy radiated by an object at a given temperature to the energy emitted by a perfect radiator or a black body at the same temperature. The thermal emissivity of a black body is 1.0, and that of most organic substances (i.e. wood, cloth, plastic, etc.) are approximately 0.95. Most rough or printed surfaces also have fairly high emissivity. The higher the emissivity, the easier it is to obtain accurate data with IR sensing. In the case of molding processes, an IR based technique could be used to monitor flow front location since the resin injected into mold is usually at high temperature and emits IR radiation. Because IR technique monitor surface temperatures, however, the somewhat complicated three-dimensional heat transfer through the mold would have to be taken into account. IR

sensors could also possibly be used for the measurement of internal temperature distributions during molding.

Infrared sensing technique have previously been used on many occasions. For example, Iris Fiber Optics of Acron, Mass. [19], has developed an IR based sensing instrument for the monitoring of multicomponent gas flows. Also, Stinson at the University of Washington, Seattle [19] has discovered a way to determine gasoline octane numbers from sensed IR spectra. IR techniques have been used for the measurement of the orientation of semicrystalline polymers [20]. In this case IR techniques have been found to be superior to other methods since crystalline polymer samples thick enough to be opaque at visible wavelengths can be investigated.
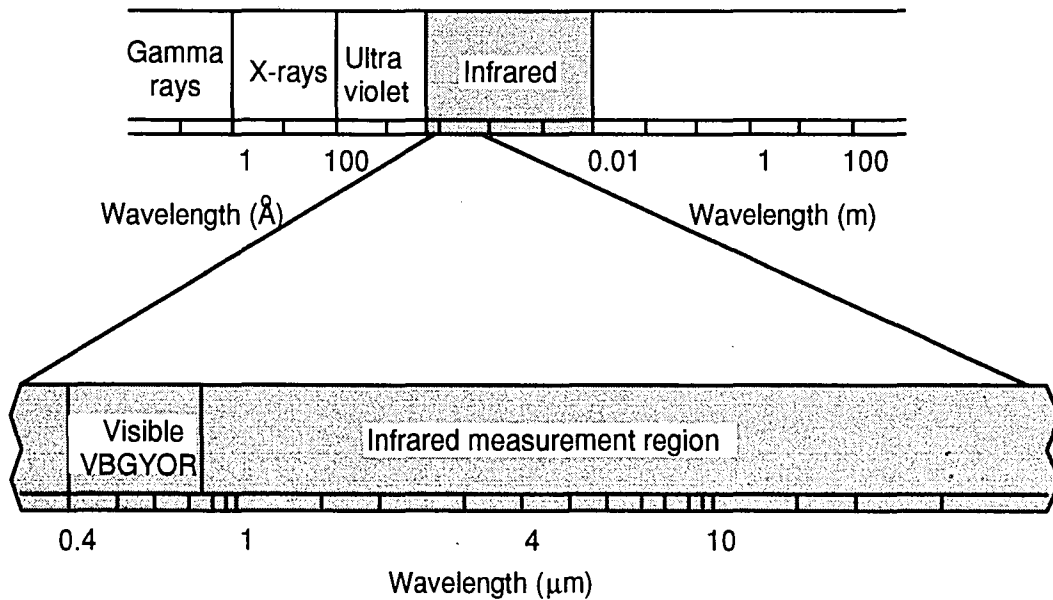
Figure 3.2.1:   Bar chart of electromagnetic spectrum

3.2.1.2   Thermochromic Liquid Crystal (TLC) films [21]:

TLC films are thin films which react to changes in temperature by changing color. TLC sensors are currently used as a thermometers for measuring air and human body temperature. The color changes of TLC films occur as a result of changes in the reflection of incident white light. TLC materials change from colorless, usually black against black background to red at a critical temperature. They, then, exhibit other color changes in the visible spectrum in sequence (orange, yellow, green, blue, violet) as the temperature increases. These color changes are totally reversible. and the color changes sequence on cooling is reversed. Readily available TLC films have an operating temperature range of -30° C (-22° F) to 115° C (239° F). Some TLC materials, however, can operate at temperature as high as 250° C (484° F). TLC films could potentially be applied to molding by placing the films onto the surface of a mold and monitoring color changes which would occur during mold filling. To successfully do this, however, three-dimensional heat transfer through the mold would have to be taken into account.

3.2.2 Embedded Sensors

3.2.2.1   Fiber optics:

During the past few years, fiber optic sensors have undergone a period of rapid development. Various types of fiber optic sensors have been used to monitor temperature, strain, pressure, and many of other environmental parameters [22]. Fiber optic sensors were initially developed for high-performance military applications, but today they are increasingly used for civil purposes.

An optical fiber is constructed from dielectric materials and is a thin strand of material composed of an inner core and an outer cladding. An additional other coating is

often included to provide mechanical and environmental protection. The core and claddings are composed of glass or plastic, with the core having a higher refraction index than the cladding. A typical diameter for optical fibers is 0.005 cm (0.002 in.), as shown in Figure 3.2.2.
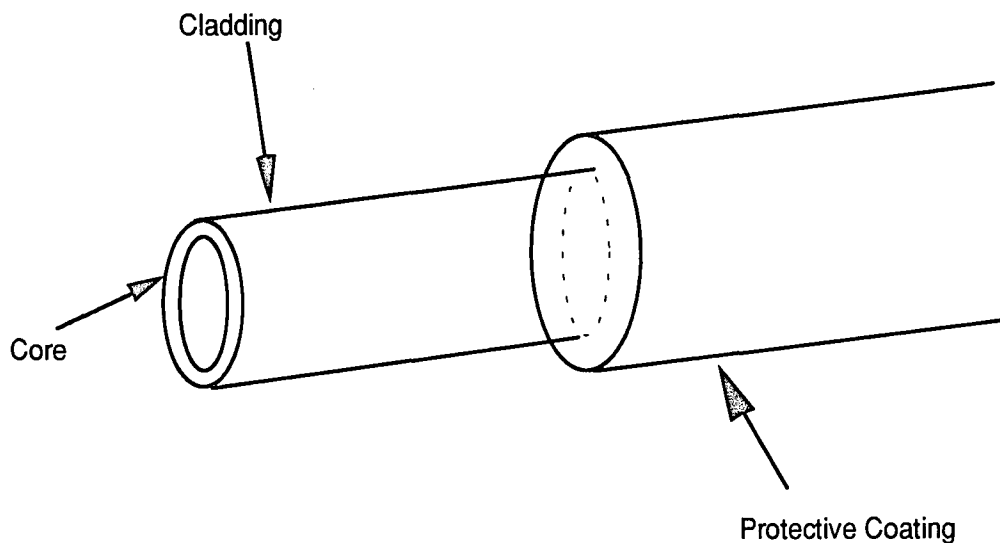

Figure 3.2.2: Typical optical fiber configuration

Optical fibers are free from electromagnetic interference and versatile since the optical beam is characterized by a large number of parameters, such as intensity, wavelength, spectrum, phase and polarization. The types of currently available fibers are divided into three types as follows [23]:

o   Multimode step-index fiber

o   Multimode graded-index fiber

o   Single mode fiber

There are two sub-classifications utilized with the optical fibers stated above, intrinsic and extrinsic. When the light remains within the fiber, the sensor is called an intrinsic sensor. Extrinsic sensor, therefore, are those in which a portion of the transmitted light beams the fiber. The sensing methods used with optical fibers are as follows:

i)   Fiber Optic Sensor alone [23-28]

ii)   Fiber optics with Optical Time Domain Reflectometry (OTDR) [29]

Both sensing methods are somewhat complicated and costly since a light source and photo detector are required. In addition, optical fibers are brittle and can be damaged easily.

i) Fiber Optic Sensors alone:

i-i)   Reflective extrinsic sensors:

Reflective extrinsic sensors are used as position sensing devices. When these sensors are applied the intensity of the detected light depends on how far a reflecting target is from the end of the fiber-optic probe.

i-ii)   Transmissive extrinsic sensors:

Transmissive extrinsic sensors are used to sense pressure, the absence of objects, and flow. They consist of two cables directed at each other as shown in Figure 3.2.3, one the transmitter and the other the detector. When the beam of light between the two fibers is broken by an object passing through or by bending due to flow, a corresponding electrical circuit is either activated or deactivated to relay a digital message.
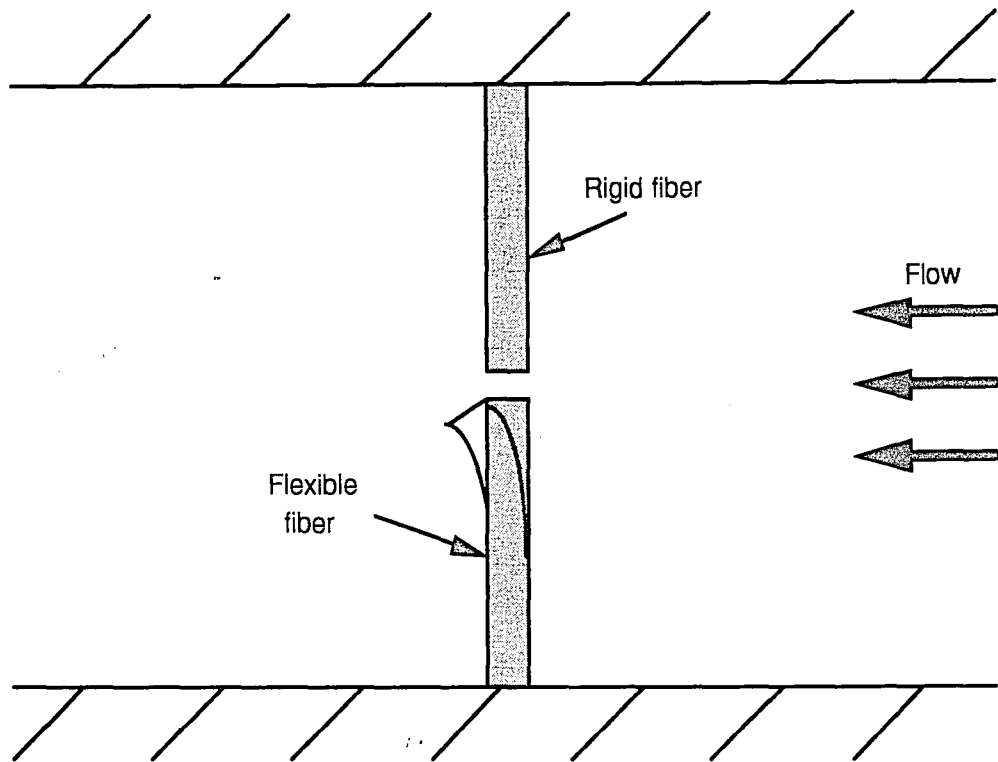
Figure 3.2.3:   Flow measurement scheme with the transmissive fiber

i-iii)   Intrinsic microbending sensors:

Intrinsic microbending sensors are used to measure pressure or stress. An example sensor is shown in Figure 3.2.4. When the fiber is bent, small amounts of light are lost through the cladding of the fiber. When pressure is applied to the microbender, it bends the fiber, so that light is lost through the cladding and not internally reflected. When the light is lost through the cladding with either conditions mentioned above, then the amount of received light is related to the value of the physical property being measured.
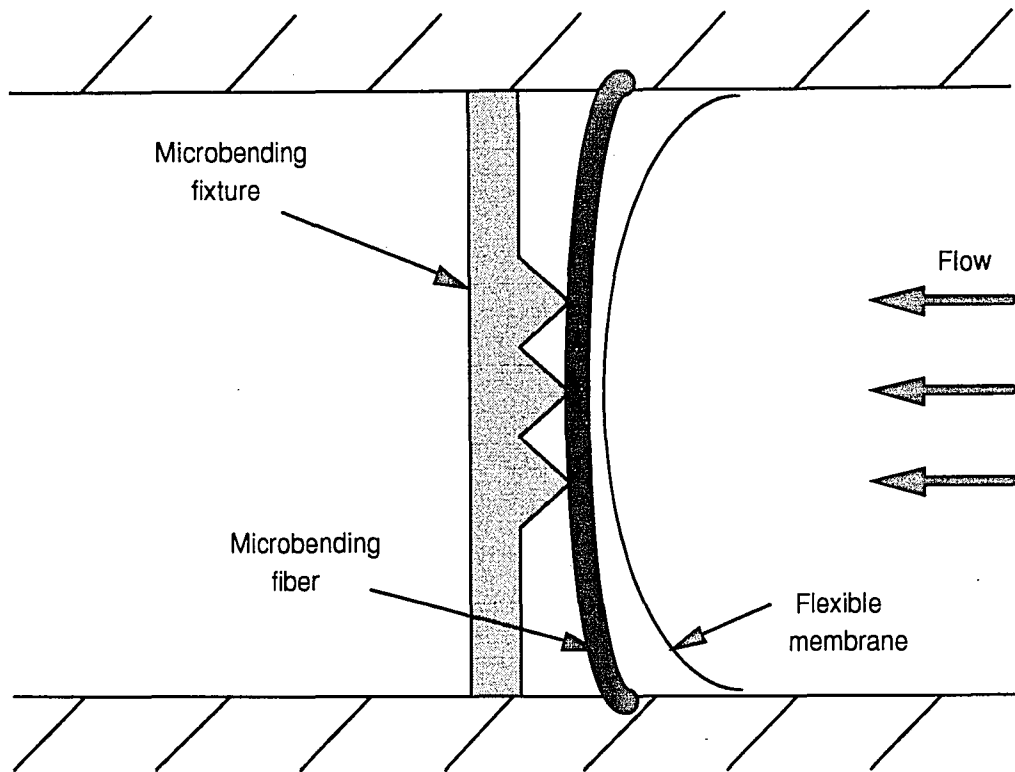
Figure 3.2.4:   Intrinsic microbending sensor scheme

i-iv)   Interferometer:

An interferometer is very a sensitive intrinsic type of sensor, and its application is in environmental sensing such as temperature and more recently in fiber optic gyroscopes. The sensor has a reference leg and a leg which is exposed to the environment to be sensed as shown in Figure 3.2.5. A laser beam is split and launched into both legs. The beams are then allowed to recombine. However, since the sensing fiber has had changes in its index of refraction and length due to environmental effects which alter the light transmission in the fiber, a phase shift occurs and the detected signal is modulated in relation to the reference fiber beam. This is detected and quantified by associated signal processing hardware.
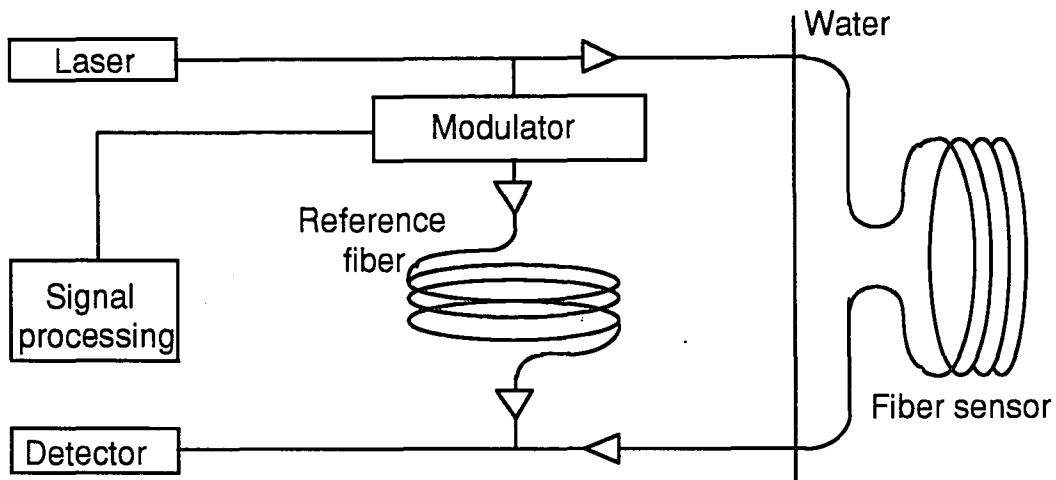
Figure 3.2.5: Fiber optic interferometer scheme

ii) Fiber optics with Optical Time Domain Reflectometry (OTDR):

The OTDR technique was originally developed by Barnoski and Jensen [29] about fifteen years ago. They coupled a pulsed GaAs injection laser with a glass fiber, and obtained its attenuation characteristics by analyzing the time dependence of the detected Rayleigh backscattered light generated by the system as shown in Figure 3.2.6. OTDR is used for the single-ended characterization of optical fiber cables. The reflectometry technique is used for testing long and short haul fiberlinks. It can locate faults by probing a fiber with optical pulses and timing the arrival of reflected and backscattered light. The concept of this generic system is based on Barnoski and Jensen's idea as shown in Figure 3.2.7.
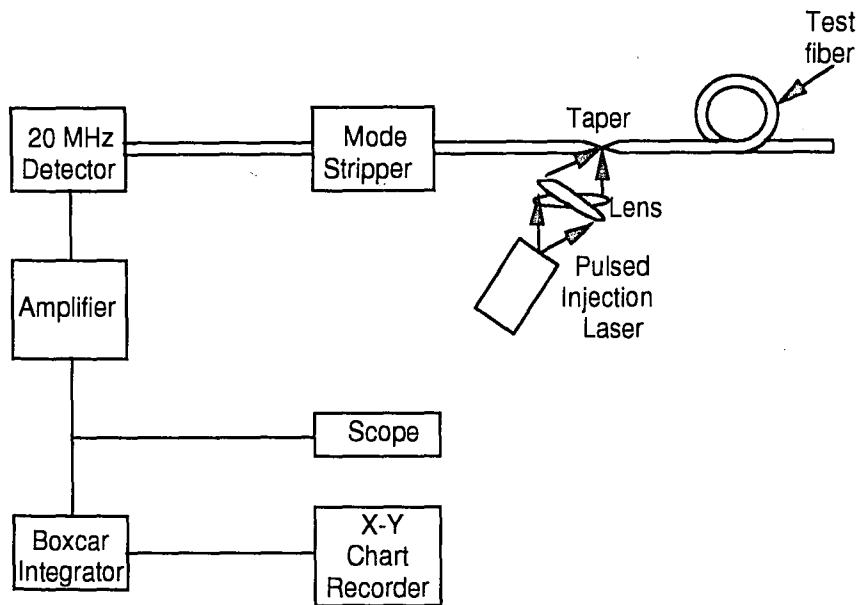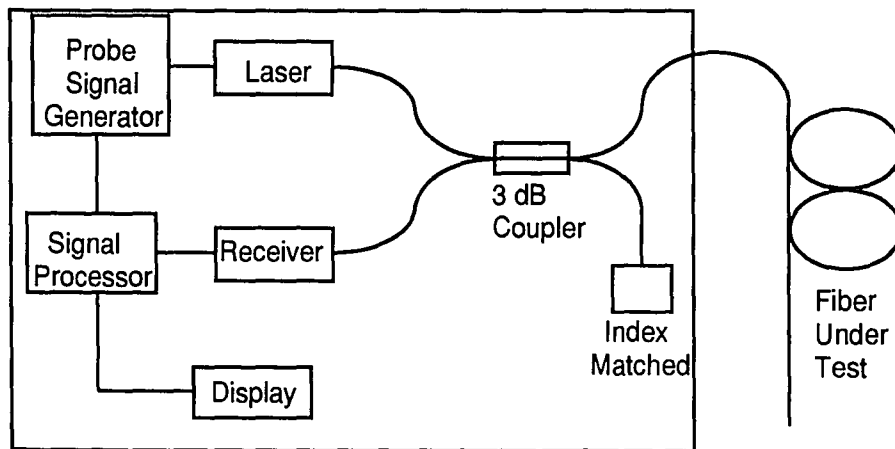
Figure 3.2.6:   First OTDR by Barnoski and Jensen

Figure 3.2.7:   Generic OTDR system diagram

For the OTDR system to work, an electrical probe signal (usually a square pulse) is used to drive a semiconductor laser source, and the resulting optical probe signal is coupled into the fiber under test by a beamsplitter or directional coupler. The splitter couples the backscattered and backreflected light from the fiber under test to a receiver and obtained backreflected light is the received signal. It is known as Rayleigh backscattered power, P_b, and defined as follows:

$$P_b = \frac{P_0 S \alpha_s W \upsilon}{2} e^{-2\alpha \frac{\upsilon t}{2}} \qquad (3.2.1)$$

where P_0 is the optical pulse of peak power, W is the optical pulse of width ($<<2 / \alpha \upsilon$), S is the recapture ratio of the Rayleigh scattered power back into the fiber, α_s is the power attenuation coefficient due to Rayleigh scattering, ($\upsilon t / 2$) is the cumulative attenuation up to a distance (in nepers) and V is the light velocity in the fiber. The exponential term in equation 3.2.1 implies the attenuation characteristics of the fiber. Time, t , corresponds to the location, l , in the fiber as follows:

$$l = \frac{\upsilon t}{2} \qquad (3.2.2)$$

Also, the received signals are processed (usually by a large amount of averaging and the correlation) before displaying. A typical signal before and after processing is shown in Figure 3.2.8. The big kick-up in the figure is the fault. The faults are caused by the qualification of losses at bad splices, faulty connectors, sharp bends or breaks. They can be obtained from the changes in the level of Rayleigh backscattering, which is the dominant loss mechanism in optical fiber, and it is displayed. The display shows the

49

slope of the signals on either side of a given discontinuity, and it provides a measure of the propagation loss of the respective fibers.

In this chapter, previously used and potential sensing methodologies applicable to molding processes were discussed. A modified and improved version of the embedded electronic fiber based methodology was selected for use during the present study. This selected methodology is described in the next chapter.
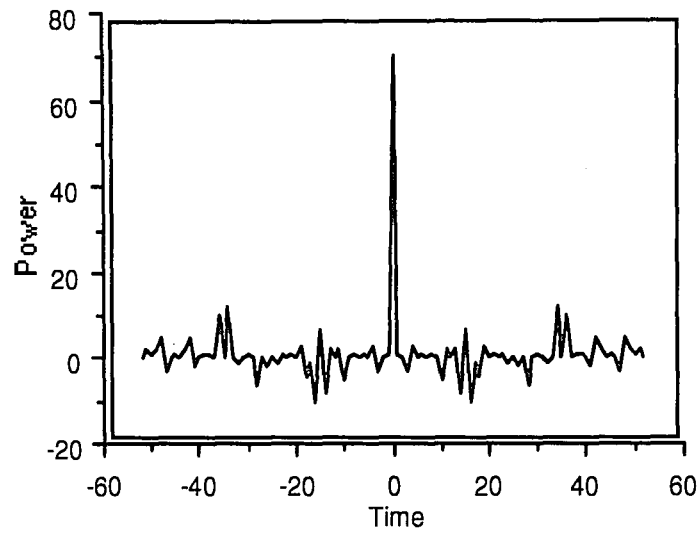
(a) before processing
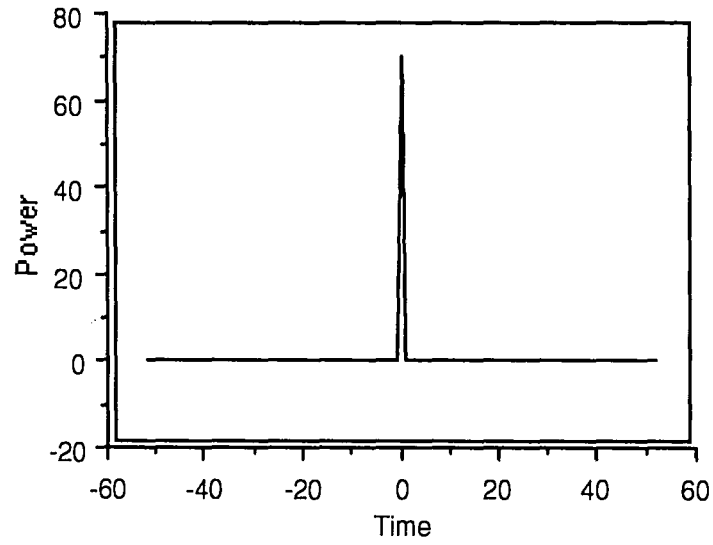
(b) after processing

Figure 3.2.8:   Signals received before and after processing

51

Chapter 4. EMBEDDED ELECTRONIC MOLDING PROCESS SENSORS: CONCEPT & THEORY

4.1 CONCEPT

The embedded electronic sensor concept is based on embedding electrically conductive fibers into opposing inner surface of the mold cavity in an orthogonally non-intersecting manner. When this is done, sensing gaps such as shown in Figure 4.1 are created.

Electrically conductive fibers
[placed orthogonally non-intersecting]

Sensing gap   Sensing gap
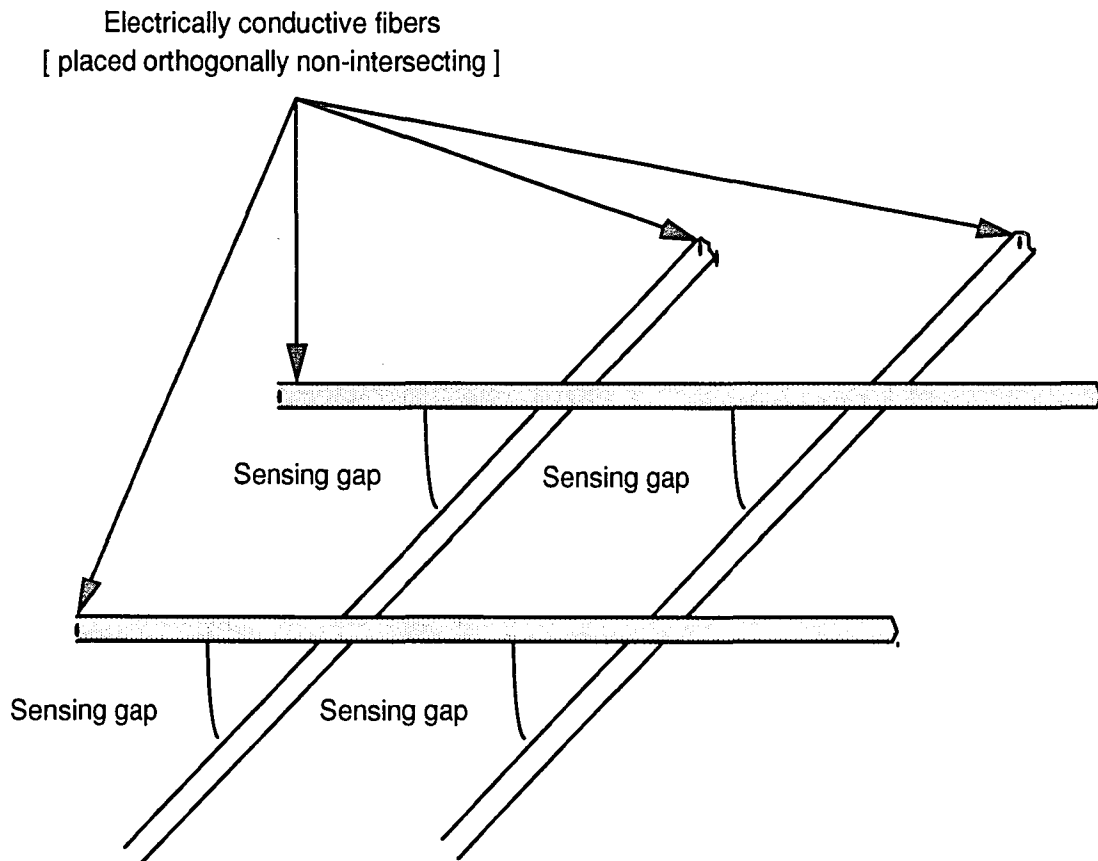
Sensing gap   Sensing gap

Figure 4.1:   Sensing gaps utilized with the selected approach

These sensing gaps act as individual sensing nodes of the present methodology. The basic idea of the embedded electronic sensor technique is to obtain the response from these nodes and the variation of response signal as resin flow front advances through the sensing gaps. When the mold is in its initial unfilled condition, open electrical circuits exist between all inner-layer wire pairs. When a material with some degree of conductivity enters a sensing gap, an electrical circuit is completed by the addition of the finite electrical resistance associated with the material. The monitoring of resistance at each sensing gap in a mold, therefore, can lead to the determination of the temporal resin flow front progression. Furthermore, the spatial and temporal rheological resin characteristics, such as viscosity and degree of cure could also be monitored since material's volumetric resistivity changes with rheological condition. Even though rheological condition measurements are possible, the present investigation focused on resin flow front progression monitoring only. All rheological characteristics were assumed to remain constant throughout the filling processes.

The basic embedded electronic sensor concept has been previously implemented by Walsh [18]. He has utilized an extremely sensitive electrometer to measure the actual resistance, which for many thermosetting polymers ranges from 10^{10} to $10^{15} \, \Omega$, across each node junction of the sensing grid. Walsh's original method was found to be effective, but required a significant amount of time for in-situ electrometer reading stabilization. Additionally, the cost associated with a high quality electrometer is quite large. Due to these reasons, a modified version of the basic sensing concept was implemented during the present study which eliminated the need for an electrometer and decreased the number of discrete measurements required to locate an advancing resin front. The modified sensing approach is based on the usage of an array of aligned one-dimensional sensing circuits, an example of which is shown in Figure 4.2.
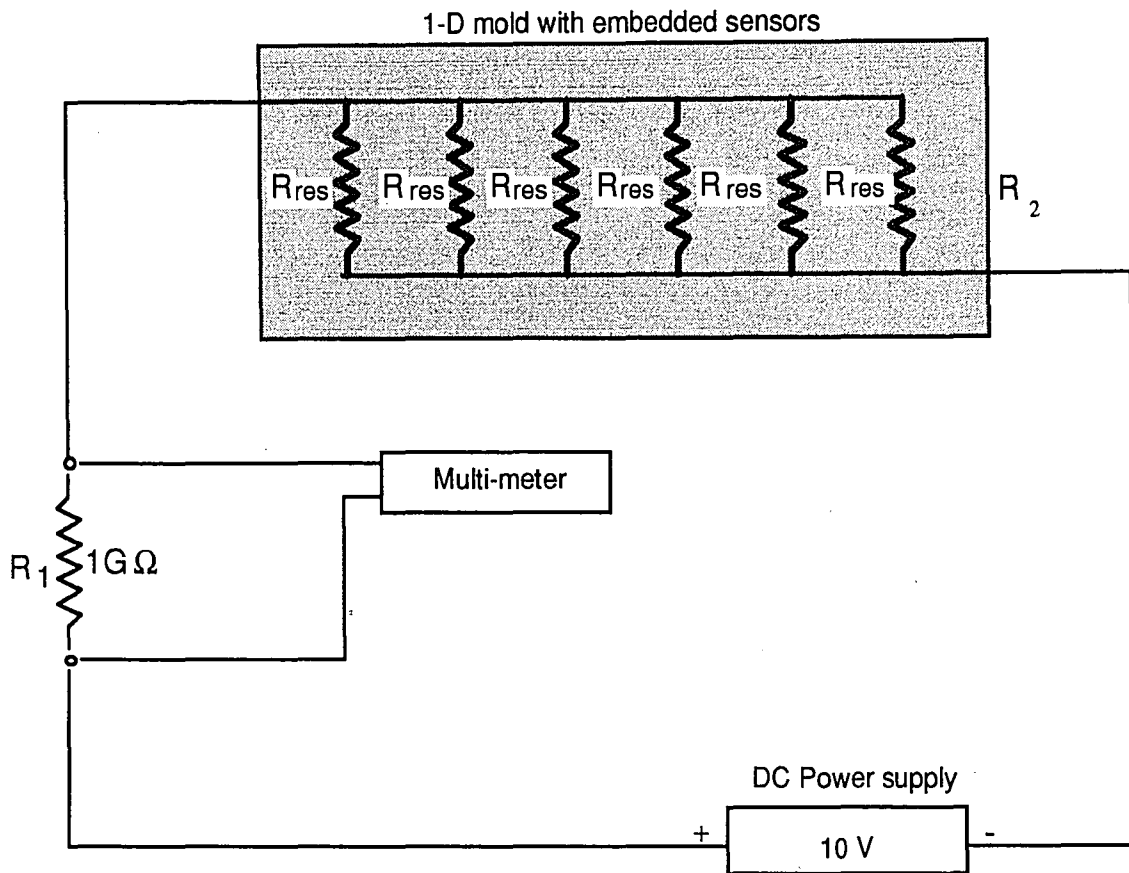
53

Figure 4.2:   One-dimensional circuit diagram

Each sensing circuit consists of a DC power supply and two resistors in series. One of the resistors, R_2, is associated with the resistance of the resin. This quantity varies as the resin flow front advances and fills multiple sensing gaps of a single one-dimensional circuit. The other resistor, R_1, has a fixed and appropriately selected resistance value. The magnitude of R_2, and hence the number of sensing gaps which are filled by resin, is determined by monitoring the voltage drop across the fixed resistor. Assuming that the mold filling process proceeds along each sensing circuit with no node junctions being

skipped, the position of the resin front along each one-dimensional circuit can be monitored in real-time. Two and three-dimensional flow front progression can be monitored using multiple one-dimensional circuits. The theoretical background associated with this modified embedded electronic sensing methodology follows.

4.2 THEORETICAL BACKGROUND

The fundamental material property associated with the present sensing methodology is the volumetric resistivity, ρ_{res}, of the material being molded. For multi-component materials, such as epoxy resin systems containing epoxy and curing agents, the volumetric resistivity can be approximated using the rule of mixtures:

$$\rho_{res} = \rho_e \phi_e + \rho_c \phi_c \qquad (4.1)$$

In this expression, ρ_e and ρ_c represent the volumetric resistivities, and ϕ_e and ϕ_c represent the mixture volume fractions of the epoxy and curing agent respectively.

Within each sensing gap, the material behaves as an electrical resistor. The electrical resistance associated with each gap depends on the volumetric resistivity as well as both the gap length, L, and the sensing node cross-sectional area, A, as follows:

$$R_{res} = \rho_{res} \frac{L}{A} \qquad (4.2)$$

Assuming equal resistance values for all filled sensing nodes, the overall effective resin resistance, R_2, for the circuit depicted in Figure 4.2 depends on the number of such nodes, N:

$$R_2 = \frac{R_{res}}{N} \qquad (4.3)$$

Lastly, the voltage drop, ΔV_1, across the fixed resistor, R_1, is related to the resin resistance, R_2, in the following manner:

$$\Delta V_1 = \frac{V_{ps} R_1}{(R_1 + R_2)} \qquad (4.4)$$

Here V_{ps} represents the constant voltage level provided by the power supply.

Thus, it can be readily seen that when the volumetric resistance of the material is known and remains constant the temporal progression of molding processes can be sensed by monitoring the voltage drop across the fixed resistor.

In some cases, the sensing of molding processes using equation 4.4 to quantitatively relate voltage drop to effective resin resistance at a particular point in time can be difficult. The reasons for this difficulty are twofold. First, it is not always possible to precisely know the volumetric resistivity of the material being molded. Supposedly similar resin mixtures created in different batches may have slightly different electrical properties, and for curing systems, these properties change as a function of time as curing progresses. Secondly, undesirable electrical noise signals can result during experimentation due to the high resistance of resin. It is desirable to utilize the present sensing methodology in a manner which is more robust in the presence of these realistic complexities.

In response to the above considerations, a simple technique was developed and used during the present study to both accommodate varied resin electrical properties to

some degree and distinguish the actual system response from noise. The technique involved the analysis of the temporal voltage drop gradient rather than the actual voltage drop. According to the theory presented above, large changes in the time derivative of the fixed resistor voltage drop should occur every time an additional sensing node location in a circuit is activated by the sudden presence of resin. The continuous calculation and analysis of this quantity makes the sensing system less dependent on the actual volumetric resistivity of the material being molded. All that is required is that the electrical changes associated with material rheological changes occur on a time scale significantly longer than the single sensing grid length resin progression time. The number of filled sensing gaps in a given circuit is simply incremented by one every time a critical voltage jump condition such as that which follows is met:

$$\frac{d(\Delta V_1)}{dt} > \varepsilon \qquad (4.5)$$

In this condition, the critical voltage drop gradient level, ε, is adjusted so as to be less than the voltage change corresponding to the wetting out of additional sensing nodes and, at the same time, greater than the changes of voltage associated with electrical noise.

During the present investigation, the modified sensing methodology was experimentally evaluated both one and two dimensional molding processes. Descriptions of the experiments that were performed are presented in the next chapter.

Chapter 5. EXPERIMENTAL DETAILS

5.1   One-Dimensional Experiment

During the present study, experimental real-time sensing was performed for both one-dimensional and two-dimensional molding cases. The experimental apparatus utilized for one-dimensional proof-of-concept molding tests is shown in Figure 5.1.
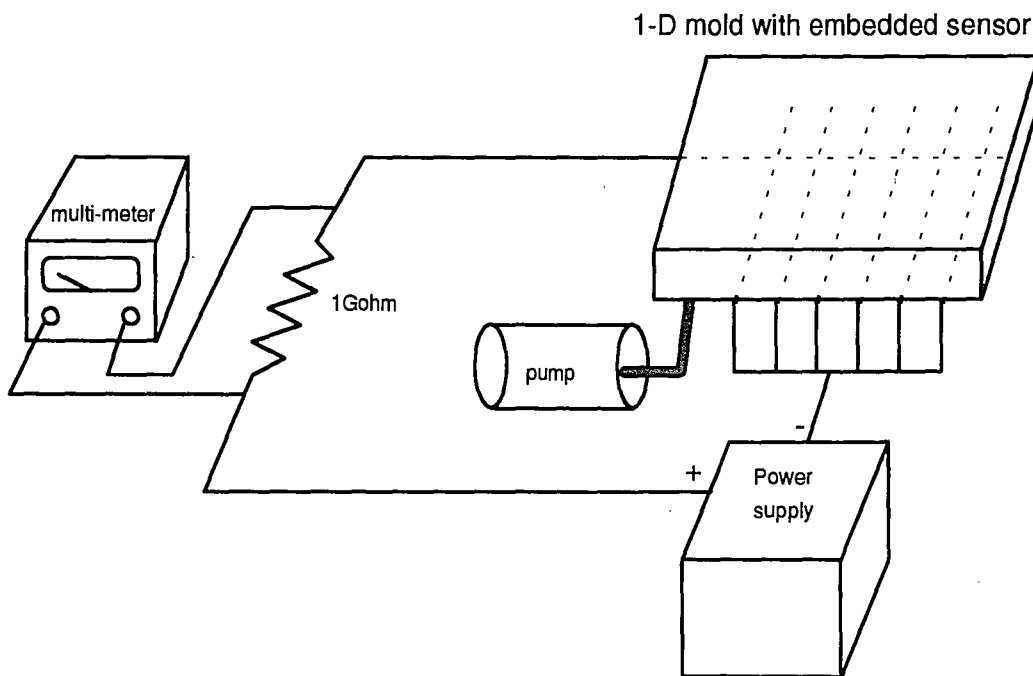

Figure 5.1:   Schematic of one-dimensional experiment

The experimental assembly included a one-dimensional transparent mold with embedded electronic sensors, a power supply, a fixed resistor, a resin supply tank, and a pump. The

mold consisted of two transparent plates and one aluminum spacer plate. A single resin inlet gate was located at one end of the mold. Figure 5.2 shows the dimension of the mold assembly. The mold dimensions were 30 cm (12 in.) long by 5 cm (2 in.) wide, and each surface plate had a thickness of 1.27 cm (0.5 in.). The spacer plate was 0.5 cm (0.1875 in.) thick including two rubber gaskets attached on both sides of the plate and with a U-shaped internal slot to create a 3.2 cm (1.25 in.) wide flow cavity. The configurations of the mold of top and bottom plates included in the embedded conductive wires are shown in Figure 5.3. Electrically conductive wires were orthogonally embedded onto the inner surface of both plates in a non-intersecting manner. Twenty horizontal wires positioned 1.25 cm (0.5 in.) apart were attached to one plate and one vertical wire to the other plate as shown in Figure 5.3. A twenty-eight gauge copper wire was used for this particular experimentation. The vertical wire was connected to the positive terminal of the power supply through a resistor of fixed value, R_1 (1G Ω). All horizontal wires were directly connected to the ground terminal of the power supply.

During experimentation, an applied voltage level of $V_{ps} = 10$ volts was utilized. A CF-920 Ono-Sokki dynamic analyzer was connected to the fixed resistor, and used to measure the voltage drop, ΔV_1, across it. The resin feeding system consisted of a tubing pump (TAT Engineering Corp., Model #410-000, Series H-92) driven by a stepping motor (Anaheim Automation, Model #34D207D) which was controlled by a Gateway 2000 personal computer through an RS232 port. A resin supply tank was attached to the pump, and the flow rate was set very low to practice both the molding process and the monitoring technique.
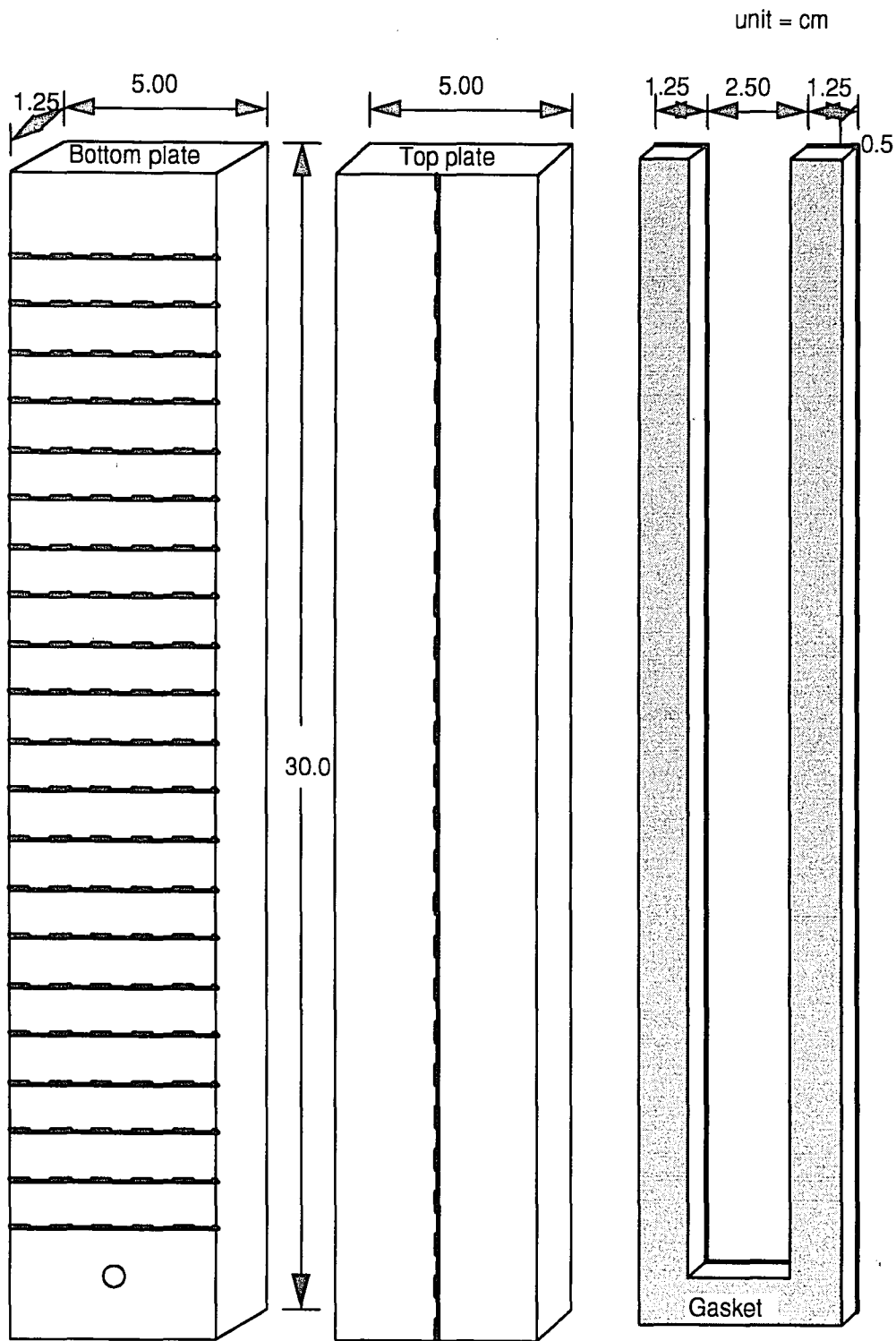
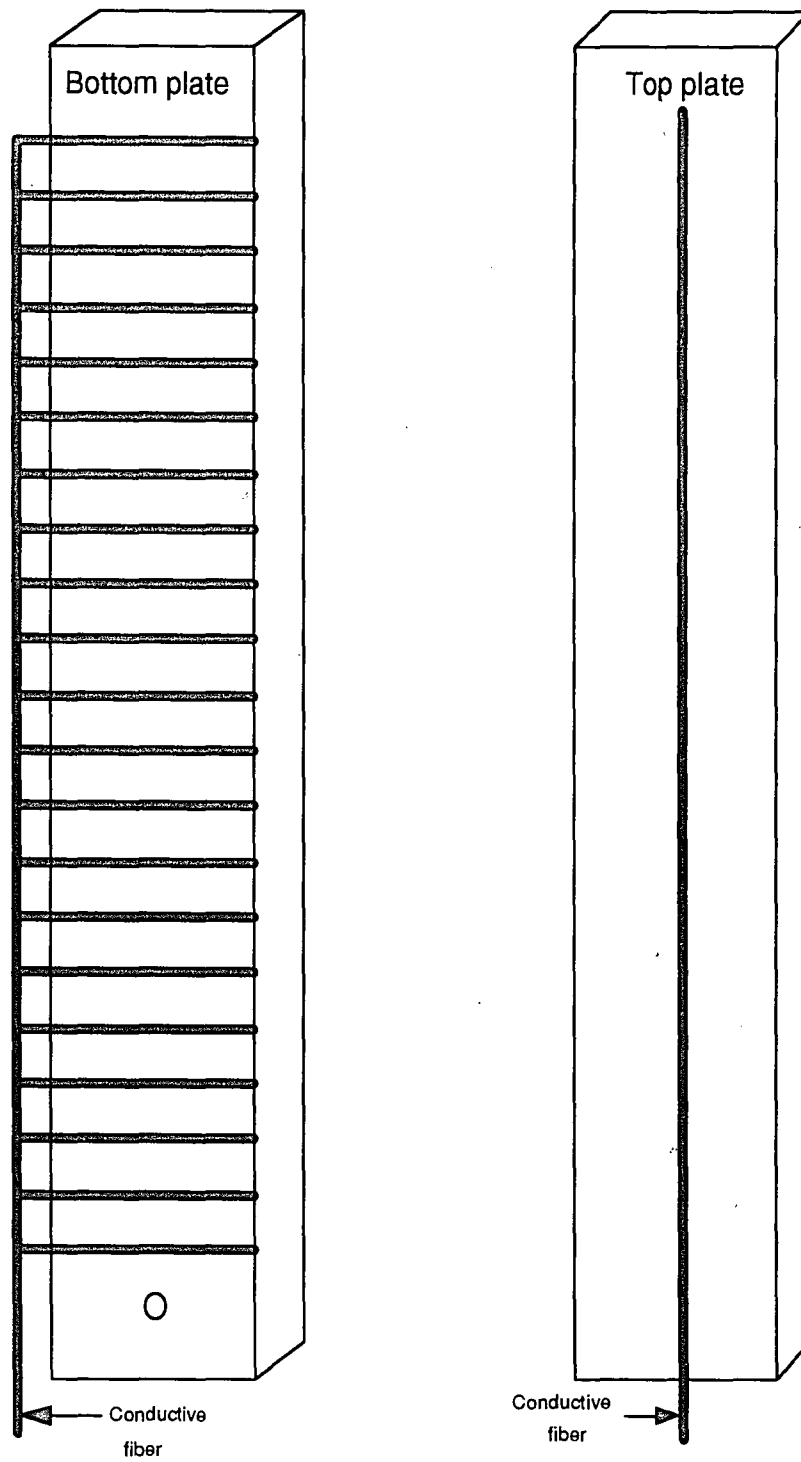Figure 5.2:   Mold utilized for one-dimensional experiment

Figure 5.3:   Top and bottom plate of one-dimensional mold with embedded conductive wires

5.2   Two-Dimensional Experiment

The two dimensional experiments were performed to prove that the one dimensional circuitry was applicable to two dimensional molding processes. The two-dimensional experimental assembly that was used during the present study is depicted in Figure 5.4. This assembly consisted of a transparent mold with embedded sensors, the multi-channel Ono-Sokki dynamic analyzer, a resistance box, two tubing pumps with corresponding pump controllers, the resin supply tank, a video camera, the power supply and the Gateway personal computer. The actual two-dimensional mold that was fabricated is shown in Figure 5.5.
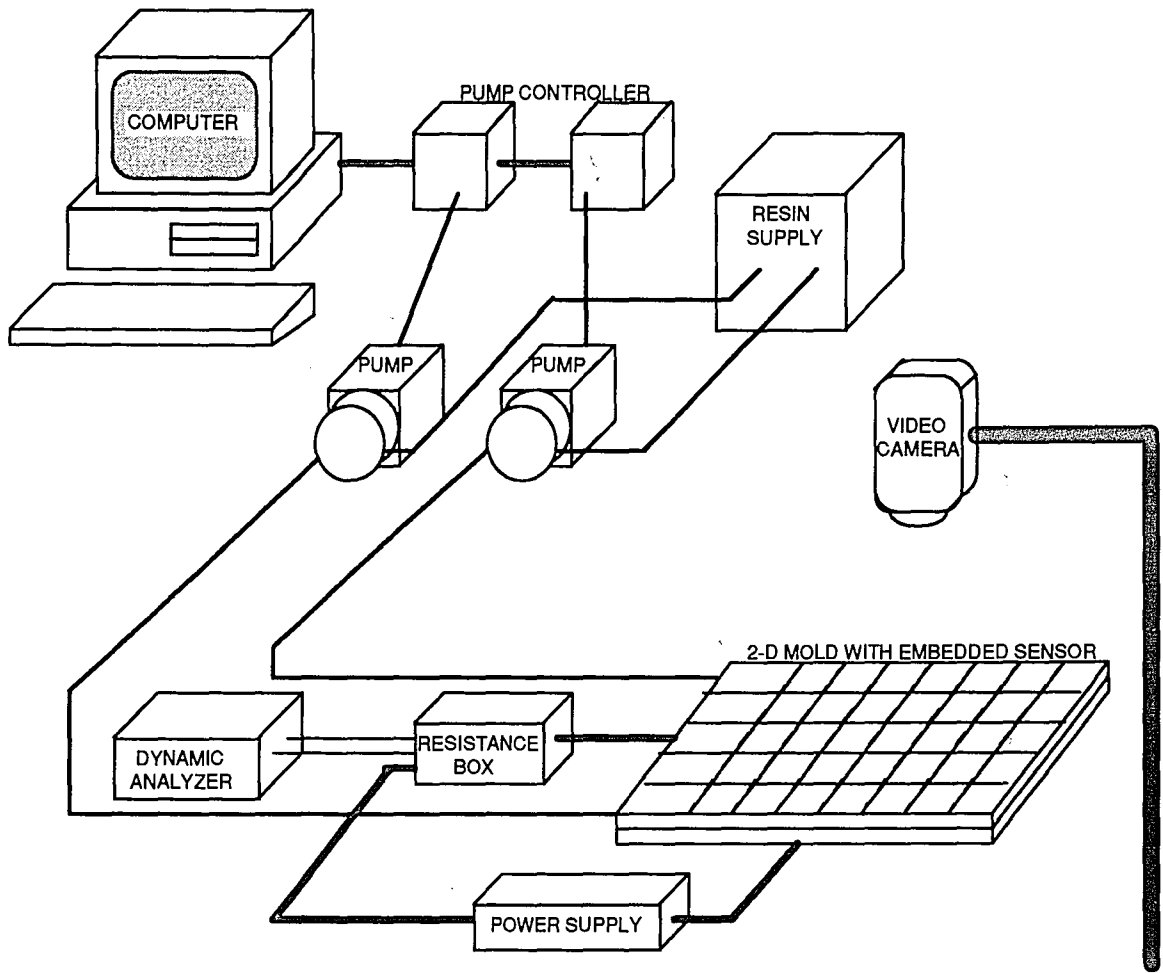
Figure 5.4:　　Two-dimensional experimental apparatus
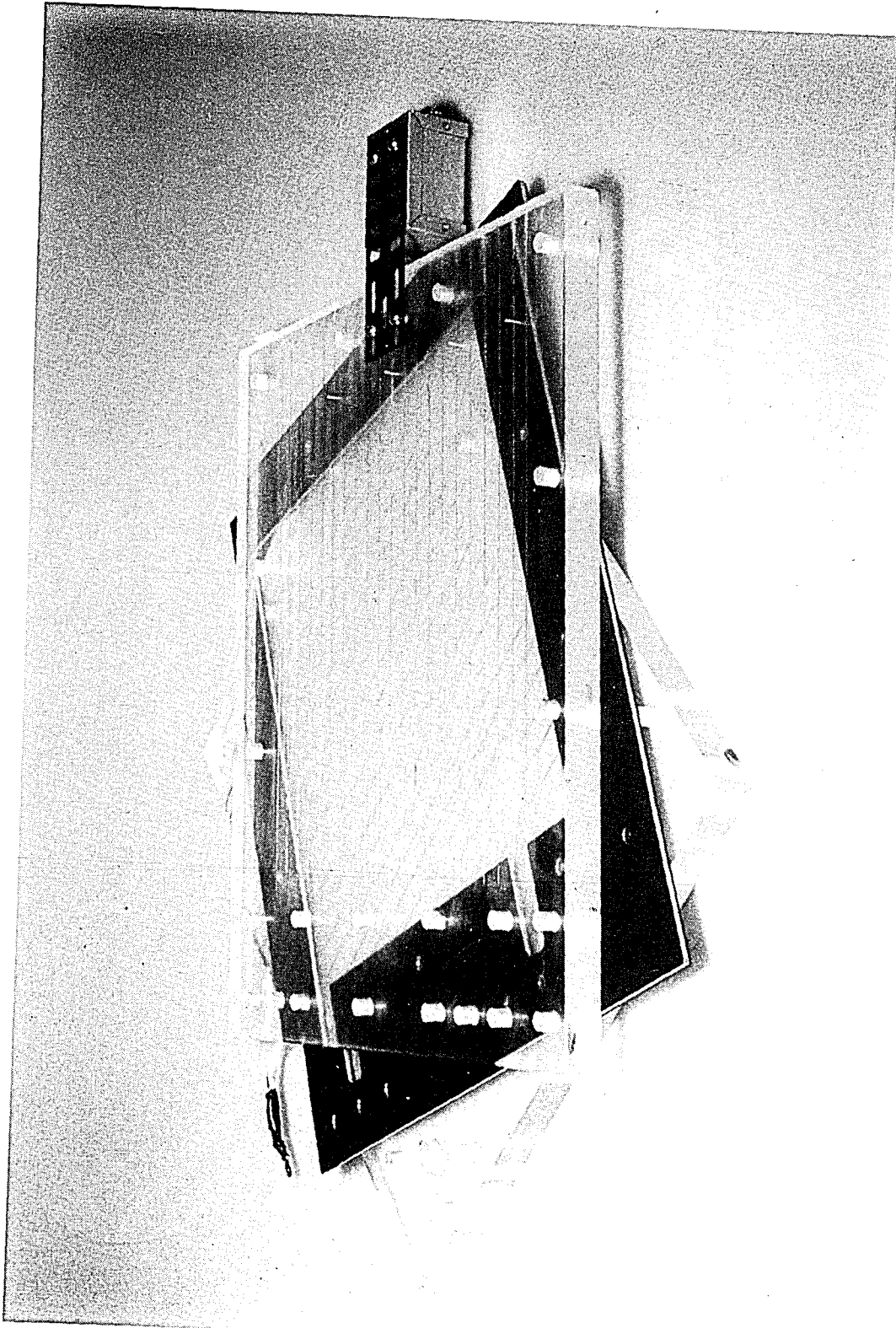
Figure 5.5:   Actual mold for two-dimensional experiment

Figures 5.6 and 5.7 show the dimensions of both the top plate and the bottom plate of the two-dimensional mold with embedded wires, and Figure 5.8 shows the dimensions of the spacer plate. The mold consisted of transparent 2.54 cm (1.0 in.) thick bottom and top plates and a 0.5 cm (0.1875 in.) thick aluminum spacer plate including two rubber gaskets attached on both sides of the plate. The top and bottom plates were 50 cm long and 40 cm wide, and the spacer plate was machined so as to create a 30 cm by 30 cm internal mold cavity. Two inlet gates were located at one end of the mold, and four vent ports were placed at the other end of the mold. The machined channel for each inlet gate was 10 cm (4 in.) by 2 cm (0.79 in.). Eleven electrically conductive wires were evenly embedded to the inner surface of the top mold plate in one direction. These parallel wires were separated from each other by a distance of 3 cm. Similarly, twenty-one electrically conductive wires were embedded to the inner surface of the bottom mold plate in the orthogonal direction. These wires were also parallel and evenly spaced by 1.5 cm. The wire size and material used was the same as for the one-dimensional case. The upper plate wires were connected to the power supply through a resistance box consisting of eleven fixed resistors, R_i's. Each of the fixed resistors had an electrical resistance of 1 GΩ. The lower plate wires were connected to the ground terminal of the power supply. The applied voltage utilized during two-dimensional testing was 20 volts. The resin feeding system consisted of two tubing pumps driven by two stepping motors which were controlled by the personal computer through an RS232 port. The pumps were set-up so as to be independently controllable, allowing for testing with varied gate flow rates. A resin supply tank was attached to the feed side of both pumps. The actual two-dimensional testing apparatus is shown in Figure 5.9. A video camera was used to monitor the flow front progression during experimentation and to verify the validity of the proposed embedded electronic sensor based monitoring technique.
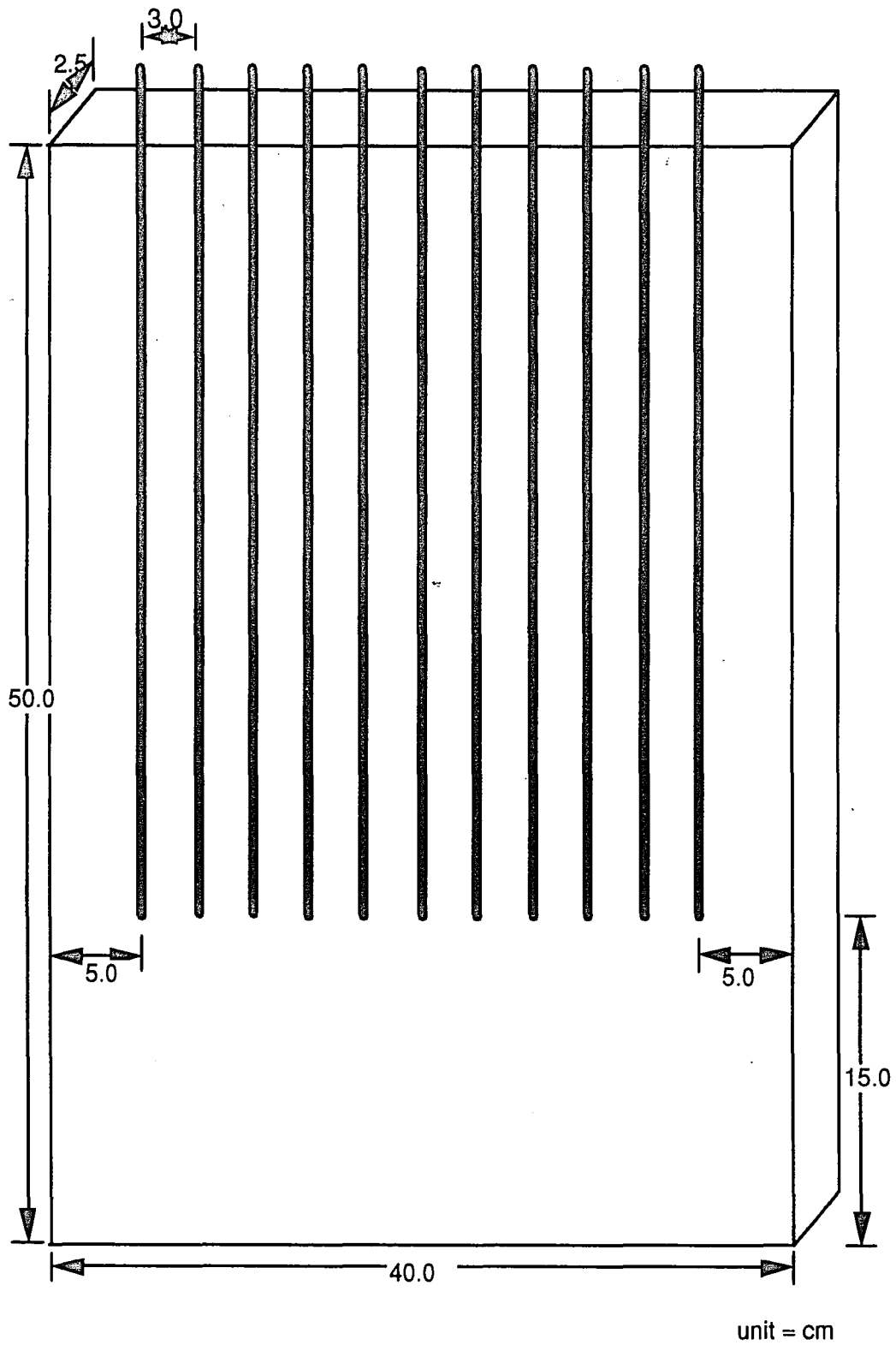
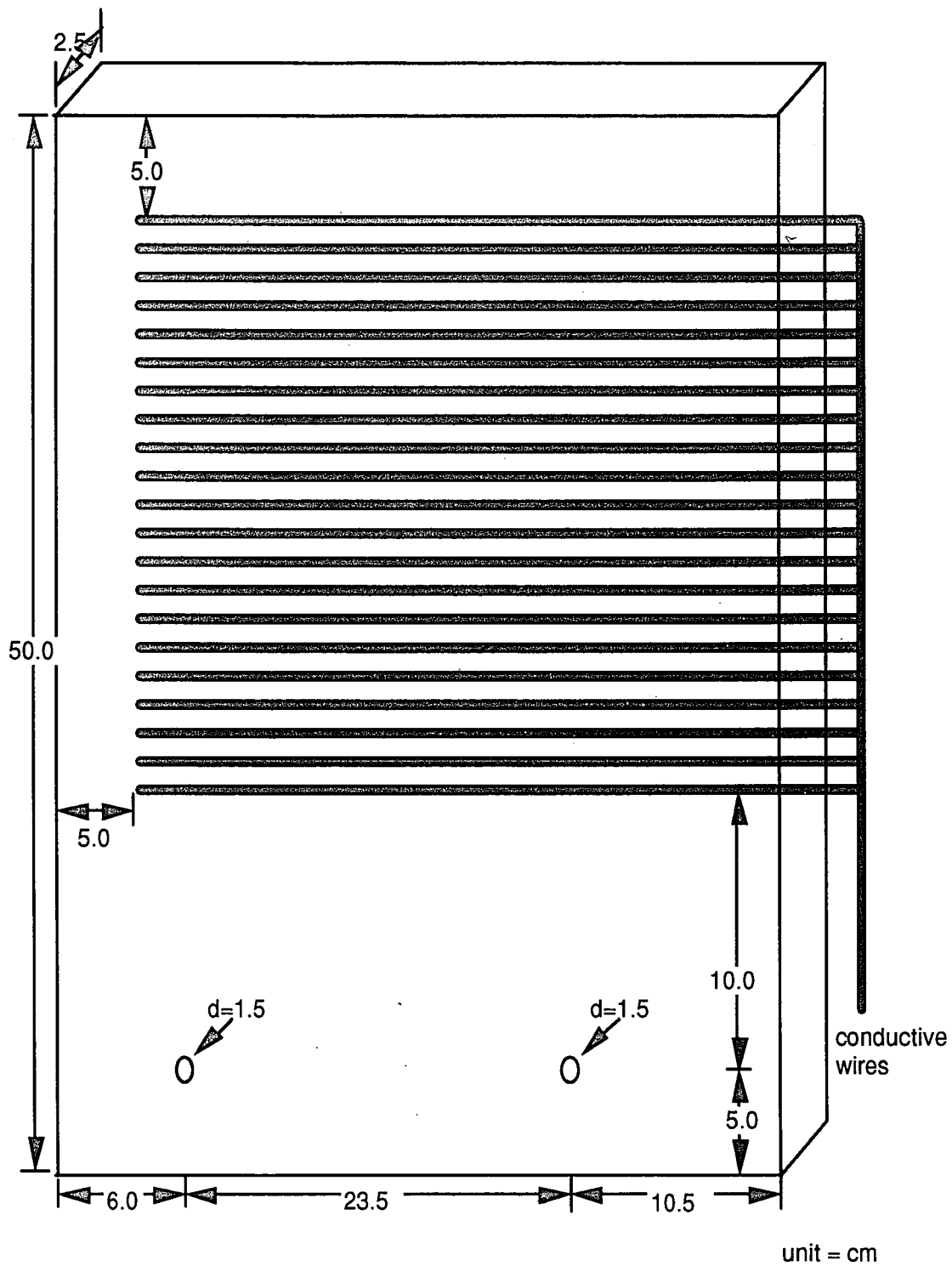Figure 5.6:   Dimensions of mold top plate for two-dimensional experiments

66

Figure 5.7: Dimensions of mold bottom plate for two-dimensional experiments
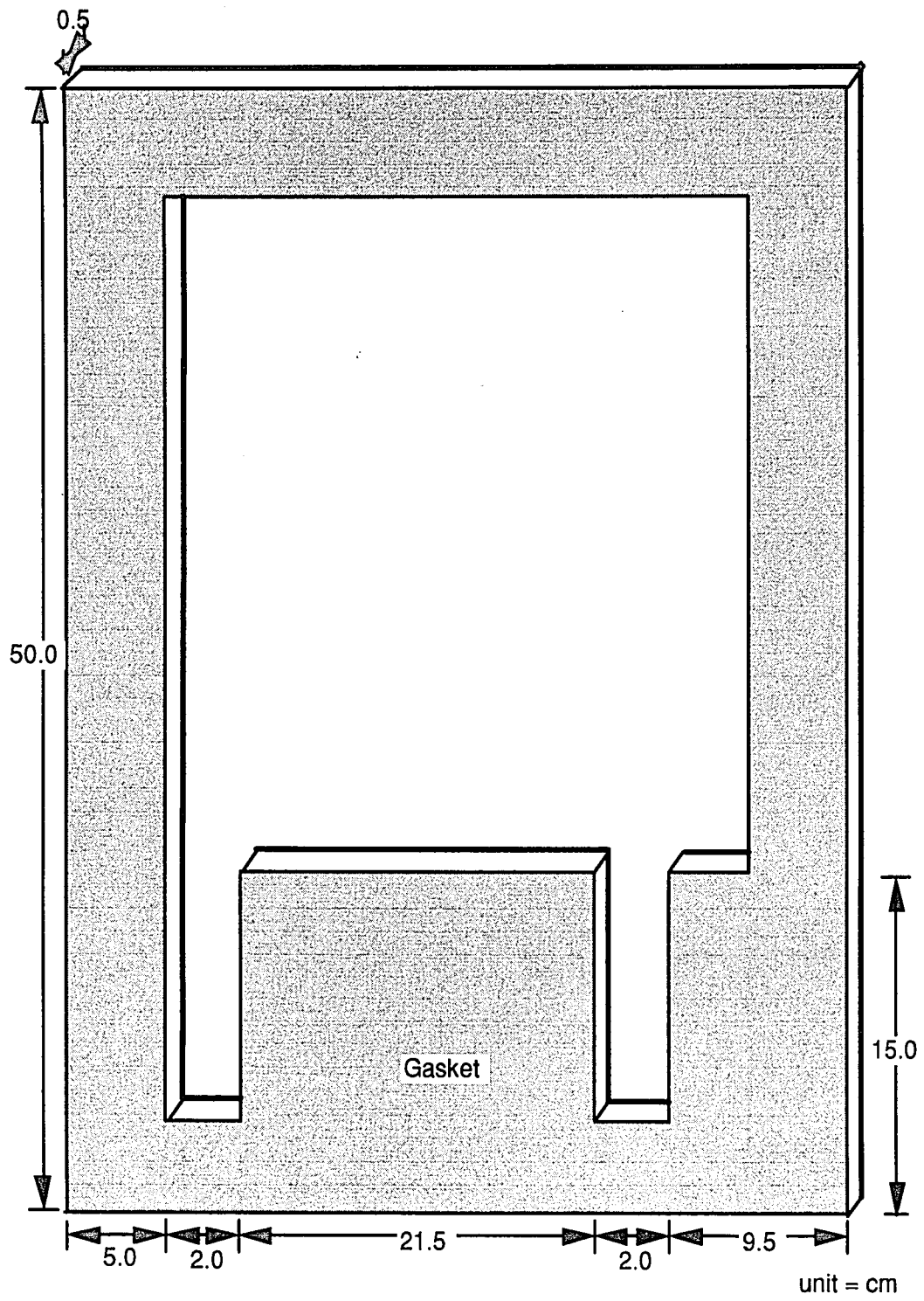
Figure 5.8:   Dimension of mold spacer plate for two-dimensional experiments

Figure 5.9: Actual two-dimensional experiment apparatus

The resin used for both one and two-dimensional molding tests consisted of a mixture of an epoxy resin (Shell EPON-826) and an anhydride curing agent (MHHPA, Anhydrides & Chemicals Incorporated). The selection of a curing agent was made carefully in order to have a slow chemical reaction rate to avoid sudden changes in viscosity and degree of cure at room temperature. The volume ratio between resin and curing agent used for the one and two-dimensional cases was 10 to 6. For 10 to 9 ratios, the manufacturer supplied a complete cure time at a room temperature approximately six days. This 10 to 6 mixture ratio was selected to provide both acceptable electrical resistivity levels and sufficiently long cure times. Both the electrical resistivity and cure time of thermosetting resin systems decrease as the amount of curing agent is increased. Prior to experimentation, the viscosity of the mixture was measured with a Brookfield viscometer and found to be 2000 centipoise at 20° C (68° F). The resin alone had a viscosity of 20100 centipoise and a density of 1.18 g/cc at 20° C (68° F). Similarly , the curing agent had a viscosity of 70 centipoise and a density of 1.18 g/cc at 20° C (68° F).

During both one and two-dimensional testing, resin was injected into the molds at fixed flow rates, and the voltage drop across the appropriate fixed resistors was monitored by the dynamic analyzer. The dynamic analyzer was set at the reading range of $\pm$ 1 volt. This analyzer was used since it can store the data for a limited time interval. It stores data every 0.39 seconds for a period of 400 seconds, every 0.195 seconds for a period of 200 seconds, or every 0.079 seconds for the period of 80 seconds, etc.. The temporal derivative of the voltage drop was subsequently calculated and analyzed. Conditioning of the resultant $d(\Delta V_1)/dt$ signals was also performed to diminish the magnitude of noise signals in the final output. The results of the testing that was performed are presented in the following chapter.

Chapter 6. RESULTS AND DISCUSSION

6.1   One-Dimensional Proof-of-Concept Testing

The embedded electronic sensor concept was first evaluated using the one-dimensional mold described previously. Resin was injected into the mold at a constant and relatively slow mass flow rate and the performance of the sensing system was evaluated.   The voltage drop, ΔV_1, across the fixed resistor was monitored, and quantitatively compared to a theoretical voltage drop that was determined once certain resin and curing agent volumetric resistivity values were assumed. For simplicity, only five sensing gaps were investigated. Typical results that were obtained for voltage drop versus time are shown in Figure 6.1.1. Included in the figure are observed results and a theoretically anticipated result which was calculated assuming constant previously measured resin properties. As shown, the observed and predicted voltage drops did not exactly agree, and the deviation between these quantities increased as the resin advanced through the mold. As alluded to in the previous theoretical section of this report, this deviation between theory and observation was attributed to uncertainty in actual resin volumetric resistivity.   If flow front determination using the initially planned direct quantitative evaluation of voltage drop is used, the case presented in Figure 6.1.1 would yield acceptable results for only the first three sensing gaps. Beyond that point, a direct voltage drop analysis scheme would produce inaccurate results, as the experimental voltage drop obtained for four sensing gaps (region E) is nearly equal to the theoretical voltage drop for three filled sensing gaps (region D). While it was initially postulated that the direct measurement of absolute voltage drop at any particular instant would lead to flow front location determination, results such as those shown in Figure 6.1.1 convinced

the investigators that the more robust time derivative based analysis scheme was necessary.

The test case presented in Figure 6.1.1 was re-analyzed using the temporal voltage drop gradient approach. The results of this analysis are presented in Figure 6.1.2, where $d(\Delta V_1)/dt$ is plotted as a function of mold filling time for the same case involving five sensing gaps. This graph shows five abrupt jumps or "spikes" in the data, each of which is associated with resin crossing an additional sensing gap. The spikes occurred at 36 sec, 80 sec, 136 sec, 191 sec and 244 sec. For this case, a critical voltage drop derivative level of $\varepsilon = 0.002$ Volts/sec was selected, and the number of sensing gaps filled was incremented by one every time the condition established by Equation 4.5 was satisfied. Noise signals were found to be below this threshold, therefore unwanted signals were easily disregarded. The verification of these experimental results was performed with visual observations. Thus, the temporal voltage drop derivative based sensing approach was concluded to be accurate and reliable for sensing mold filling processes in real time.
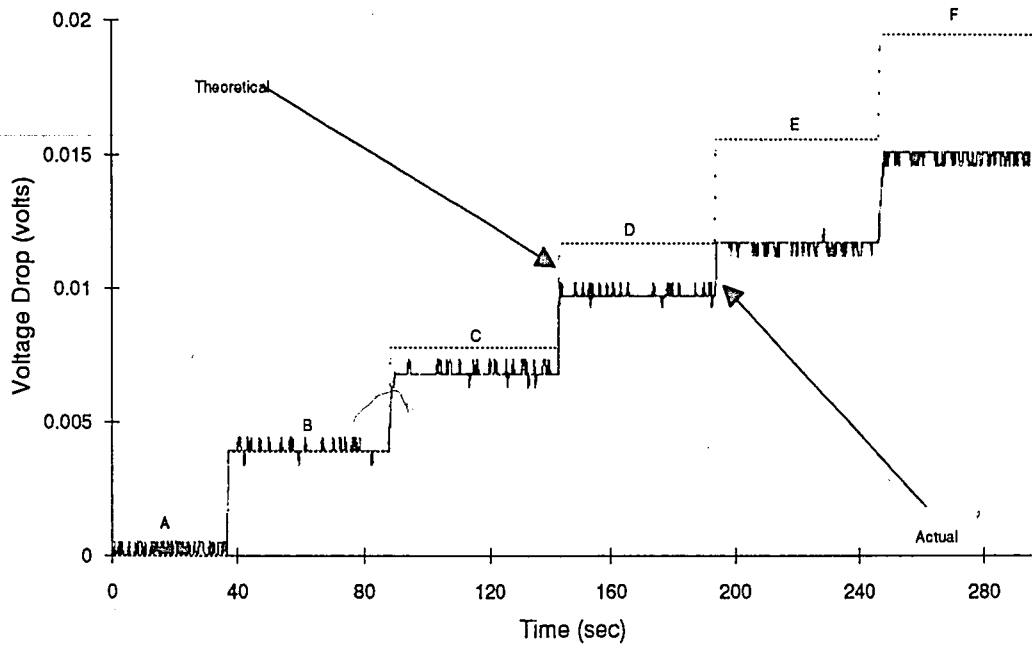
Figure 6.1.1:   One-dimensional experimental result of voltage drop versus time
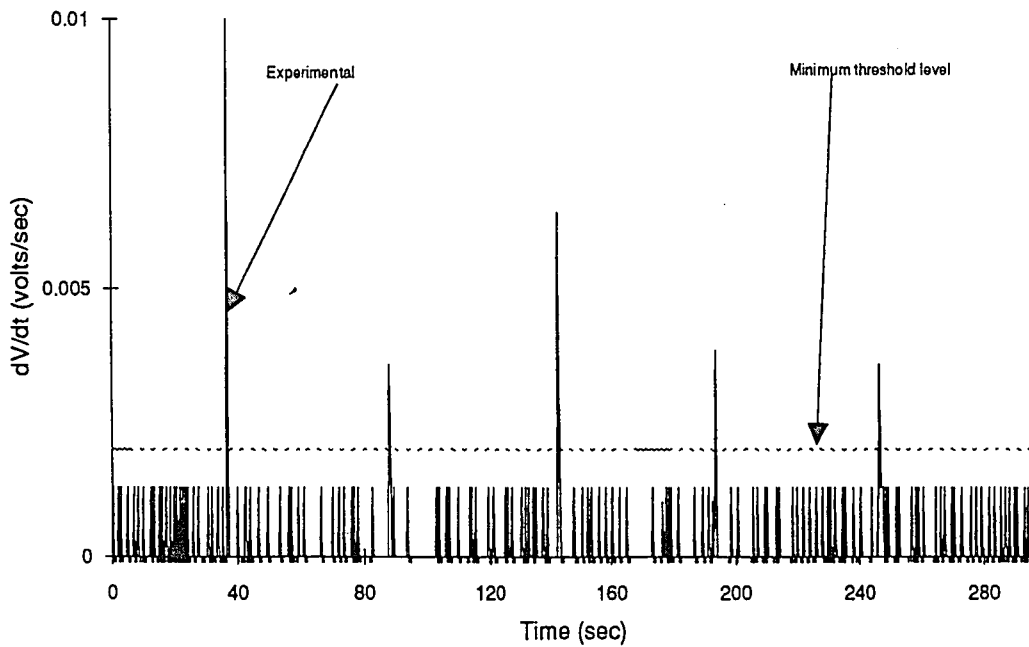
Figure 6.1.2:   One-dimensional experimental result of dV/dt versus time

73

For additional information, other experiments were run to investigate the effectiveness of the volumetric resistivity by varying the mixture ratio of the resin system. During this phase of study, volumeric resin to curing agent ratios of 10 to 0, 10 to 3, 10 to 6 and 10 to 9 were evaluated. Figure 6.1.3 shows typical results obtained from experiments with ratios of 10 to 6 and 10 to 9. As seen in figure, two curves with higher mixture ratio are only seen because resin system with both the 10 to 0 and 10 to 3 ratio mixture yielded very low volumetric resistivity values, and as a result the voltage drops, ΔV_1, across the fixed resistor were smaller than the minimum reading range of the dynamic analyzer. As shown in Figure 6.1.3, however, the two higher curing agent content mixture ratios clearly showed steplike results. At the 20th sensing gap, the voltage drop, ΔV_1, across the fixed resistor was 0.044 volts for the 10 to 6 mixture ratio and 0.065 volts for the 10 to 9 mixture ratio. Also $d(\Delta V_1)$ between each sensing gap was 0.0022 volts for the 10 to 6 mixture ratio and 0.00325 volts for the 10 to 9 mixture ratio. Upon evaluation, the mixture volumetric resistivity did not seem to follow the linear rule of mixtures relationship previously presented as Equation 4.1.

The higher curing agent content mixture ratios lower the volumetric resistivity and raise $d(\Delta V_1)$ between each sensing gap. This leads to the conclusion that the higher curing agent content mixture ratios are preferable as mentioned previously. At this point, the 10 to 6 mixture ratio was selected for the remainder of the investigation. The 10 to 6 mixture proved both acceptable electrical properties and an acceptably high viscosity level for further in-situ molding process monitoring.
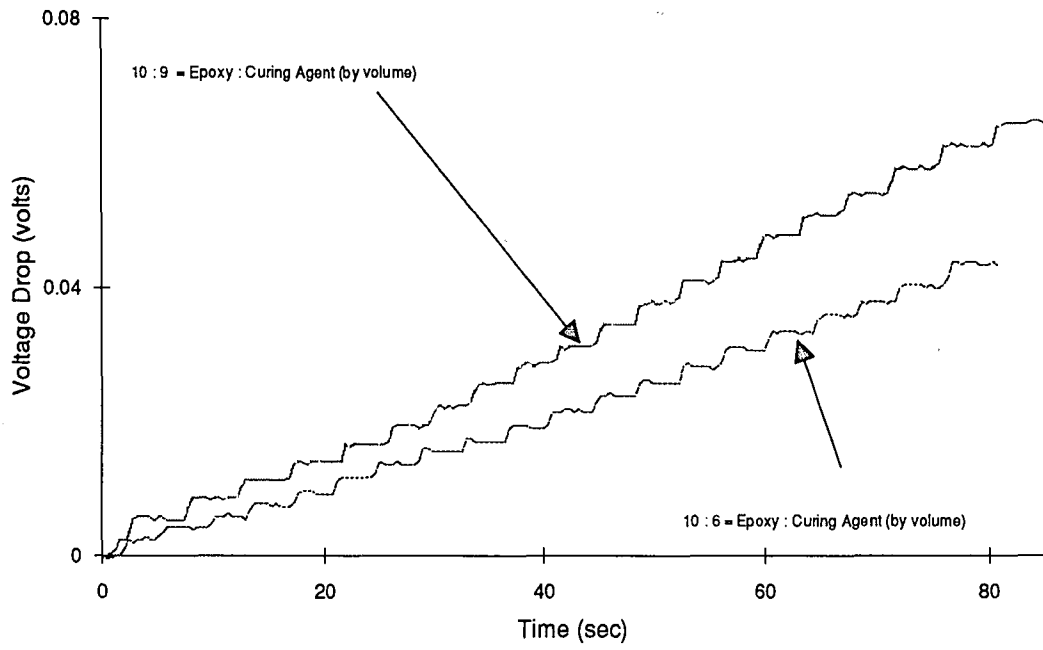
Figure 6.1.3:
One-dimensional experimental result of voltage drop versus time with two different resin system mixtures

6.2 Two-Dimensional Testing

The verification of the sensing methodology for one-dimensional mold filling processes was followed by the evaluation of the concept for two-dimensional processes. The apparatus depicted in Figure 5.4, 5.5 and 5.9 was utilized and resin was injected at each inlet gate with a volumetric flow rate of 1.15 cm^3/s. For clarity, a diagrammatic description of the mold with the eleven linear sensing circuits labeled is shown in Figure 6.2.1. During experimentation, the voltage drop across each of the eleven fixed resistors associated with these sensing circuits was recorded every 0.195 seconds. The total mold filling time that resulted was on the order of 180 sec.

Resultant temporal voltage drops for the eleven linear resin front sensing circuits are shown in Figure 6.2.2 through 6.2.12. The stepwise increasing trend in voltage drop obtained for each circuit was similar to that observed for the previously discussed one-dimensional case. As before, steplike increases in voltage drop occurred whenever a sensing gap was suddenly filled with resin. Overall, it was concluded that the step changes resulting for each circuit were consistent, but individual step change magnitudes for different circuits were not identical. For example, for the sensed signals corresponding to each circuits, average voltage drop step increments were not identical as shown in Table 6.1. Slight irregularities in sensing gap cross sectional areas and circuit resistance values could have accounted for this. The final voltage drop values for each of circuits after the mold was completely filled are also presented in Table 6.1.

Another result that is shown in Figure 6.2.2 through 6.2.12 is that the actual voltage drop signals recorded contained a considerable amount of undesirable noise. A conditioning scheme was applied to the raw data to eliminate this noise and thus provide a more appropriate sensing signal. This scheme involved the averaging of voltage drop over

small incremental time periods (in this particular experiment, three time increment) and the comparison of resultant sequential averages. When the difference between sequential average voltage drops exceeded a minimum threshold level, κ, a stepwise jump in voltage drop corresponding to the filling of an additional sensing gap was assumed. On the other hand, no stepwise jump was assumed when sequential average voltage drop differences were less than κ. Resulting conditioned voltage drop signals for each of the eleven circuits are included in the figures. The threshold level applied in this case was zero.

Circuit #	Average voltage drop increment (volts)	Voltage drop when mold was filled (volts)
1	0.0019	0.0399
2	0.0025	0.0525
3	0.0030	0.0630
4	0.0028	0.0588
5	0.0020	0.0420
6	0.0021	0.0441
7	0.0020	0.0420
8	0.0020	0.0420
9	0.0020	0.0420
10	0.0020	0.0420
11	0.0016	0.0340

Table 6.1:   Average voltage drop increment and voltage drop at 21st sensing gap
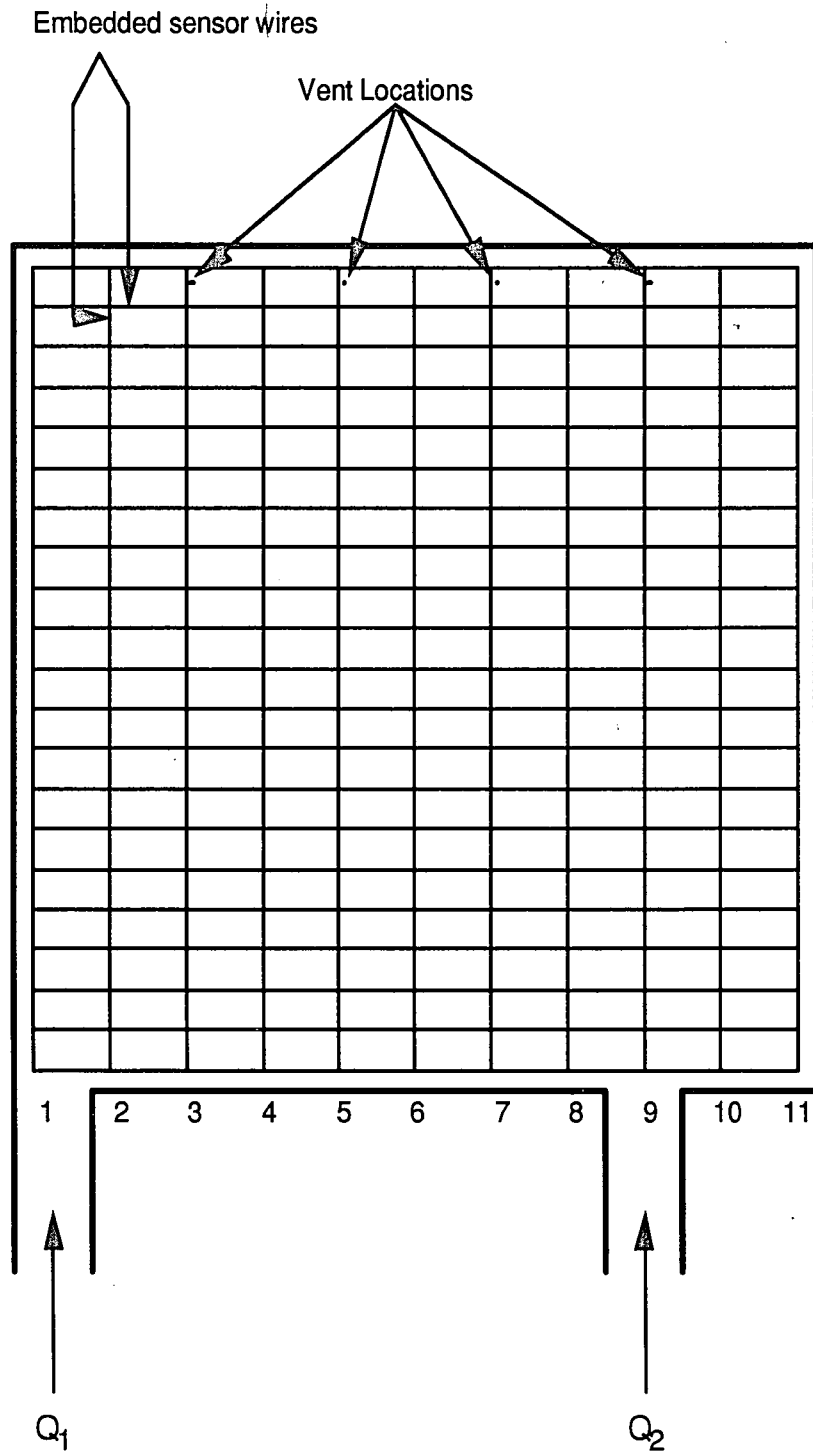
Figure 6.2.1: Two-dimensional mold with linear sensing circuits labeled
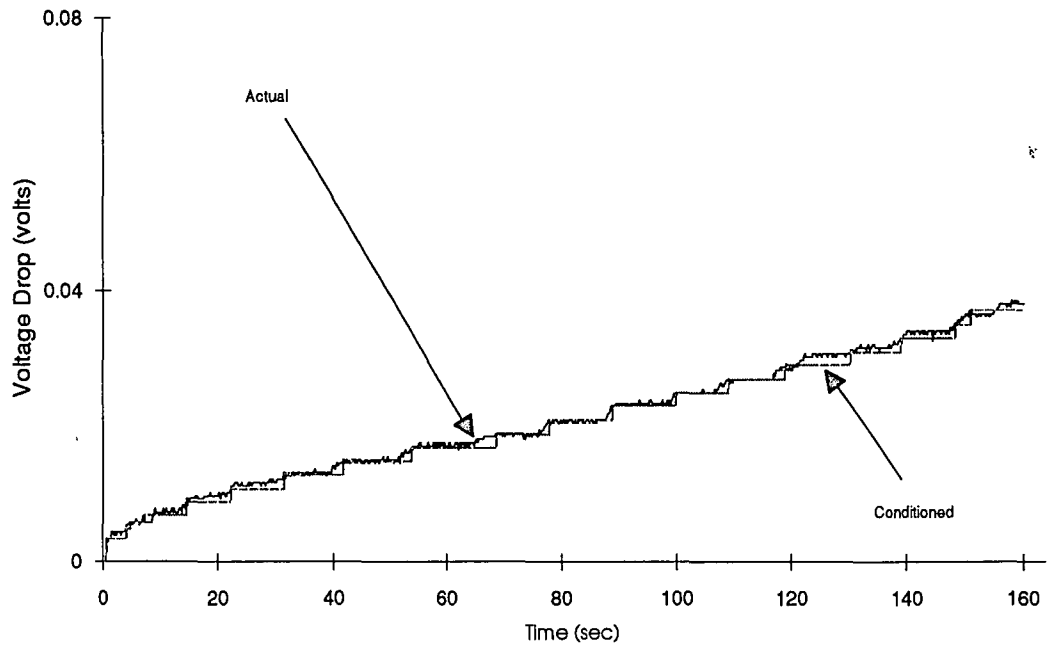
Figure 6.2.2:
Two-dimensional experimental result of voltage drop versus time for circuit 1
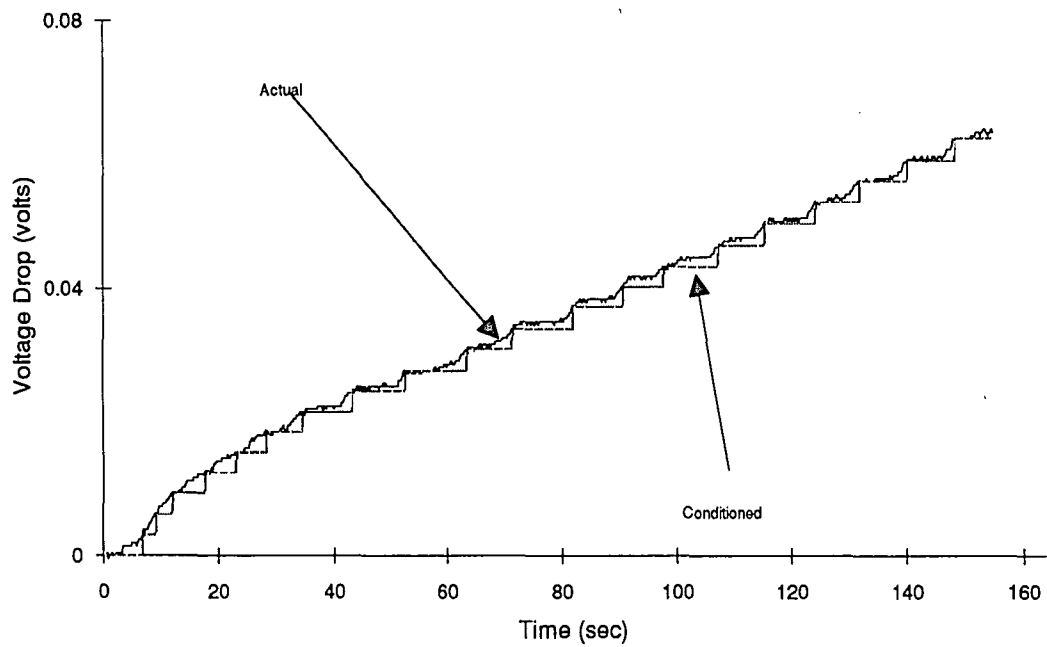
Figure 6.2.3:
Two-dimensional experimental result of voltage drop versus time for circuit 2
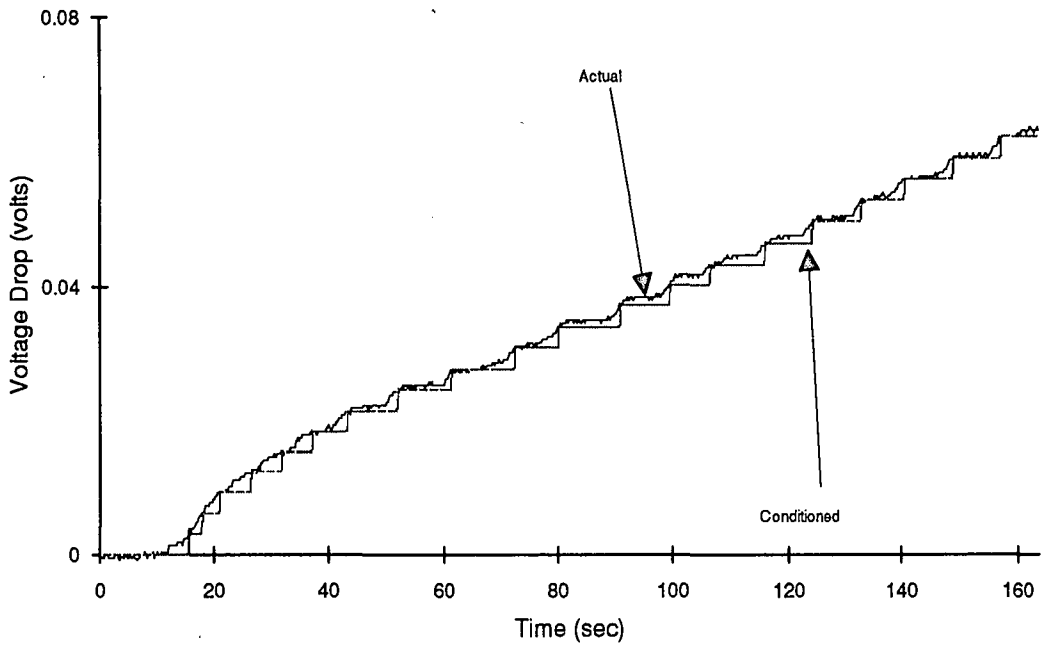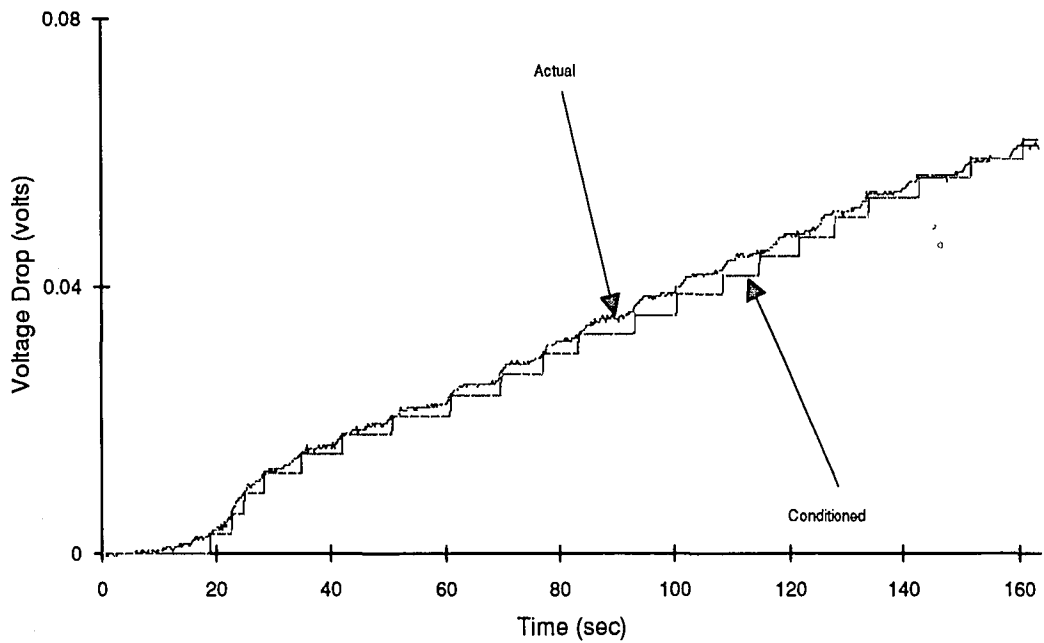
79

Figure 6.2.4:
Two-dimensional experimental result of voltage drop versus time for circuit 3

Figure 6.2.5:
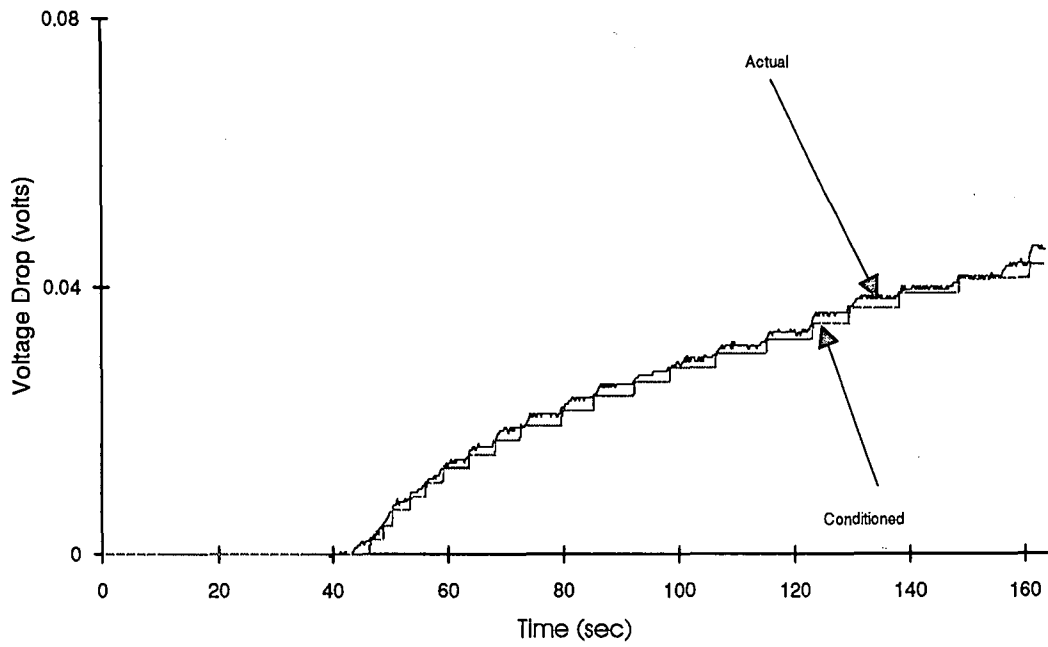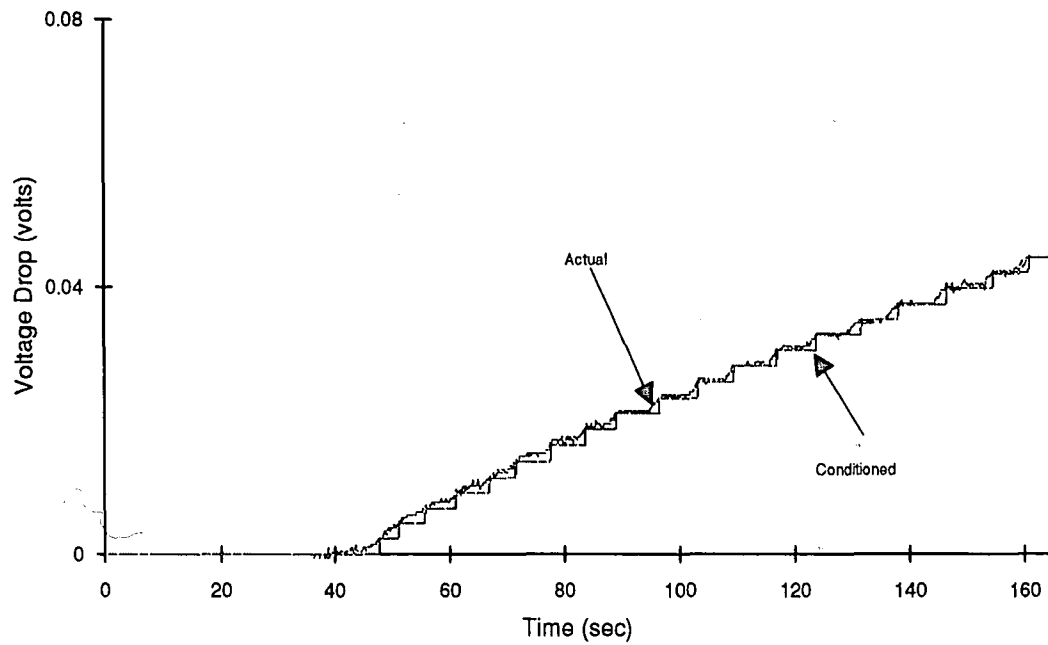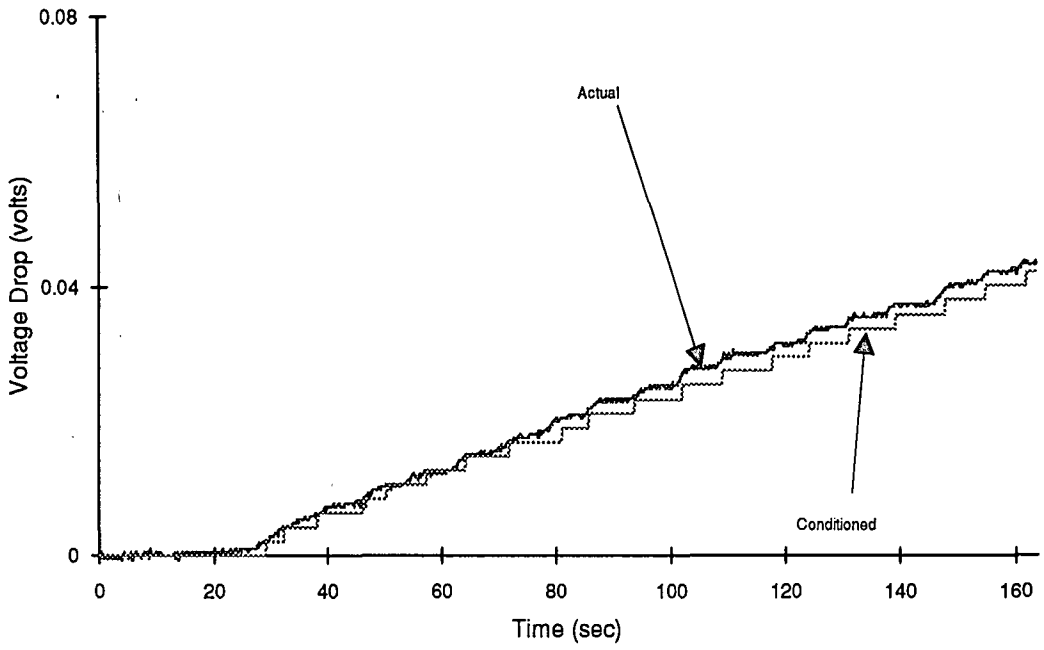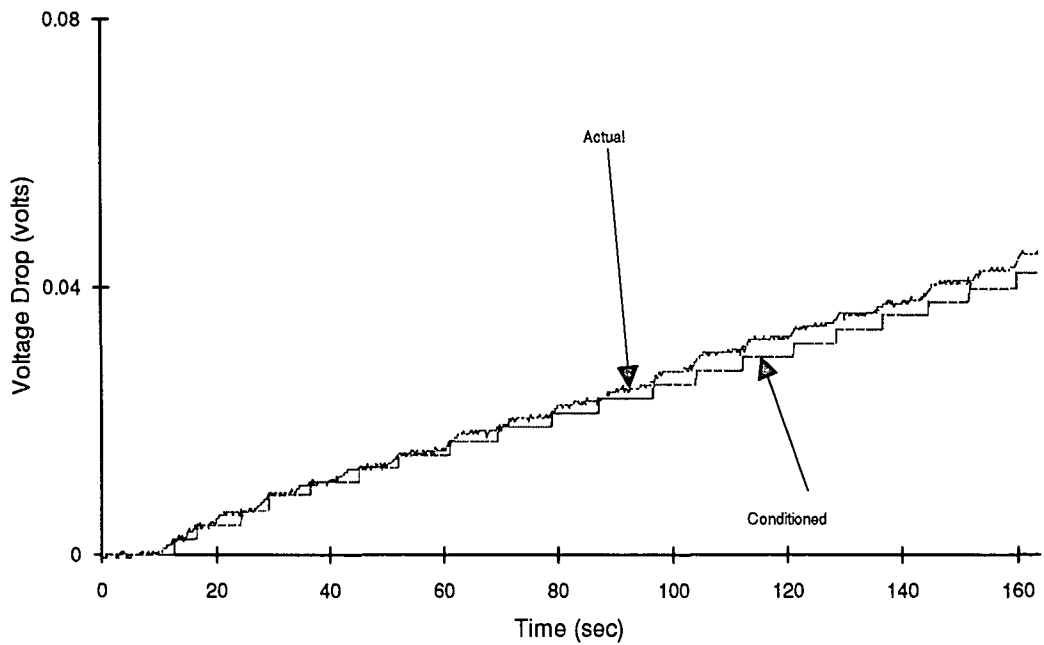Two-dimensional experimental result of voltage drop versus time for circuit 4

Figure 6.2.6:
Two-dimensional experimental result of voltage drop versus time for circuit 5
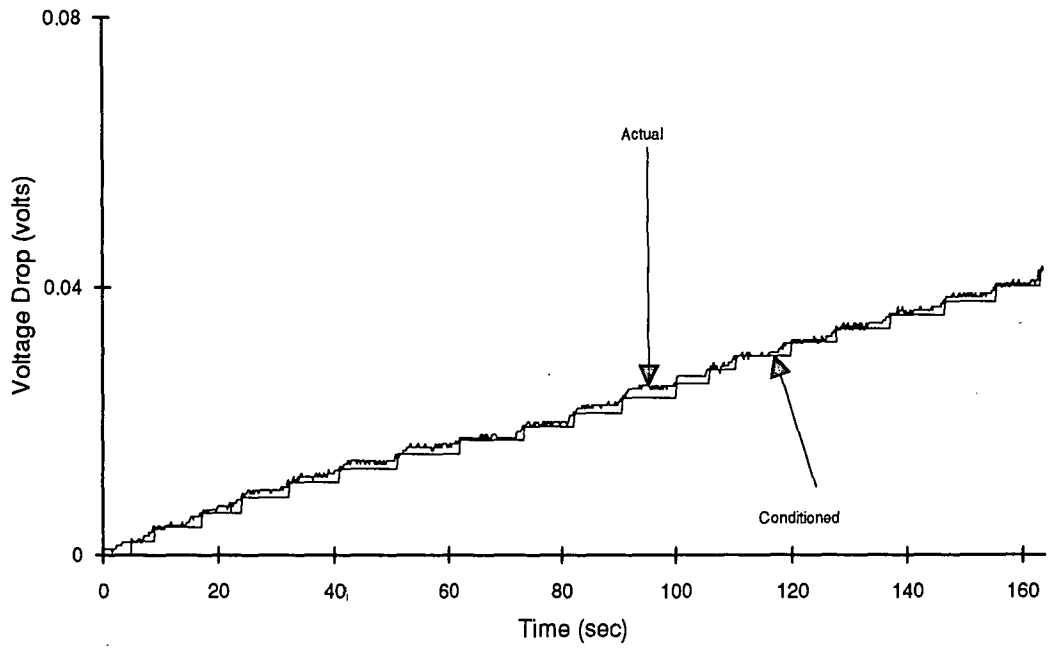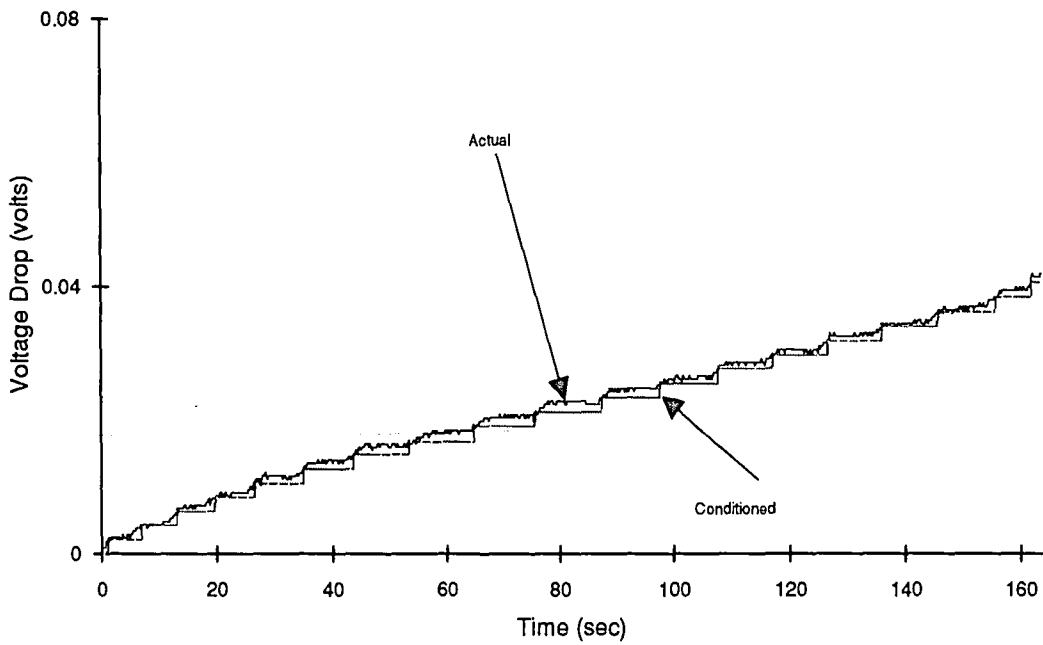

Figure 6.2.7:
Two-dimensional experimental result of voltage drop versus time for circuit 6

81

Figure 6.2.8:
Two-dimensional experimental result of voltage drop versus time for circuit 7

Figure 6.2.9:
Two-dimensional experimental result of voltage drop versus time for circuit 8

Figure 6.2.10:
Two-dimensional experimental result of voltage drop versus time for circuit 9

Figure 6.2.11:
Two-dimensional experimental result of voltage drop versus time for circuit 10
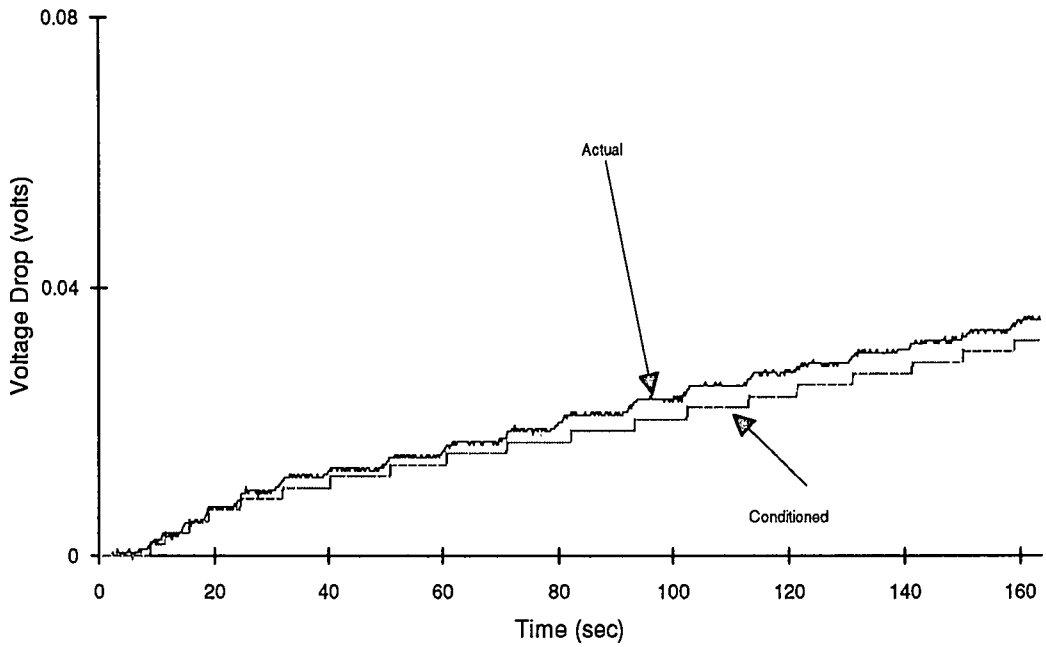
83

Figure 6.2.12:
Two-dimensional experimental result of voltage drop versus time for circuit 11

As was done successfully for the one-dimensional case, the voltage drop gradient approach was employed for the determination of temporal flow front locations. The resultant temporal voltage drop gradient distributions for each circuit are presented in Figure 6.2.13 through 6.2.23. As can be seen in the figures, these results show the spike-like behaviors similar to that obtained for the one-dimensional case, with each spike above a present threshold noise level representing the filling of an additional sensing gap in the linear circuit.
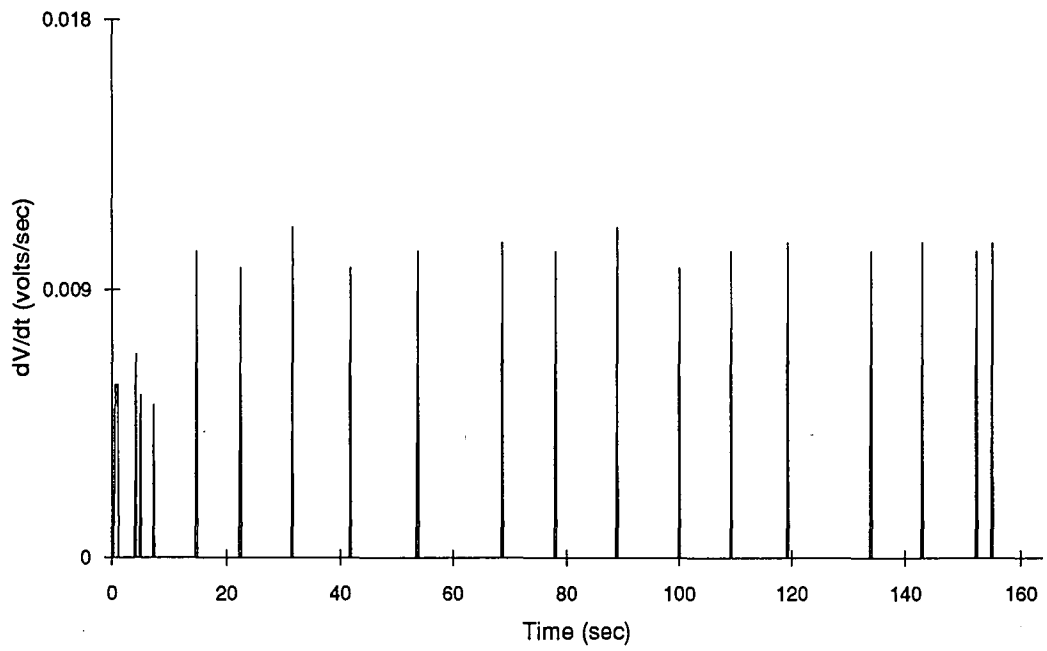
Figure 6.2.13:
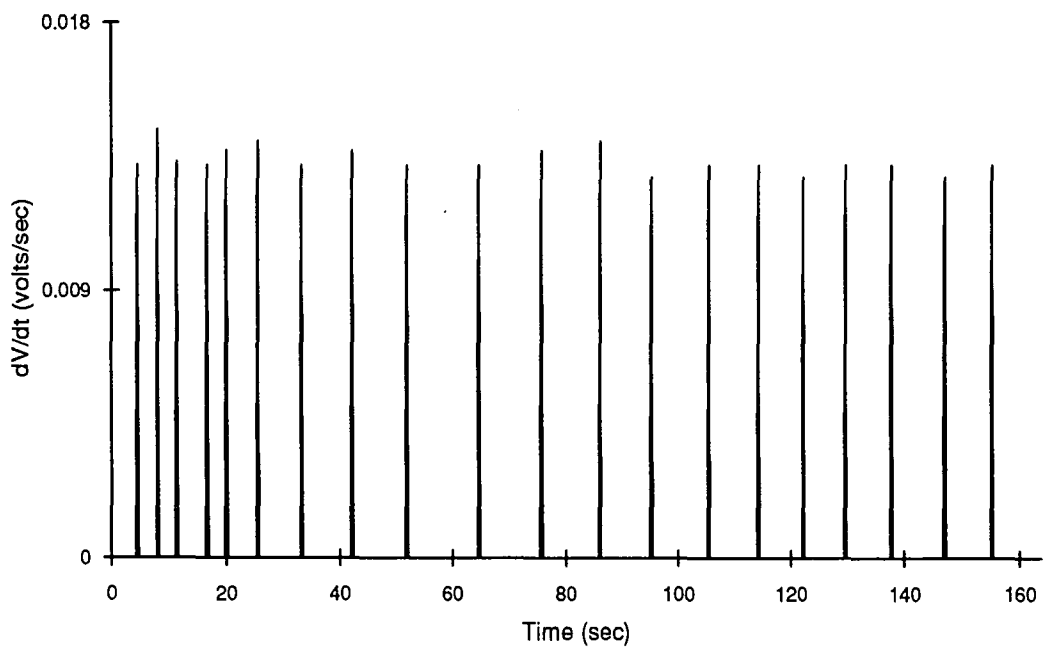Two-dimensional experimental result of dV/dt versus time for circuit 1

Figure 6.2.14:
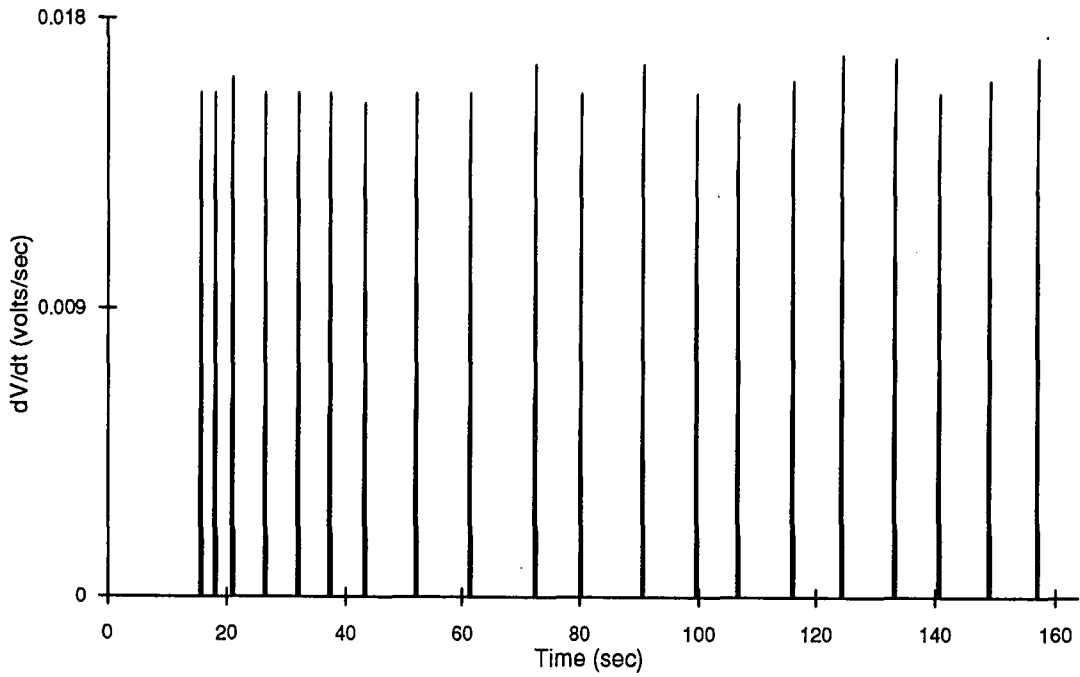Two-dimensional experimental result of dV/dt versus time for circuit 2

. Figure 6.2.15:
Two-dimensional experimental result of dV/dt versus time for circuit 3

Figure 6.2.16:
Two-dimensional experimental result of dV/dt versus time for circuit 4

86

Figure 6.2.17:
Two-dimensional experimental result of dV/dt versus time for circuit 5

Figure 6.2.18:
Two-dimensional experimental result of dV/dt versus time for circuit 6

Figure 6.2.19:
Two-dimensional experimental result of dV/dt versus time for circuit 7
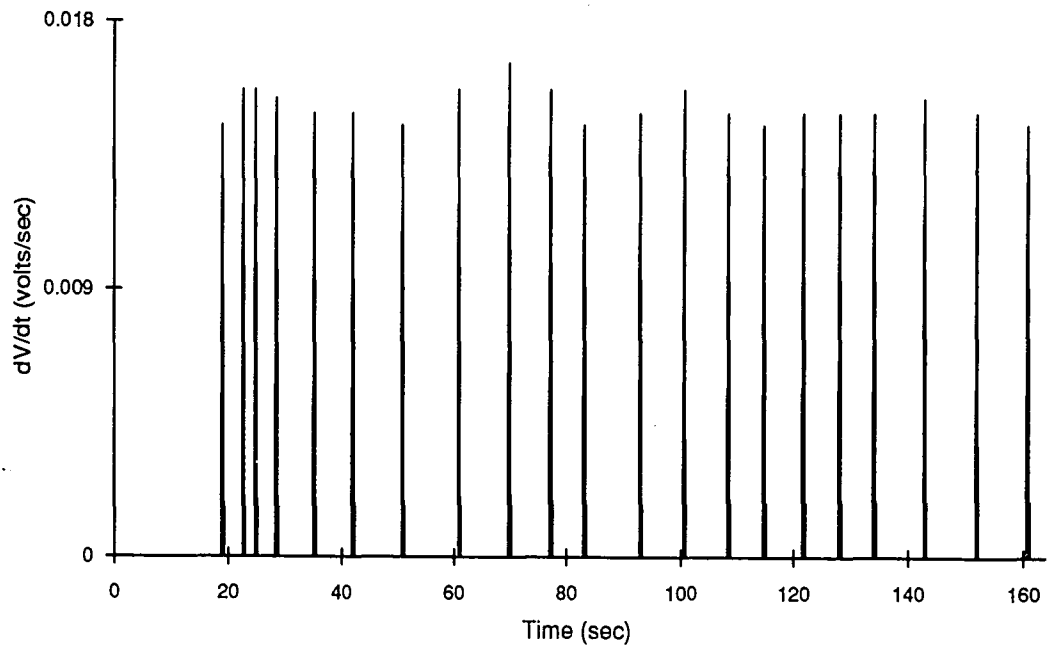

Figure 6.2.20:
Two-dimensional experimental result of dV/dt versus time for circuit 8

Figure 6.2.21:
Two-dimensional experimental result of dV/dt versus time for circuit 9
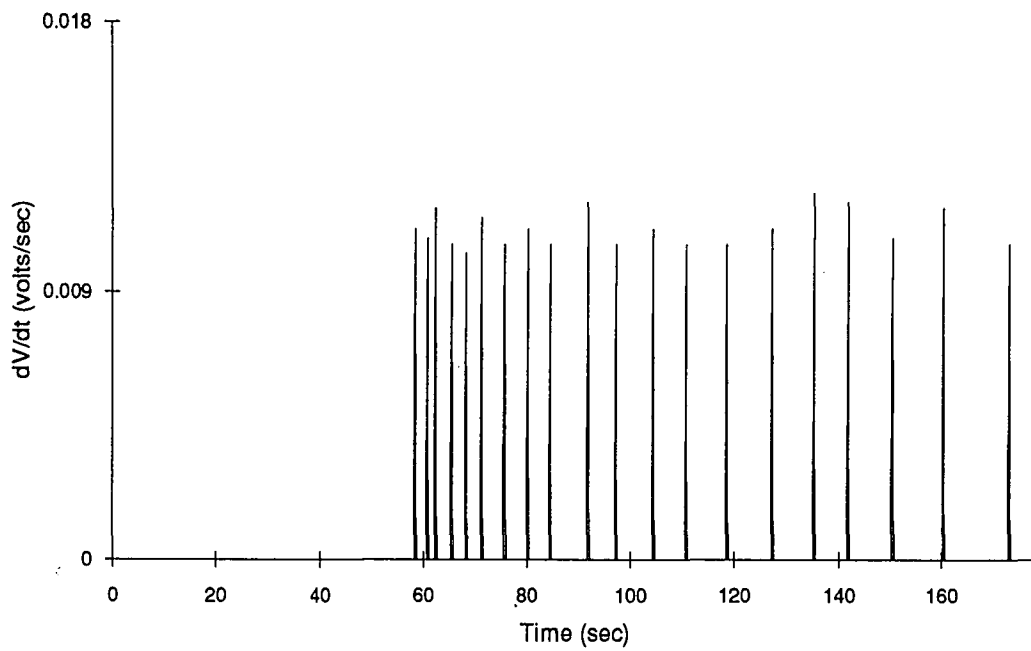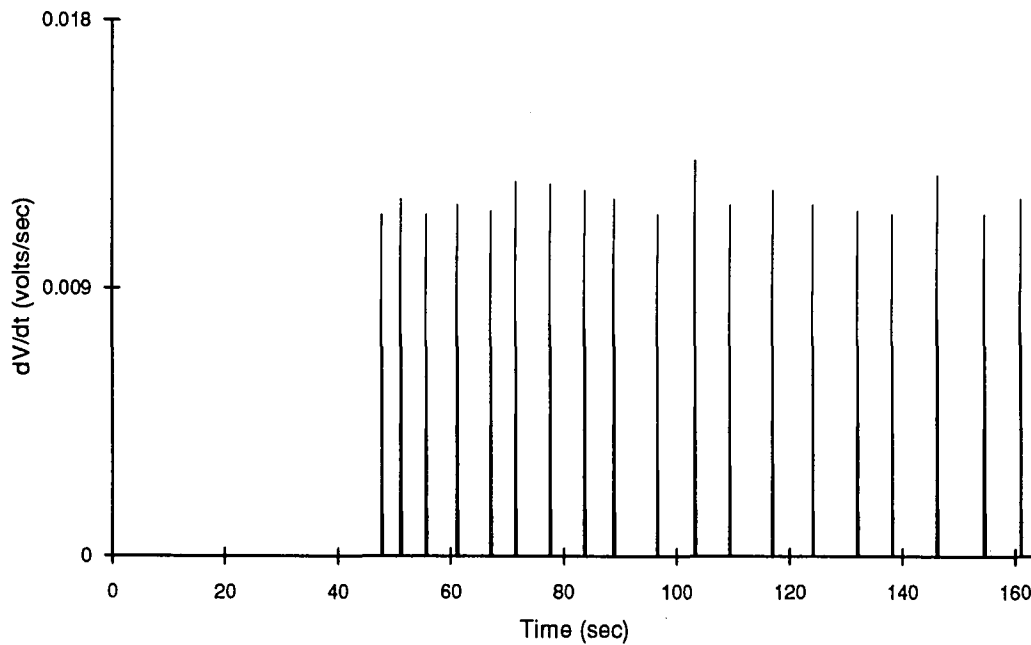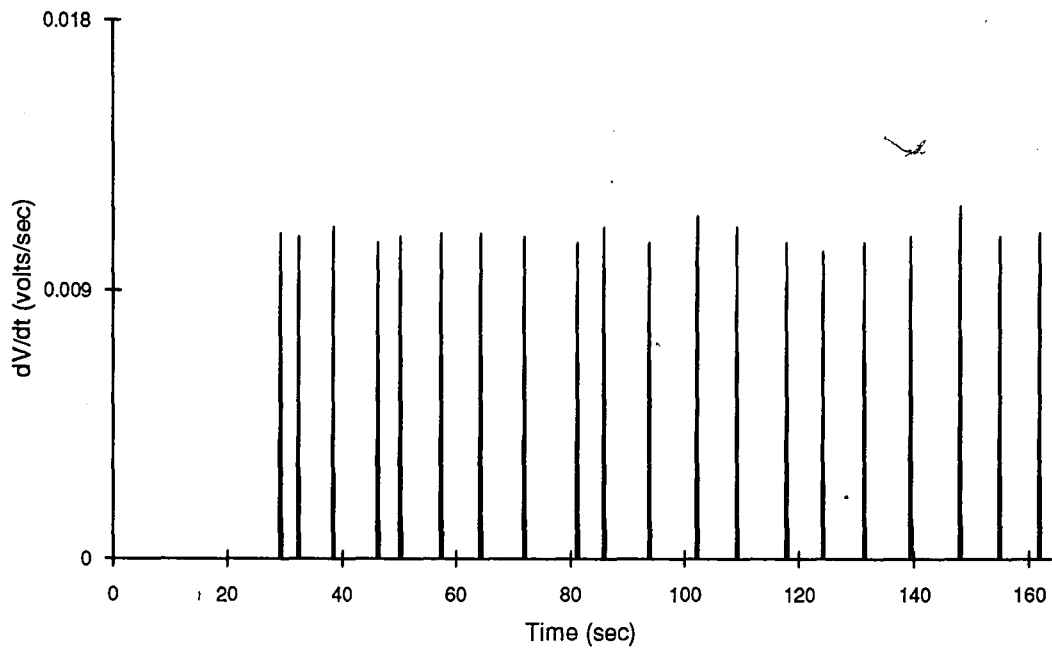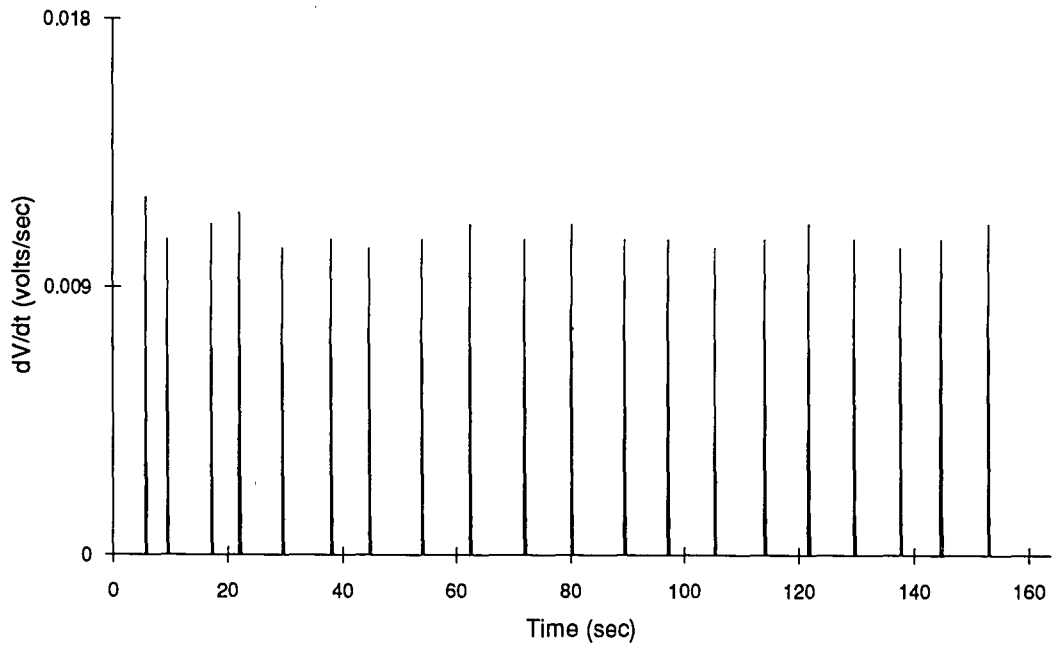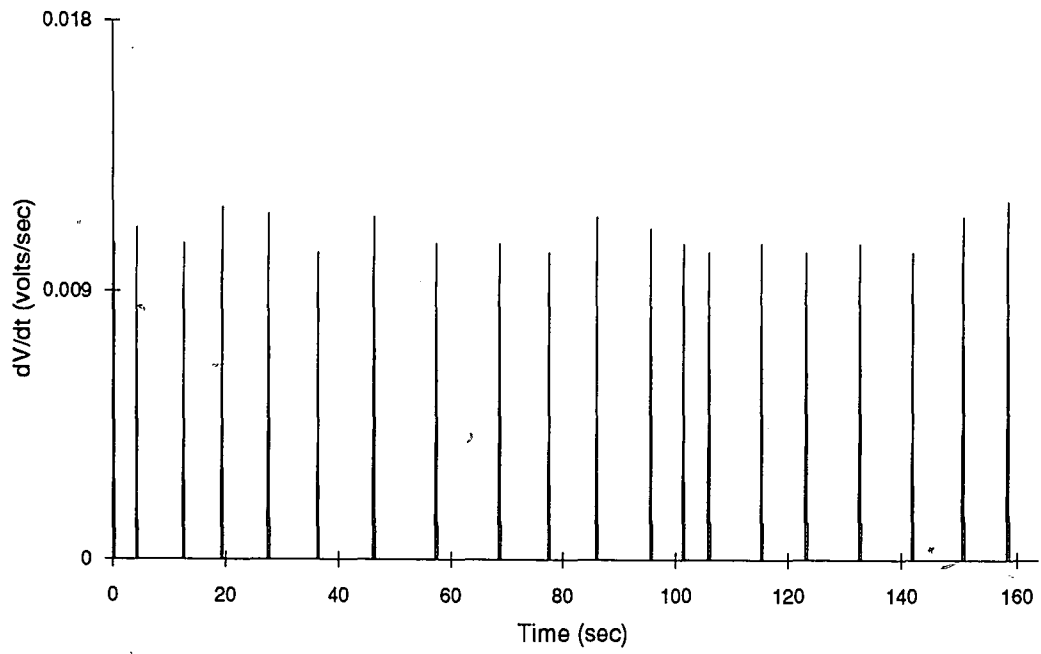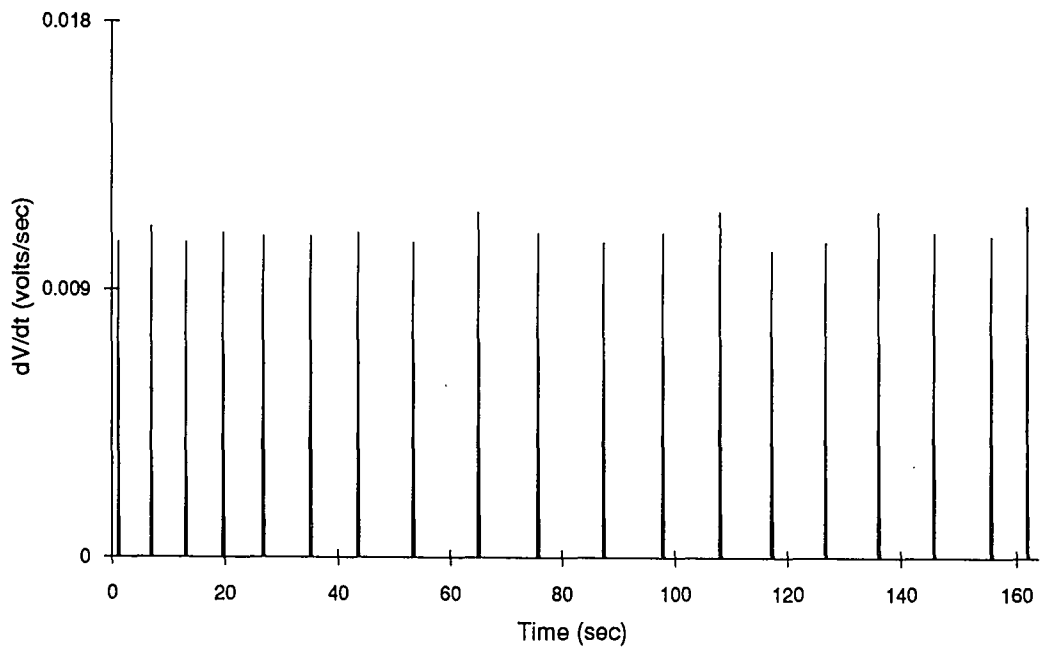

Figure 6.2.22:
Two-dimensional experimental result of dV/dt versus time for circuit 10
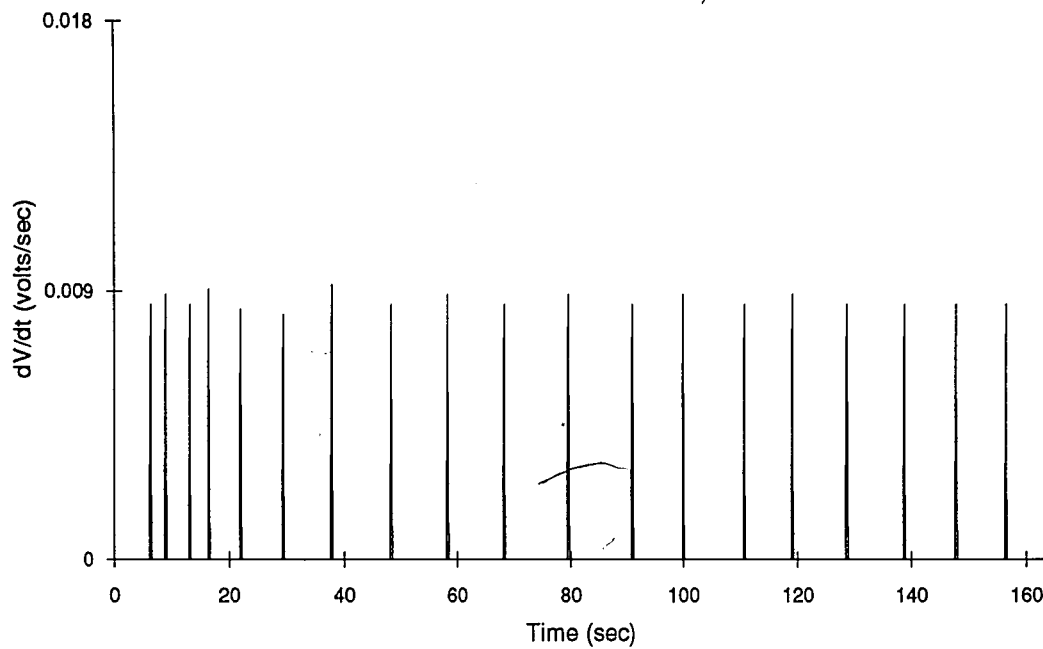
Figure 6.2.23:
Two-dimensional experimental result of dV/dt versus time for circuit 11

For each of the eleven circuits, the number of spikes at any particular time was used to determine the flow front location along that line. Collectively, the eleven linear flow front movement curves provided the overall molding process progression information desired.

The overall flow front progression profile determined during the two-dimensional testing is presented in Figure 6.3. The profiles as presented are for 20 second increments during the molding process. The spatially stepwise nature of the flow front information generated by the electronic sensing scheme can clearly be seen. The smoother profiles from the electronic sensing system could be obtained by decreasing the sensing grid unit cell size. The validity of these results were verified via recorded flow visualization of the process using a video camera. The visually recorded flow fronts corresponding to each of the appropriate time increments are included in Figure 6.3. It was concluded that the

comparison between visually observed and electronically sensed resin front profiles were quite acceptable.
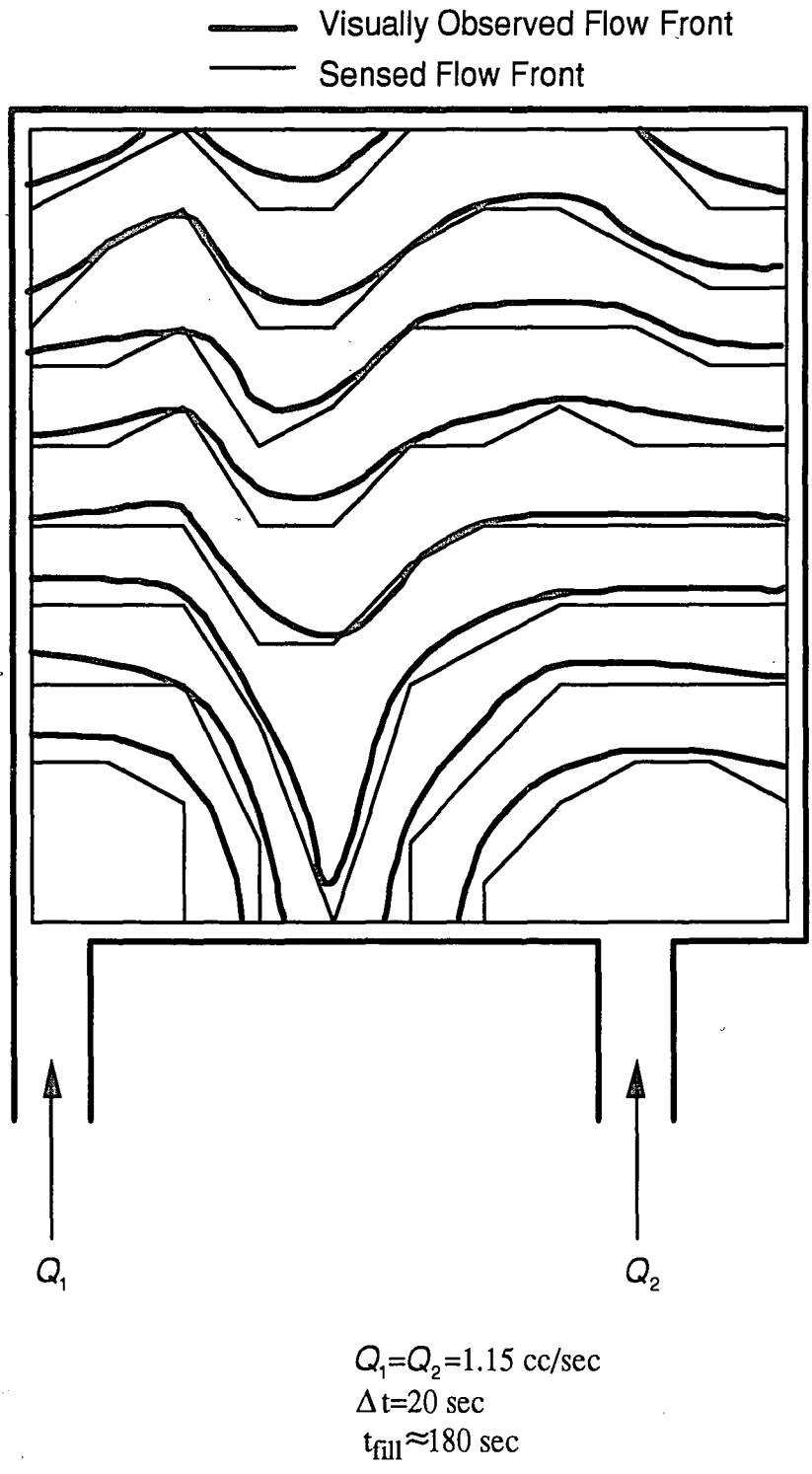
Figure 6.3:
Electronically sensed and video recorded resin front progression during two-dimensional molding

Chapter 7. CONCLUSIONS and RECOMMENDATIONS

In general, the embedded electronic sensor technique investigated during the present study was found to be applicable for the monitoring of flow front progression during molding processes in real-time. In order to monitor the flow front progression in real-time, an improved data acquisition system must be developed. This includes an inter-communication system between sensors and the computer. With further development, this approach could be utilized to monitor spatial and temporal material rheological conditions as well as resin front progression. Additional issues such as material and mold electrical properties need to be considered, but overall the present method appears to be promising.

If, properly developed, generic sensing subsystems for material transformation processes will contribute to improved capabilities for the intelligent manufacturing as shown in Figure 2.4.1 of high quality and low cost products. Such capabilities will be required for physical product based organizations to be successful in the rapidly changing and increasingly competitive international business environment of the future.

REFERENCES

1.   Uchida, M., Suzuki, M., & Nakamura, T. (1986). *Advanced Composite Materials*. Kogyo-Chosakai.

2.   Yamaguchi, S. (1985). *Engineering Plastics Handbook*. Tokyo: Gijutsu-Hyoron-sha.

3.   Rosato, D. V., DiMattia, D. P., & Rosato, D. V. (1991). *Designing with Plastics and Composites: A Handbook* (1 ed.). Van Nostrand Reinhold.

4.   Coulter, J. P., & Guceri, S. I. (1988). Resin Transfer Molding: Process review, modeling and research opportunities. In *Proceeding of Manufacturing International '88. v 1*, IV (pp. 79-86). Atlanta, GA. USA: ASME.

5.   Ware, M. (1985). Thermal Expansion Resin Transfer Molding (TERTM)-A Manufacturing Process for RP Sandwich Core Structures. *40th Annual Conference, Reinforced Plastics/Composites Institute, The Society of the Plastics Industry, Inc.*(Jan.28-Feb., 1985), Session 18-A,1-4pp.

6.   Johnson, C., Chavka, N., Jeryan, R., Morris, C., & Babbington, D. (1987). Design and Fabrication of HSRTM Crossmember Module. *ASM International*, 197-217.

7.   Dane, L. M., & Brouwer, R. (1988). A Resin Transfer Moulded Graphite Bismaleimid Composite Engine Cowling Beam. In SAMPE (Ed.), *33rd International SAMPE Symposium*, .

8.   Robertson, F. C. (1987). Resin Transfer Moulding of Aerospace Resins-A Review. *British Polymer Journal*, 20(1988), 417-429.

9.   Kranbuehl, D., Delos, S., Hoff, M., Weller, L., Haverty, P., & Seeley, J. (1987). Dynamic dielectric analysis: Monitoring the chemistry and rheology during cure of thermosets. In ACS (Ed.), *Polymeric materials science and engineering, Proceedings of the ACS.*, 56 (pp. 163-168). Denver, CO. USA: ACS,.

10. Kranbuehl, D., Delos, S., YI, E., Mayer, J., Jarvie, T., Winfree, W., & Hou, T. (1986). Dynamic dielectric analysis: Nondestructive material evaluation and cure cycle monitoring. , 26(5), 338-345.

11. Kranbuehl, D. E., Delos, S. E., & Jue, P. K. (1986). Dielectric properties of the polymerization of an aromatic polyimide. , 27(1), 11-18.

12. Hart, S., Kranbuehl, D., Loos, A., Hinds, B., & Koury, J. (1992). Intelligent sensor-model automated control of PMR-15 autoclave processing. In SAMPE (Ed.), *37th International SAMPE Symposium*, (pp. 224-230). SAMPE.

13. Kranbuehl, D., Delos, S., Hoff, M., Haverty, P., & Freeman, W. (1989). Use of the frequency dependence of the impedance to monitor viscosity during cure. , 29(5), 285-289.

14. Kranbuehl, D., Hoff, M., Eichenger, D., Hamilton, T., & Clark, R. (1988). Frequency dependent electromagnetic sensing: Life monitoring of materials during use in space. In *Proceeding of the ACS division of polymeric materials: Science and engineering - Fall meeting*, 59 (pp. 839-843). Los Angeles, CA, USA: ACS, Books & Journal division.

15. Kranbuehl, D., Kingsley, P., Hart, S., Loos, A., Hasko, G., & Dexter, B. (1992). Sensor-model prediction, monitoring and in-situ control of Liquid RTM advanced fiber architecture composite processing. In SAMPE (Ed.), *37th International SAMPE symposium*, (pp. 907-913).

16. Kranbuehl, D. E. (1990). In-situ cure monitoring of coatings for plastics. In *Proceedings of the ACS Division of Polymer Materials: Science and Engineering*, 63 (pp. 90-93). Washington, D.C., USA: ACS, Books and journals division.

17. Kranbuehl, D. E., Haverty, P., Hoff, M., & Hoffman, R. D. (1989). Monitoring the cure processing properties of unsaturated polyesters in- situ during fabrication. , 29(15), 988-992.

18.   Walsh, S. M. (1990). Artificial intelligence: Its application to composite processing. In SAMPE (Ed.), *35TH INTERNATIONAL SAMPE SYMPOSIUM*, (pp. 1280-1291).

19.   Stinson, S. C. (1989). Advances Made in Applying IR Sensors to Process Control. *C&EN*(January), 30-31.

20.   Boldizar, A., & Jacobsson, S. (1988). Far Infrared Birefringence versus Other Orientational Measurements of High Pressure Injection Molded High-Density Polyethylene. *Journal of Applied Polymer Science*, 36, 1567-1581.

21.   HALLCREST (1990). Thermochromic Liquid Crystal Products (Catalogue No. HALLCREST.

22.   Dianov, Y. M. (1988). Radio Engineering. *Radioteknika*(No. 8), 3-4.
Farris, R. D. (1987). Composite Front Crossmember for the Chrysler T-115 Mini-Van. , 63-73.

23.   Hochberg, R. C. (1986). Fiber-Optic Sensors. *Transactions on Instrumentation and Measurement*, IM-35(December), 447-450.

24.   Grossman, B. Alavie T., Ham F., Franke J., Thursby M., (1989). Fiber-Optic Sensor and Smart Structures Research at Florida Institute of Technology. *SPIE*, 1170, 123-135.

25.   Jackson, D. A., Jones J. D. C.., (1986). Fibre Optic Sensors. *Optica Acta*, 33(No.12), 1469-1503.

26.   Lee, C. E. T., Taylor H. F., (1989). Fiber Optic Sensor Research at Texas A&M University. *SPIE*, 1170(Fiber Optic Smart Structures and Skins II), 113-122.

27.   Lieberman, R. A., Blyler, L., & Cohen, L. G. (1990). A Distributed Fiber Optic Sensor Based on Cladding Fluorescence. *Journal of Lightwave Technology*, 8(February), 212-220.

28.   Shanglian, H., Fei, L., & Yingjin, P. Distributing Fiber Optic Pressure Sensor using High-Birefringent Fiber No. Department of Opto-Electronic Instruments, Chongqing University, Chongqing, Sichuan, China.

29.   Tateda, M., & Horiguchi, T. (1989). Advances in Optical Time-Domain Reflectometry. *Journal of Lightwave Technology*, 7(August), 1217-1224.

30.   Aoyagi, H., Uenoyama, M., & Guceri, S. I. (1992). Analysis and Simulation of Structural Reaction Injection Molding (SRIM). *International Polymer Processing*, VII, 71-83.

31.   Coulter, J. P., I., B. L., & Demirci, H. H. (1993). Neural Networks in Material Processing and Manufacturing: A Review. *Journal of Materials Processing & Manufacturing Science*, 1(April), 431-444.

32.   Hansen, S. (1990). RTM Processing and Applications. *Conference: Resin Transfer Molding Clinic*
March 6-7, 1990, EM90-214:1-25.

33.   Kalpakjian, S. (1992). *Manufacturing Engineering and Technology* (2 ed.). Addison-Wesley Publishing Company.

34.   Kelleher, P. G. (1990). Report on the State of the Art: Injection Molding of Fiber Reinforced Thermoplastics. Part 2. Design and Manufacture. *Advances in Polymer Technology*, 10(No. 4), 277-284.

35.   Rogers, J. (1989). SRIM and RTM Sprint Toward High-Volume Uses. *Plastics Technology*(March, 1989), 51-58.

36.   Rogers, J. (1990). RTM and SRIM-ready for mainstream markets? *Modern Plastics*(Nov, 1990), 44-48.

37.   Stover, D. (1990). Resin-Transfer molding for advanced composites. *Advanced Composites*(March/April 1990), 61-80.

38.   Warren, C. (1990). INFRARED THERMOMETERS Out of the lab and into the factory. *Machine Design*(November), 85-88.

Vita

Akihisa Kikuchi was born June 10, 1964 in Tokyo, Japan to parent of Mr. and Mrs. Kikuchi. The author began his undergraduate studies at the University of Delaware in September 1985. After graduating from the University of Delaware with a Bachelor of Science degree in Mechanical Engineering in June 1990, the author continued his studies at the center for composite materials at the University of Delaware as a research assistant for one year. Then, he continued his studies as a National Science Foundation funded research assistant at Lehigh University under the direction of Dr. John P. Coulter. In January 1994, the author received has Master's of Science degree in Mechanical Engineering. Presently, the author has accepted the job as a developmental engineer for a company specializing in injection molding.

END
OF
TITLE